12-2021

Experimental and Computational Studies of Electron Rich Alkenes

Alexa May
University of Arkansas, Fayetteville

Experimental and Computational Studies of Electron Rich Alkenes

A dissertation submitted in partial fulfillment
of the requirements for the degree of
Doctor of Philosophy in Chemistry

by

Alexa May
Oklahoma State University
Bachelor of Science in Chemistry, 2015

December 2021
University of Arkansas

This dissertation is approved for recommendation to the Graduate Council.

_____
Matt McIntosh, Ph.D.
Dissertation Director

_____
Nan Zheng, Ph.D.
Committee Member

_____
Wesley Stites, Ph.D.
Committee Member

_____
Joshua Sakon, Ph.D.
Committee Member

Abstract

Thermal homolysis is one of the most fundamental reactions in organic chemistry. Free radical reactions are generally initiated by light or a radical initiator to generate the first radical, which can then propagate or terminate the reaction. Direct thermal homolysis requires no chemical initiators, just an increase in temperature depending on the homolysis energy. There are few studies of direct radical homolysis in complex systems or under mild conditions. The reactions involving C-N homolysis under mild conditions are reported in Chapter 1. Though the authors do not all propose a radical mechanism, we believe they can all be explained by a radical mechanism similar to our own chemistry reported in the later chapters. These all involve an electron rich alkene intermediate, which we believe to be especially prone to homolysis based on DFT calculations and our own research presented in this work.

We have uncovered multiple C-N homolysis reactions from electron rich alkenes. The first, is a Breslow intermediate that undergoes facile rearrangement from the enolate when a benzyl group is installed on the azolium nitrogen atom. This reaction leads to products consistent with a radical mechanism, and those previously reported by our group. Second, is a reaction that generates 2-alkyl pyridines from an electron rich enamine. This C-N homolysis requires heat, but the products are also consistent with a radical mechanism. Currently efforts are underway to expand the scope of this chemistry to include heterocycles with fused rings.

Acknowledgements

I would like to thank my family for supporting me through this long journey. I would also like to thank the many friends and colleges I have made throughout my time here which made this process a bit easier and a lot more fun.

Most importantly I would like to thank Dr. McIntosh for taking me in and introducing me to a whole new world of chemistry that was exciting to explore. Also, for helping me develop my skills as an organic chemist both in the lab and in the classroom. I regained my confidence in his lab and for that I am forever grateful. I thank Dr. Weaver, my undergraduate advisor for helping me get into graduate school and for my initial training in organic chemistry. His passion for organic chemistry made me excited for what organic chemistry can do.

I would like to thank Wei Shi and his group as well, for showing me the ropes in carbohydrate synthesis and giving me several role models to look up to. Also, I am very thankful for my committee members for pushing me to be better and guiding me in the right direction. Lastly, I want to say thank you to anyone not mentioned that helped me along this journey.

Table of Contents

Chapter 1: Low Temperature C-N homolysis

1.1 Introduction

Thermal homolysis is a fundamental reaction in organic chemistry and it only requires heat to generate the two radicals. The general homolysis reaction mechanism is shown in Figure 1a, where the bond between two atoms is broken homolytically to generate two radicals. Some common examples of homolysis reactions are shown in Figure 1b and 1c as allylic bromination and radical halogenation[1]. Common features of these reactions include high temperatures and/or chemical/photo initiators such as, peroxides and Azo compounds like AIBN. The initiator will

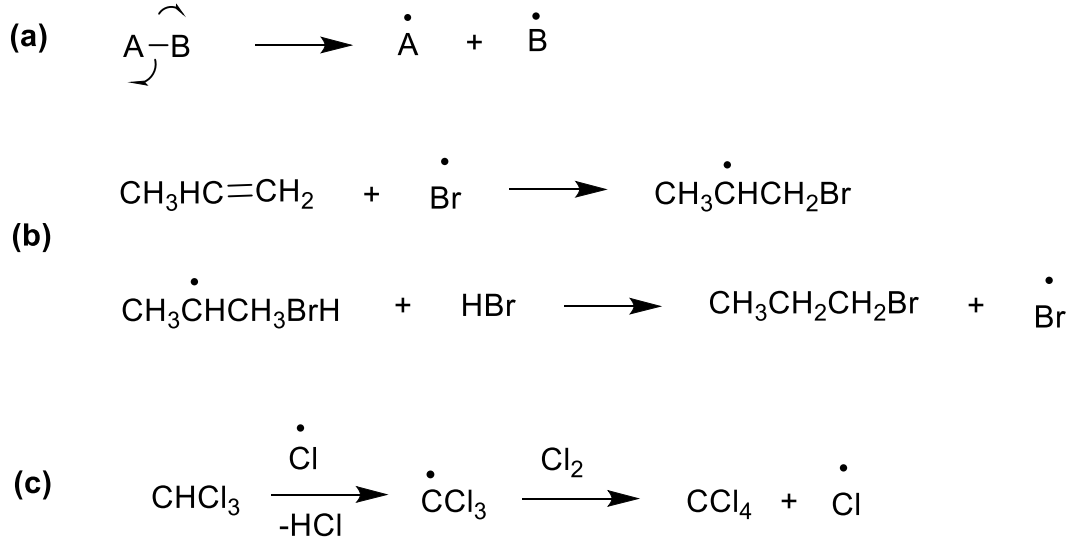

Figure 1: (a) general homolysis reaction (b) allylic bromination. (c) radical halogenation

generate the first radical which can then create a second radical and propagate the reaction until termination occurs. Since, radicals are high energy species they are generally have very strong bonds. Breaking a C-C, C-N or C-O bond homolytically requires exceedingly high temperatures of greater than 300 °C, since the bond dissociation energies of these strong bonds are around 75-85 kcal/mol or even higher. However, there are reports in literature of low temperature homolysis of C-N bonds.

Additionally, the mechanism of more complex radical reactions is not as well understood, most computational studies are of very simple structures or of reactions that involve initiators. In the context of this work there are two main reactions, homolysis followed by recombination, or a homolysis followed by disproportionation. This review will focus on generating radicals at low temperatures via C-N homolysis of some electron rich alkenes that can then undergo recombination or disproportionation. Through the course of these reactions, we would also like to look at what influences these reactions to better understand the mechanism.

1.2 Oka: Studies on vitamin B_1 and related compounds

In 1970 Oka[2] et al. reported a cleavage of thiamine and homologs by reacting them with benzaldehydes in methanol at reflux to give an alcohol **3**, aromatic ketone **2**, a pyrimidine product **1**, and Benzoin **4** (**Scheme 1**).

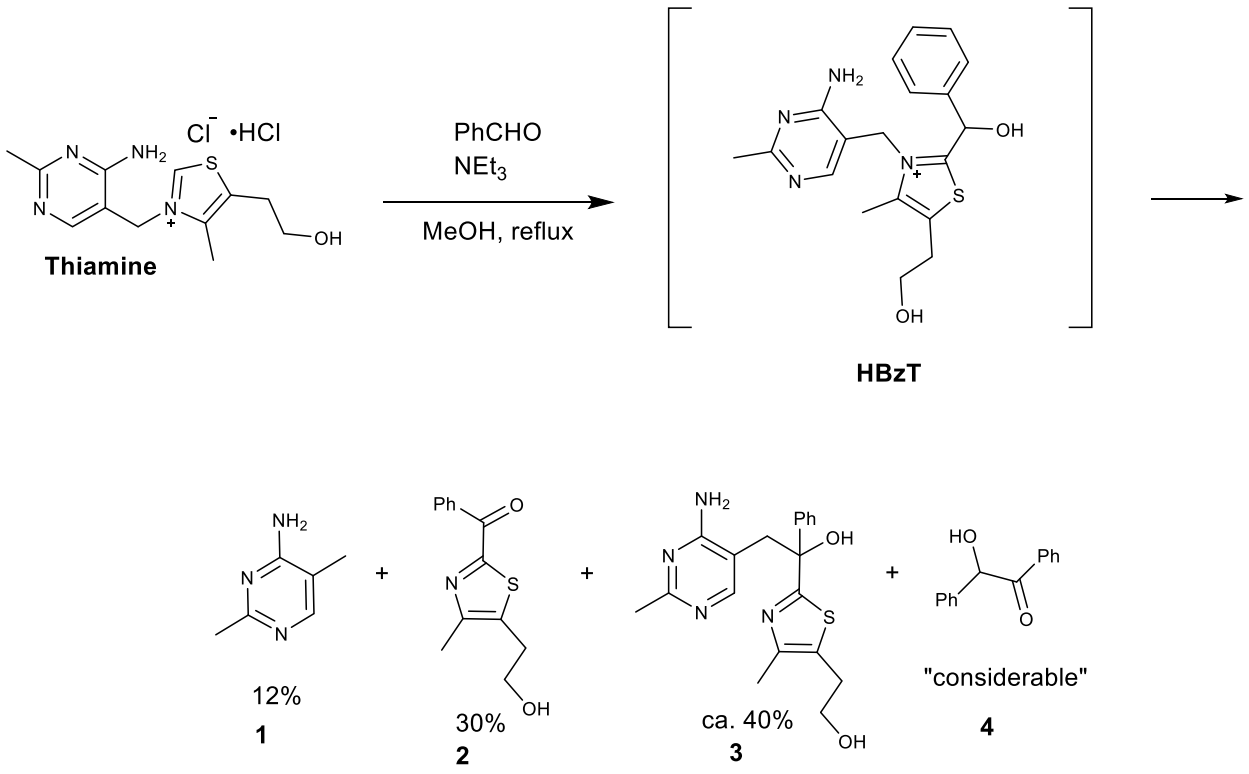

Scheme 1: Oka fragmentation products

They proposed a polar mechanism for this fragmentation process by way of an α-hydroxybenzylthiamin (**HBzT**) intermediate and postulated the 4-amino group in the pyrimidine to be necessary for the rearrangement like product **3** and ketone product **2**, since in the absence of the amino group they did not see either product. This mechanism seems unlikely since it does not go through a Breslow intermediate and in our lab, other functional groups besides pyrimidine, have given us the analogous products.

1.3 Hemmerich: Studies in the Flavin series Alkylation and rearrangement reactions of dihydroalloxazines

Hemmerich[3] and coworkers described the rearrangement of dihydroalloxazines in 1971. They found N(5), N(10), and C(4a) to be the possible alkylating spots for their reactions (**Scheme 2A**). They also found the position of alkylation was dependent on the alkylating reagent, whether it is activated by pi-orbitals or has a saturated alkyl group.

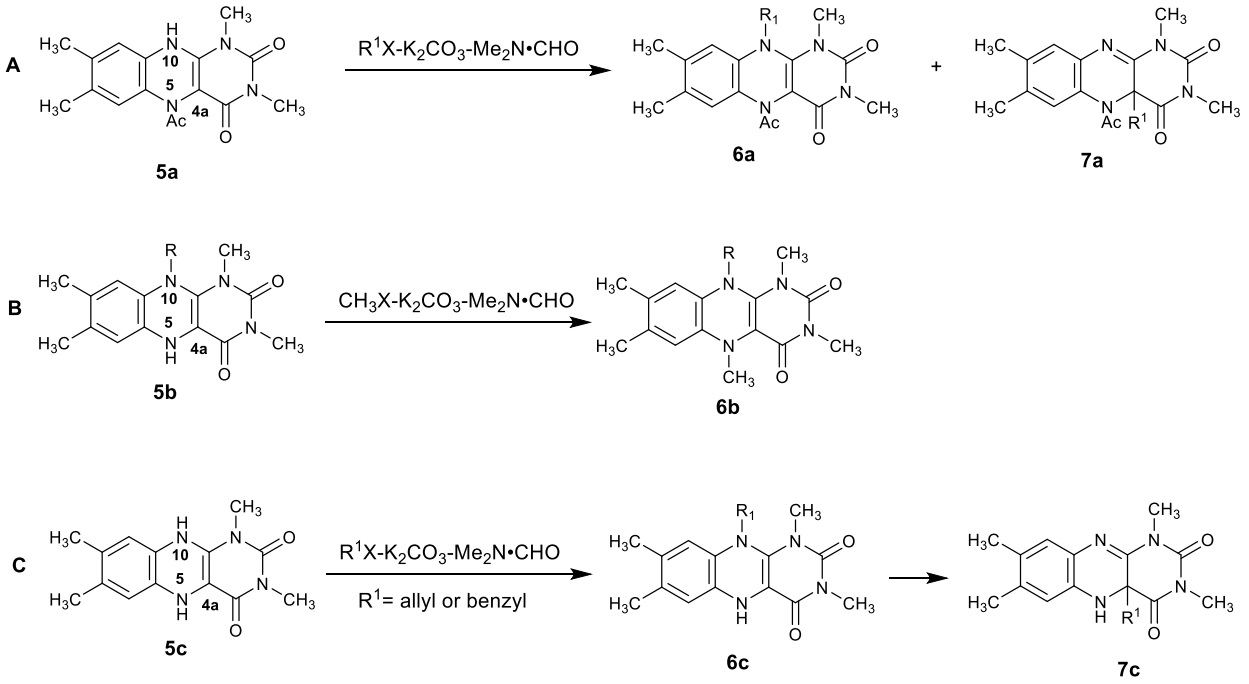

Scheme 2: (A) possible products after alkylation. **(B)** Methyl Iodide alkylation after removal of the N(5) acetyl group. **(C)** alkylation with allyl or benzyl after removal of N(5) acetyl

Reagents such as dimethyl sulfate, ethyl iodide, and isopropyl iodide gave exclusively the N(10) alkylated product (**6a**), while benzyl, allyl, and methyl gave a mixture of N(10) and C(4a) alkylated products (**6a** and **7a**), albeit very small in the case of methyl iodide (**Scheme 2A**). Based on the product ratios, and sizes of the substituents the reaction did not seem to be controlled by sterics. Removal of the acetyl group at N(5) resulted in a greater difference between the alkylating reagents, with methyl iodide giving exclusively N(5) alkylation (**Scheme 2B**) and benzyl and allyl giving exclusively C(4a) alkylation, which was confirmed by NMR (**Scheme 2C**). Based on these results Hemmerich and co-workers proposed that the position of alkylation depended on the nature of substituents on the molecule before alkylation and therefore the planarity of the dihydroisoalloxazines. Thus, when N(10) is acetylated the dihydroisoalloxazines are less planar and that changes the reaction from frontier molecular orbital controlled to charge controlled. The bending of the C-N bond is something our group has hypothesized to lower the radical homolysis energy and it appears this that this supports that hypothesis similar to what was seen in the previous section. This is one reason why the alkylation with methyl iodide gives exclusive alkylation at N(5) and the allyl and benzyl groups gave exclusively C(4a) alkylation when the acetyl group was removed. In addition to this observation, the difference in products we believe could be explained by the radical stability of the group on the nitrogen. Methyl is a far less radical stabilizing group than allyl or benzyl and therefore would not undergo homolysis to give a product like **8d** when the acetyl group is removed (**Scheme 3**). The removal of the acetyl group also makes the molecule more electron rich which is consistent with our observation that the more electron rich the compound the more likely homolysis is (see chapters 2 and 3).

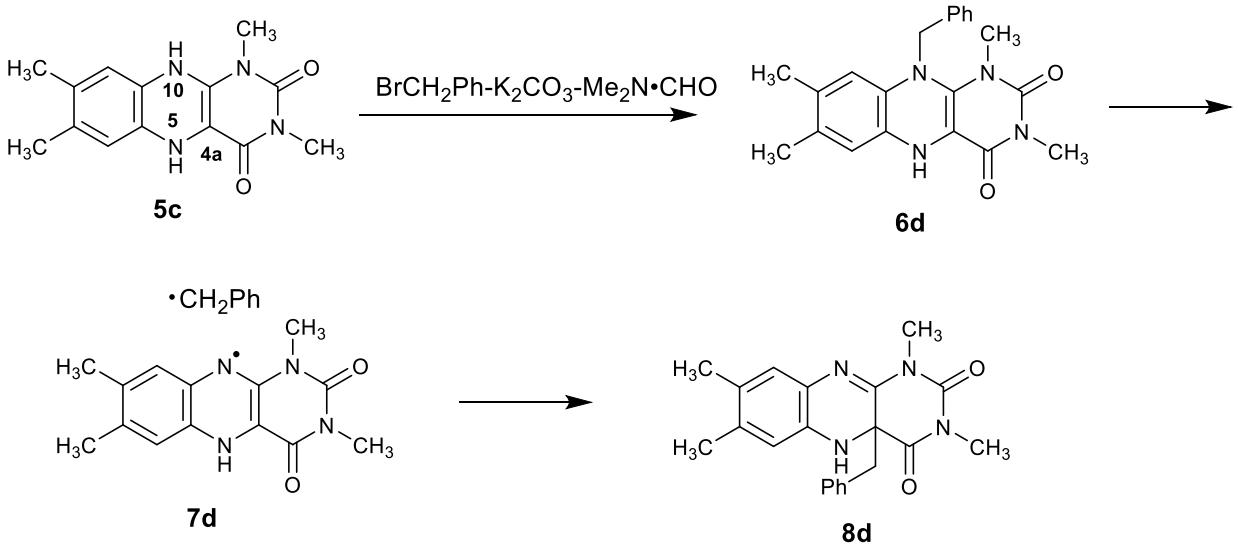

Scheme 3: Proposed C-N homolysis when R^1 is benzyl

1.4 Baldwin: Reactions of N,N,S,S substituted ethylenes

In 1974 Baldwin[4] reported the formation of N,N,S,S substituted ethylenes that were found to undergo a radical [1,3] or a concerted [3,3] rearrangement depending on the temperature and nitrogen substituent (**Scheme 4**).

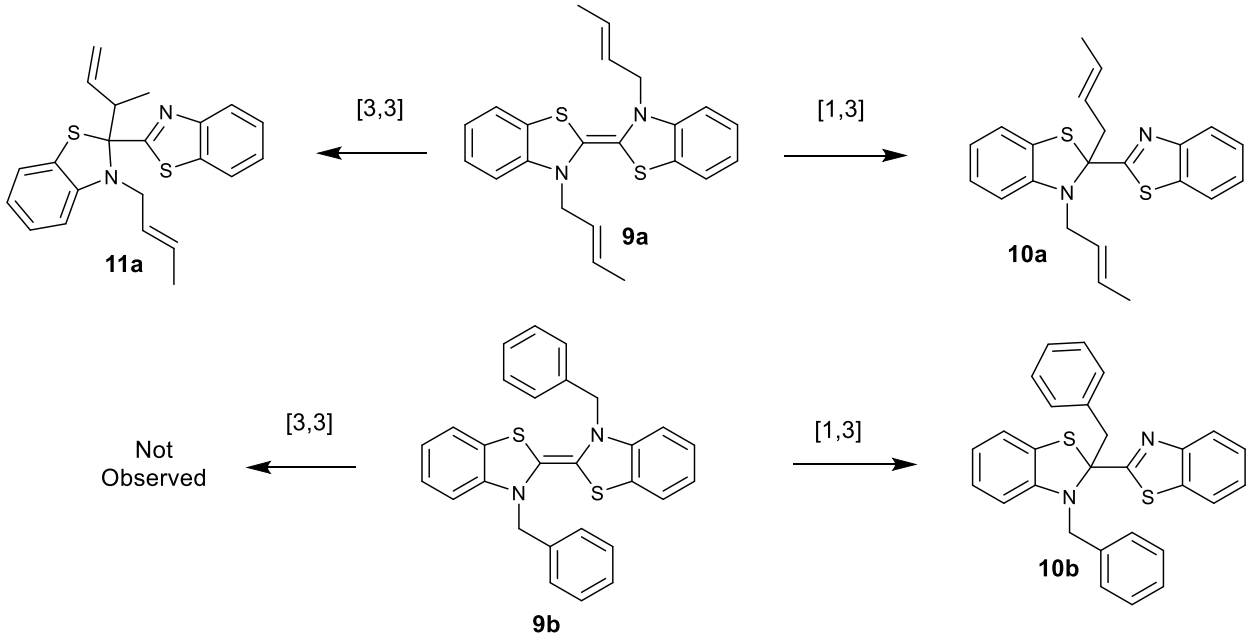

Scheme 4: Degree of [1,3] vs [3,3] rearrangement with different N-substituents

They found that simple allyl groups preferentially underwent [3,3] rearrangement (**11a**), while substituted allyl and benzyl substituents preferentially underwent [1,3] rearrangement especially at elevated temperatures (up to 100 °C). Benzyl groups only provided the [1,3] rearrangement product **10b** and none of the [3,3]. Baldwin argues for a radical mechanism for the formation of the [1,3] rearrangement product. Further mechanistic studies involving a crossover reaction with deuterium labeled benzyl groups supported a radical mechanism.[5] The authors used a mixture of benzothiazolium salts and subjected them to the reaction conditions, which resulted in the formation of a cross over product. The stable dideutoerio dimer was confirmed by Mass Spectrometry as 28 ± 2% of the total (**Scheme 5** inset).

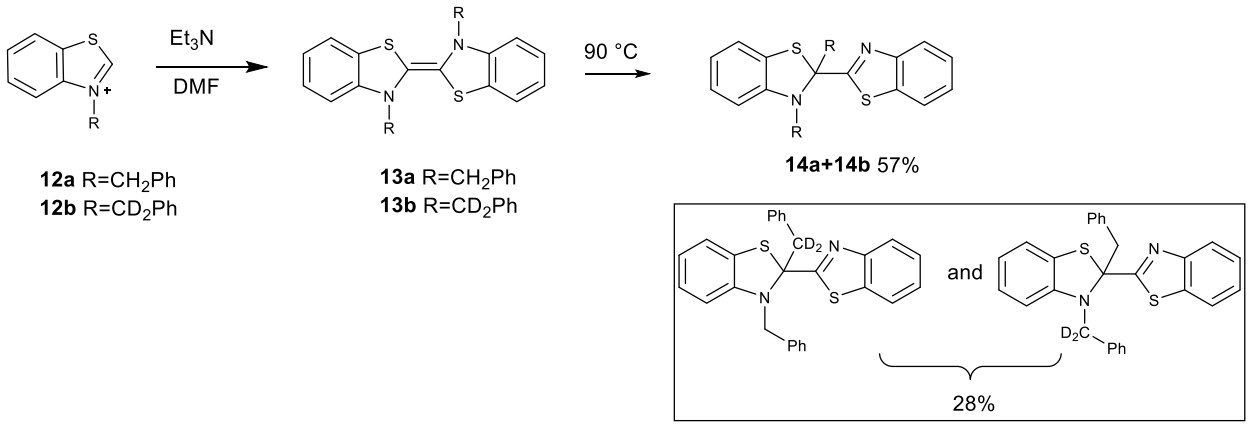

Scheme 5: Deuterium labeling mechanistic study

They speculated that the low yield of the intermolecular cross over products produced, was due to a solvent cage effect. They also obtained 57 ± 2% of the intramolecular rearrangement products **14a** and **14b** which they propose is due to a fast recombination of the two radicals within the solvent cage. The reversibility of the formation of the dimer was ruled out after the monomethylated dimer was not detected by Mass spectrometry in a crossover reaction between the monomethylated and non-methylated dimers (**Scheme 6**). The last piece of evidence for a radical mechanism was the detection of bibenzyl in the Mass spectrometer.

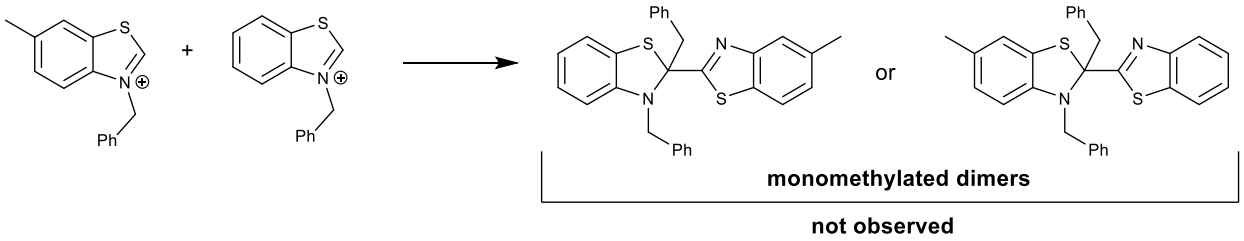

Scheme 6: Synthesis of benzothiazolium dimer cross over products

1.5 Lown: Sterochemistry and mechanism of thermal [1,3] alkyl shift of stable dihydropyrazines

Around the same time as Baldwin, Lown and coworkers[6] reported on the thermal reaction

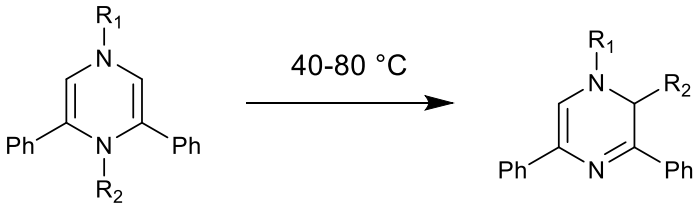

Scheme 7: Dihydropyridine rearrangement

mechanisms of 1,4-Dialkyl-1,4-dihydropyridines. The general reaction conditions show a pyrazine undergoing rearrangement with heat (**Scheme 7**). They found evidence of the [1,3]-alkyl shift being a radical mechanism. Crossover reactions done by changing the hydrogens to deuterium in pyrazine **15**, gave rearrangement product **19** with the deuterated part unchanged (**Scheme 8**). When the benzylic position was deuterated (**16**) instead the analogous product **20** resulted. These deuterated starting materials were heated until the rearrangement was completed and the crossover product percentage of 12 indicated the reaction was mainly intramolecular (**Scheme 8**). This is the amount of radicals that escape the solvent cage, and when changing to hexanes, a lower viscosity solvent for the crossover experiment, 14% of the crossover product was observed. The same mixture was reacted under the rearrangement conditions with a radical

scavenger, butanethiol, which resulted in no crossover product and the formation of butane disulfide **21** (**Scheme 8**). This supports that the mechanism is not free radical, but instead a caged radical process.

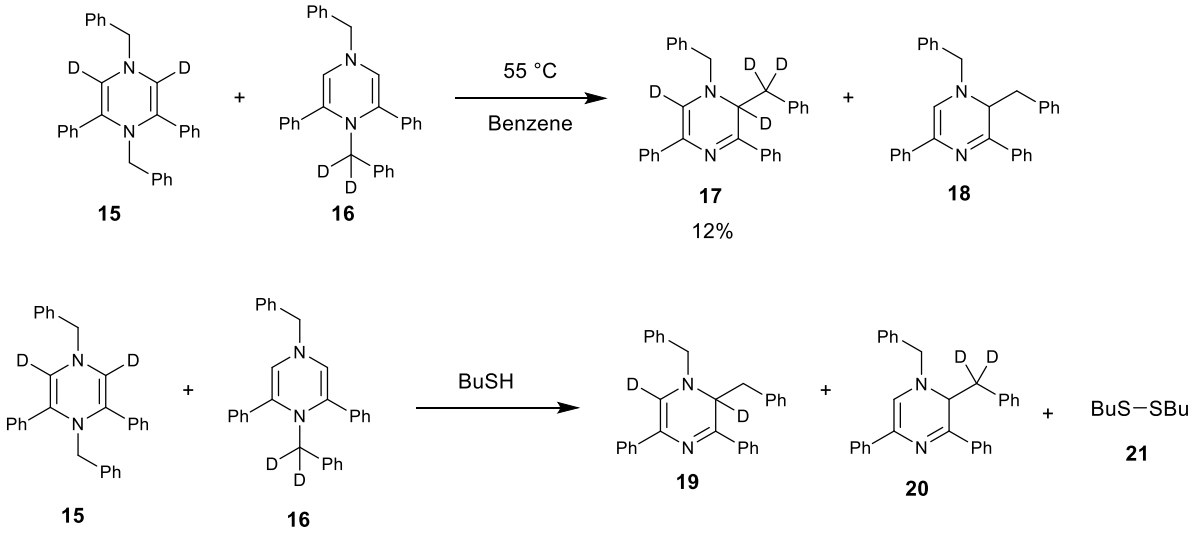

Scheme 8: Crossover experiments with radical scavenger

The stereochemical consequences of this probable intracage process were investigated by heating a deuterium labeled starting material in the S conformation. The idea was that a completely free radical reaction would result in racemization, and overall inversion would signify the involvement of the sigmatropic mechanism inside the cage. If the reaction was stepwise loss of optical activity would occur only if the radical pair that forms from C-N-

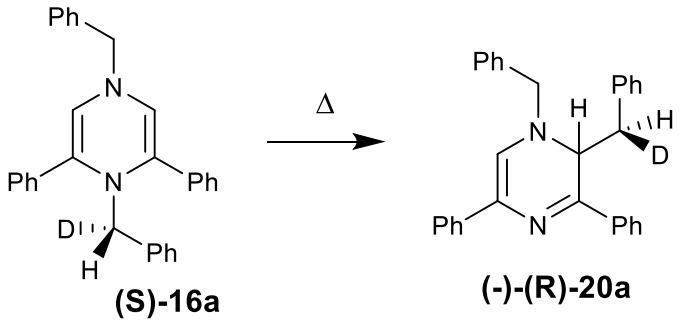

Scheme 9: Reaction investigating stereochemistry

homolysis has a long enough lifetime to permit reorientation of the radicals. The resulting product (-)-(R)-20a (**Scheme 9**) was optically active with inversion. This confirms the involvement of the sigmatropic pathway inside the solvent cage. The degree to which the inversion occurs was assessed by heating up **16a** with the butanethiol scavenger used previously. This reaction showed a rearrangement product with increased specific rotation indicating that the racemized rearranged product was forming outside the solvent cage. Therefore it was concluded that the rearrangement was going by both a sigmatropic and a radical dissociative mechanism depending on the migrating group and the reaction temperature. Additional details on the regiospecificity of the rearrangement were examined as well. It was determined that the stability is established by the geometry of the heterocycle which is controlled by the position of the substituents on the ring and the ability of the nitrogen lone pair to be in conjugation with the rest of the system. The authors conclude that a nonplanar structure is likely for the dihydropyrazine system studied here, where one nitrogen is out of plan. This is consistent with our own experimental and computational work that suggests radical C-N homolysis occurs more easily when the nitrogen substituent is bent out of plane. **Figure 2** illustrates this phenomenon with methyl groups instead of the N-benzyl and neighboring phenyl groups.

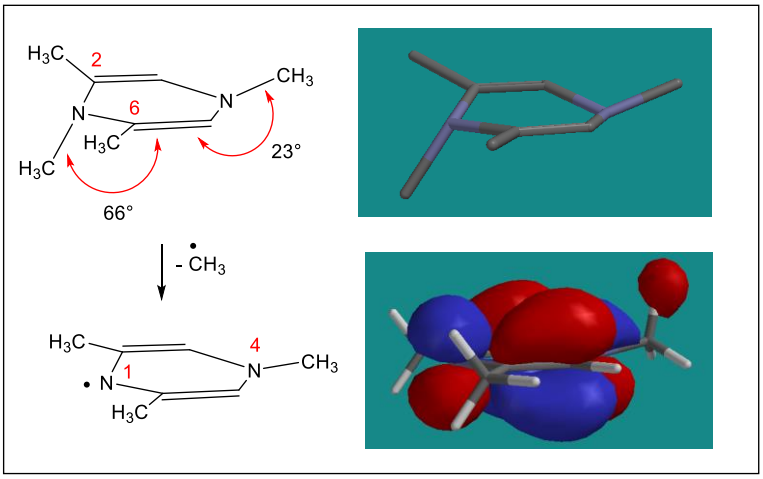

Figure 2: DFT computations showing the difference in dihedral angles for N-substituents

1.6 Lappert: Synthesis of 1,3,1',3'-tetrabenzyl-2,2'-biimidazolidinylidines

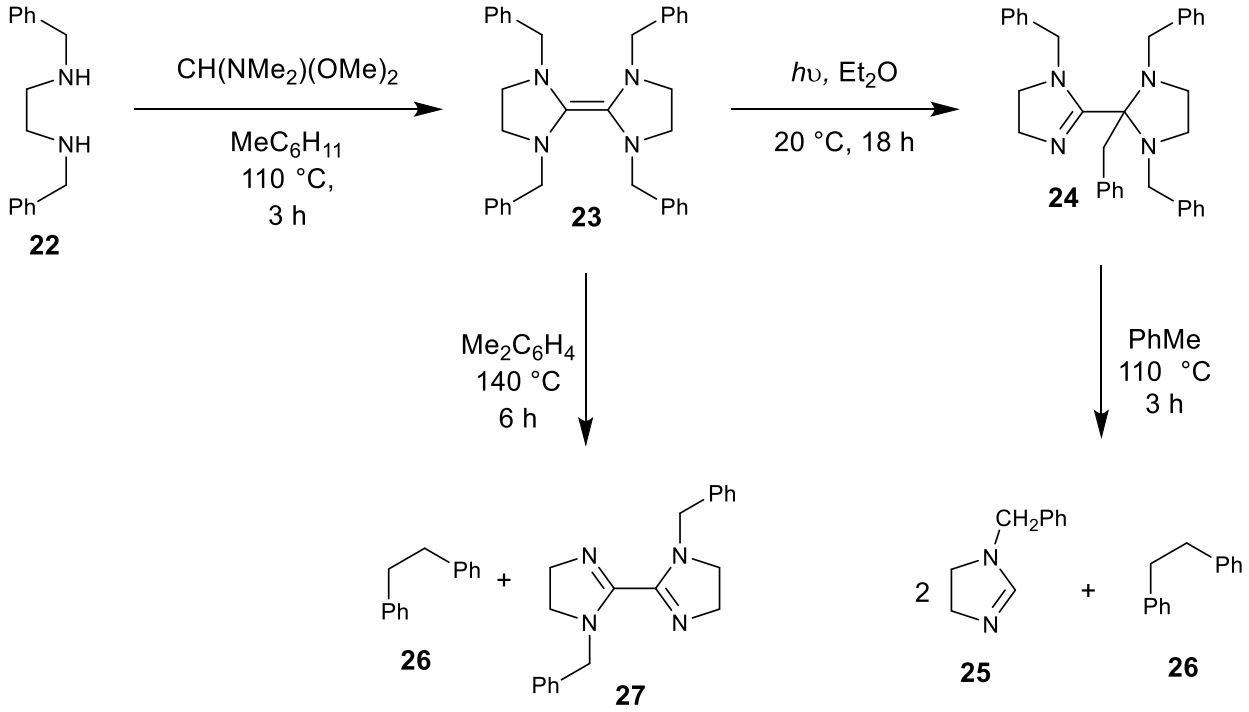

Scheme 10: Synthesis and radical homolysis products of enetetramine **23**

In 1998 Lappert[7] and his group studied the degradation reactions of different enetetramines (N-benzyl variation is shown in (**Scheme 10**). They were able to synthesize **23,** as well as the N-$CH_2CH{=}CH_2$ and N-ethyl analogs and studied their thermal and photochemical reaction products. Under photochemical conditions **23** gave rearrangement product **24,** and under thermal conditions biimidazoline **27** and bibenzyl **26** were obtained. The reactions to form **25** and **27** are proposed to be radical since they both formed bibenzyl (**26**). After full characterization Lappert and co-workers attempted to obtain the tetrabenzyl compound **28** (**Scheme 11**). The tetrabenzyl compound was not able to be confirmed using any of the conditions and instead each reaction underwent debenzylation to give **31**. Notably, product **31** is

analogous to the previously formed enetetramine **27,** which was proposed to go by a radical mechanism because of the bibenzyl biproduct.

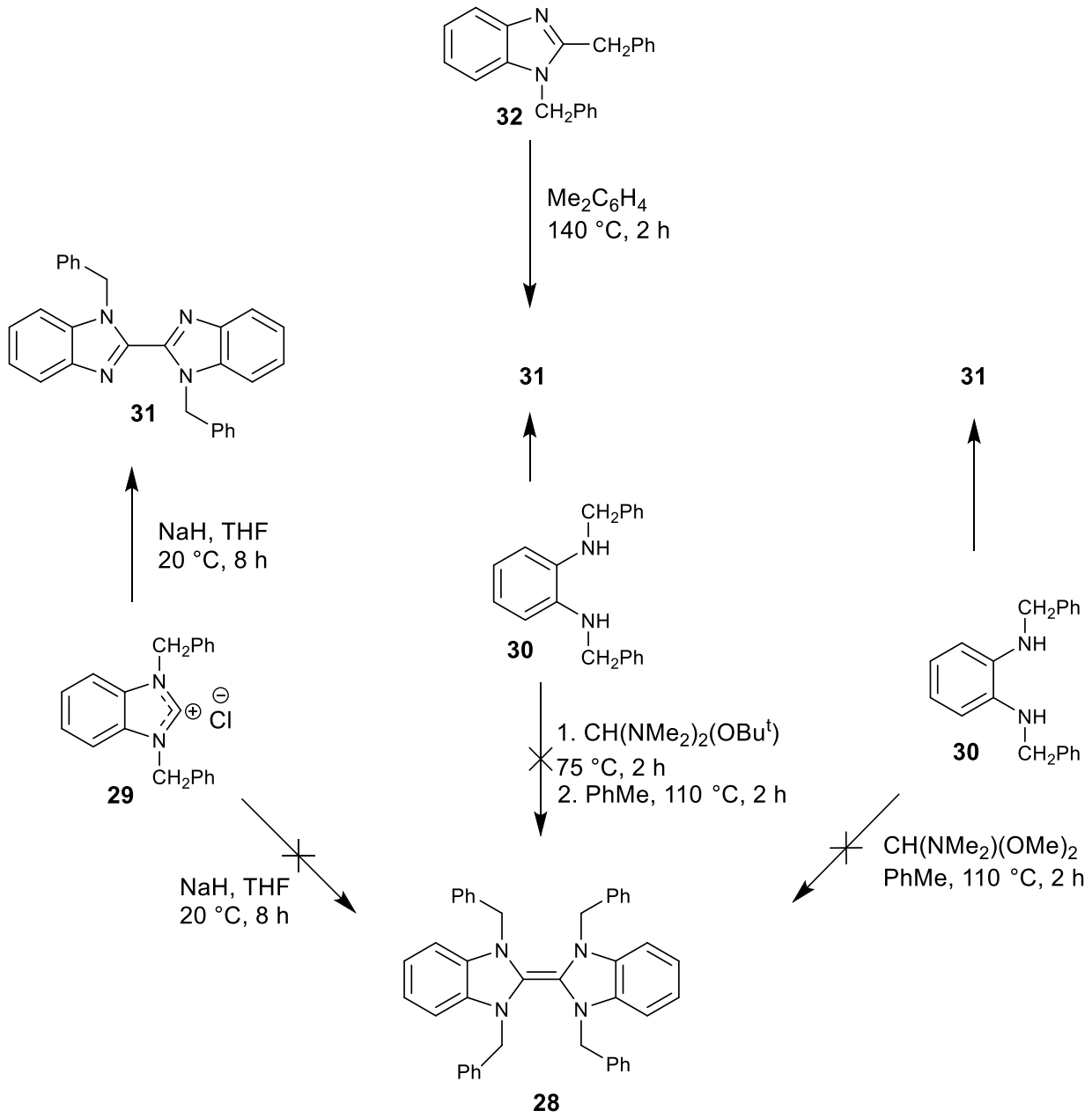

Scheme 11: Synthesis of enetetramine **28** resulting in the formation of **31**

The crystal structure of the methyl analog[8] shows the two ends of the molecule are twisted by ca. 21° about the C=C bond to reduce the steric strain between the adjacent methyl groups (**Figure 3**

right). The crystal structure of the benzyl analog which was previously synthesized[9], shows the NCN' planes are twisted by ca. 17° about the C=C bond as seem in the X-ray crystallographic data (**Figure 3** left). They attribute the difference in stability between the tetrabenzylene-tetramine and the other tetraaminoethylenes to be because of the steric interactions between the two methyl groups which causes the C=C bond to twist.

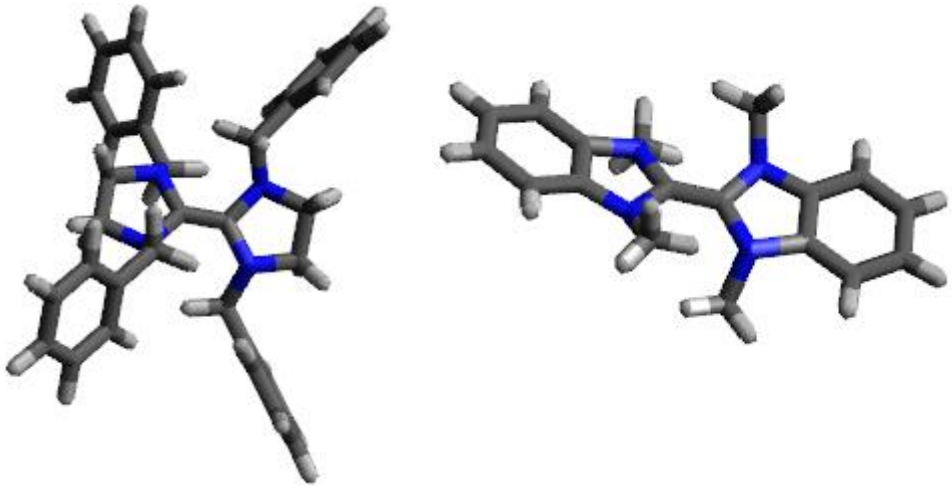

Figure 3: Left: tetrabenzylenetetramine. Right: tetramethylenetetramine

1.7 Hahn: Rearrangement of electron-rich N-allyldibenzotetraazofulvalenes

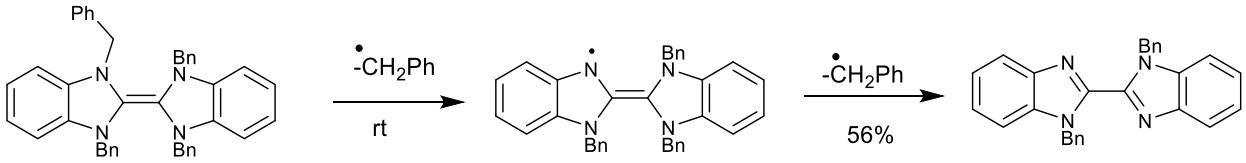

Scheme 12: Mechanism of double dealkylation

Hahn and coworkers[10] in 2006 studied the mechanism of rearrangement (**Scheme 12**) and the degradation of electron rich N-substituted dibenzotetraazafulvalenes. They found that they could not isolate a dibenzotetraazofulvalenes by deprotonation of C2, instead it formed compound **36a** or **36b** (**Scheme 13**) where you get cleavage of two N-R bonds, depending on the N-substituent. To investigate the reaction mechanism, they performed DFT calculations for the formation of the

rearrangement type prodcuts. There are at least two options for mechanism, a radical homolysis/recombination or a sigmatropic rearrangement. When comparing the energies of the radical pairs and the transition state energies of the sigmatropic rearrangements, it was found that the 3-aza-cope rearrangement adopts a chair like structure in the transition state **37**- (**Scheme 14**).

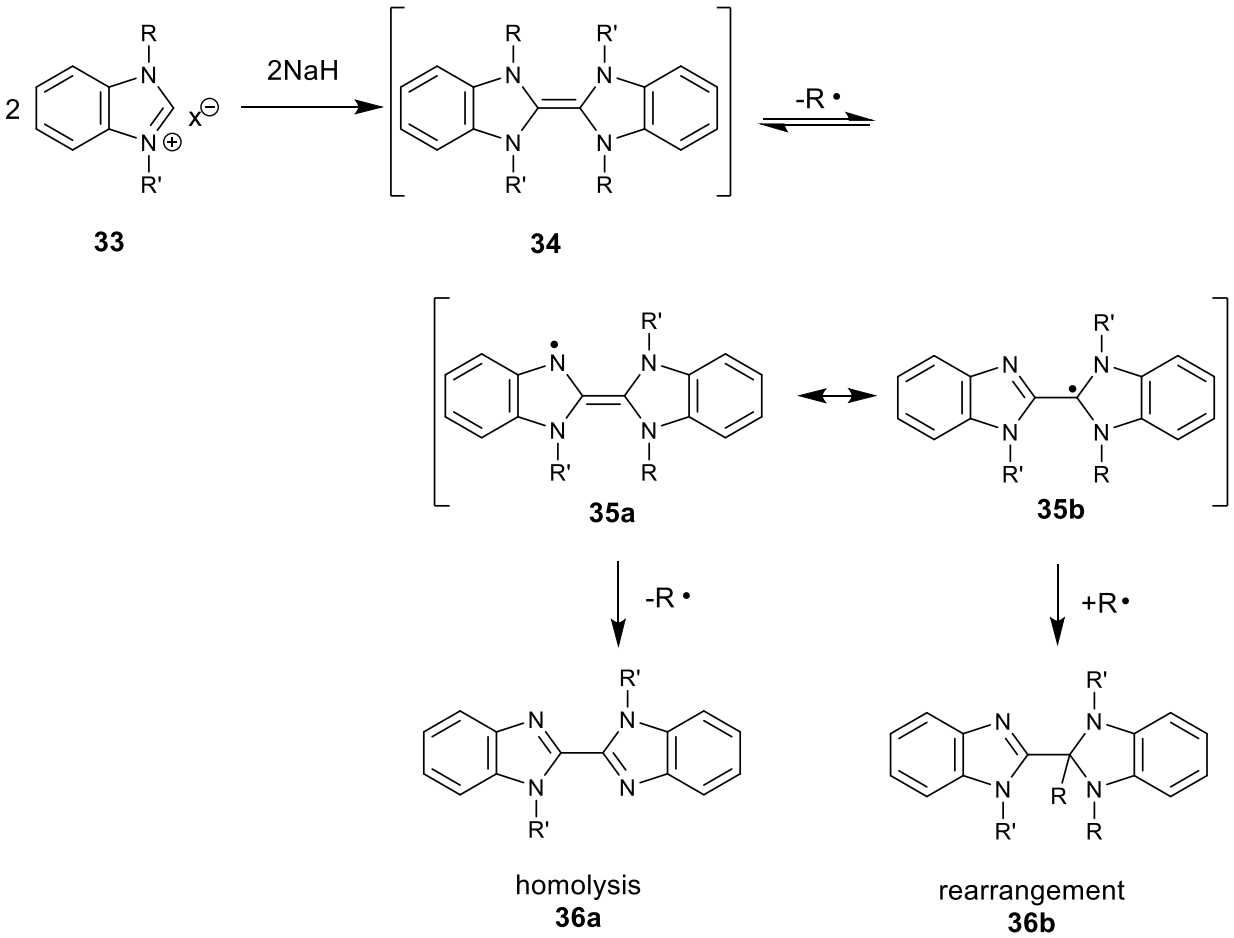

Scheme 13: Two pathways to products **21a** and **21b** by a radical mechanism

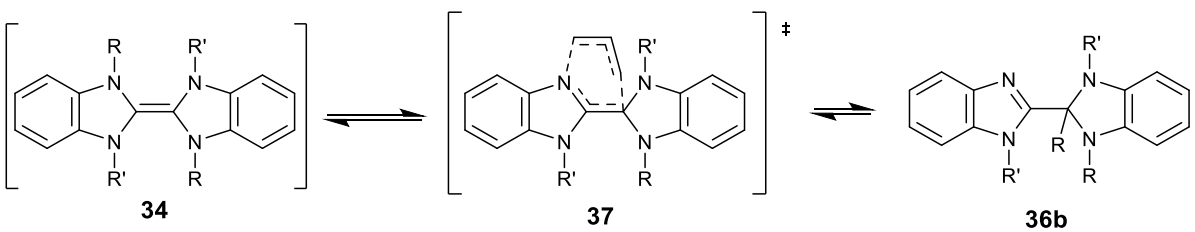

Scheme 14: Mechanism for the 3-aza-cope rearrangement with transition state

For the structures with 2 or 4 allyl groups as the N-substituents there was not much difference in the activation energy for the transition states (less than 1 kcal/mol). However, for the bulkier allyl and the benzyl substituents the transition states could not be identified. Overall, the energies for the radical path were much lower for the dibenzotetraazafulvalenes than the 3-aza-Cope rearrangements, or in the case of the bulkier groups the only energy that could be calculated. The other possible pathways result in the loss of a second R group to give a homolysis product **36a** or the loss of one R group to give a rearranged product **36b**. DFT calculations done for the R==R'=allyl and the R=allyl and R'=methyl showed a difference of 30 kcal/mol or more between the rearrangement and homolysis pathways, however both products are observed experimentally. This indicates that once the products **36a** and **36b** are formed the back reaction to the radicals is slow under the reaction conditions so there are some kinetic factors to consider, in addition to the thermodynamics. Additionally, DFT calculations were done on the N-allyl-N'-benzyldibenzotetraazafulvalene which has 3 potential reactions: double deallylation, double debenzylation (**36a,** R=R'=CH_2Ph**)**, or mixed deallylation-benzylation. They found no significant differences in the energies, though experimentally only the debenzylation product was found, indicating that other factors not considered were important.

To gain more insight into the kinetic effects on the radical reactions of these types of electron rich double bonds, DFT calculations were done on the N-3-methylbut-2-enyl substituted dibenzotetraazafulvalene. They found that the first homolysis from **38** to give **39'** (**Scheme 15**) was 6.8 kcal/mol indicating a radical pathway was likely. After the formation of **39'** there are two possible pathways one is a recombination type product **40/40'** or a second C-N homolysis can occur to give a homolysis type product **41**. The recombination product as two possibilities due to resonance structure you can draw for the 3-methylbut-2-enyl radical. Experimentally,

recombination at the tertiary carbon atom of the radical to give **40** did not occur, which is supported by the calculated reaction energies that showed this reaction to be the least exothermic at -7.1 kcal/mol. A steric effect is suggested to be hindering this rearrangement reaction.

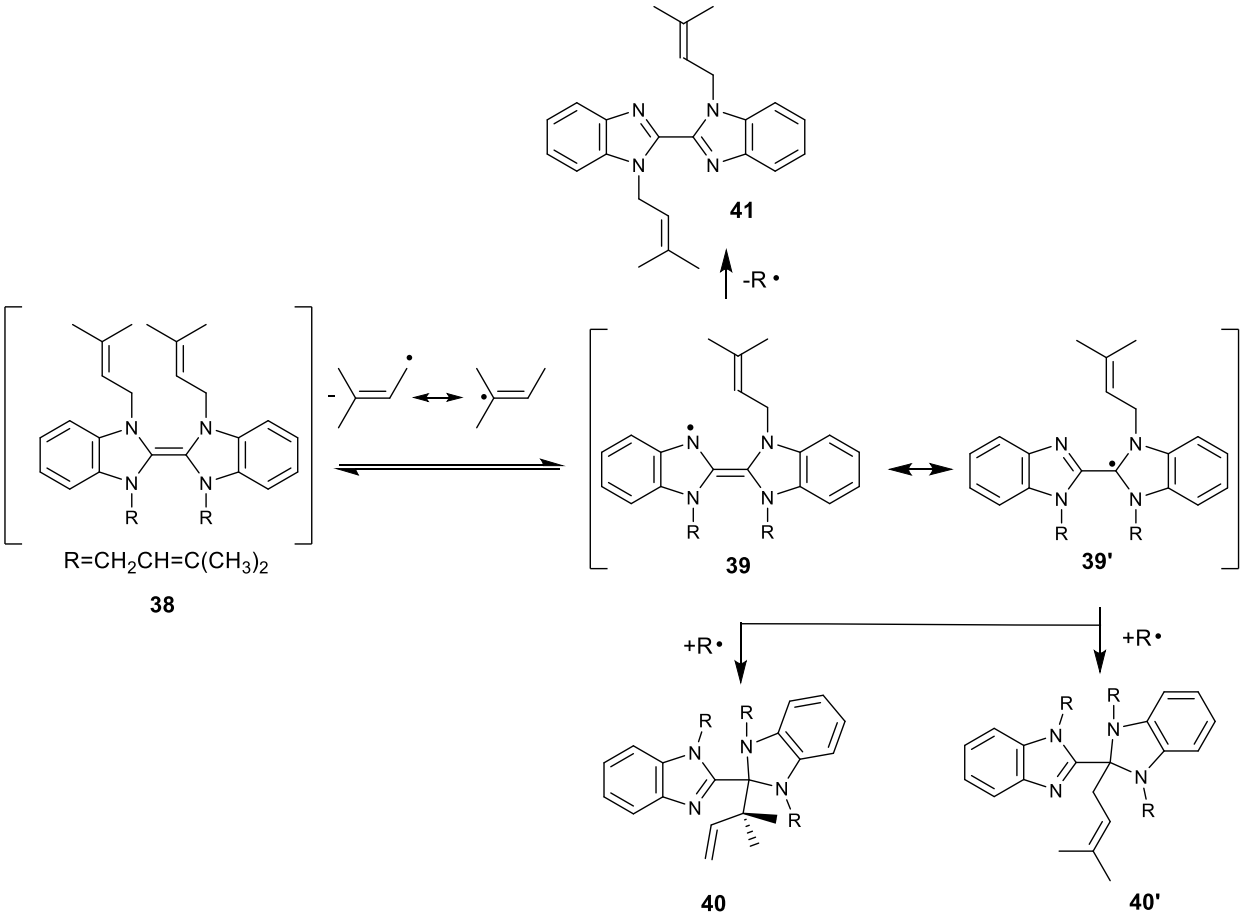

Scheme 15: Possible reaction pathways for **39** and **39'**

Computationally the reaction energies to form **40'** or **41** from **38** were more exothermic at -26.9 and -60.8 kal/mol respectively. From a thermodynamic perspective these two reactions could both occur, but experimentally only **41** was observed. They conclude this is likely due to a difference in reaction rates so thermodynamics alone cannot accurately predict the product.

1.8 Tsoleridis: Synthesis of 2-keto-imidazoles utilizing N-arylamino-substituted NHCs

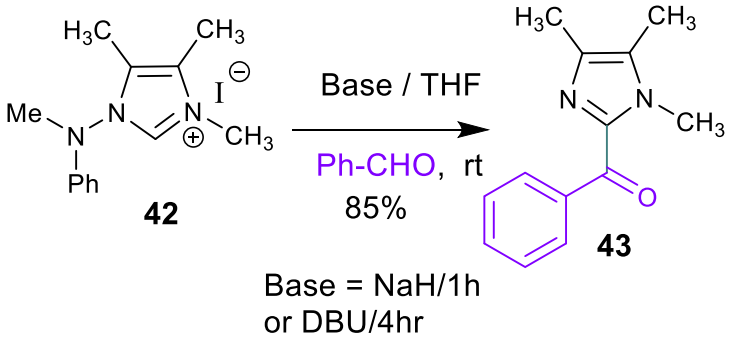

43ac, Y=C_6H_4-Br-4, 94%
43ah, 2-Furyl, 79%
43aj, 3-Thienyl, 72%
43ak, $CH_2CHCHC_6H_5$, 82%
43am, $CH_2CHCHC_6H_5$-Cl, 87%

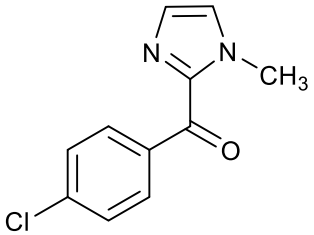

43cf, 92%

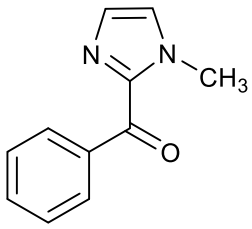

43ca, 90%

Scheme 16: Scope of 2-keto-imidazole formation reaction

Tsoleridis and coworkers[11] developed a synthesis for 2-aroyl, 2-heteroaroyl-, and 2-cinnamoyl-substituted imidazoles. They found they could functionalize C2 of the imidazoles by formation of an NHC and then trapping with an aldehyde. The reaction proceeded smoothly with various substituted aromatic aldehydes and alpha, beta-unsaturated aldehydes. (**Scheme 16**). Additionally, some bisaldehydes were found to undergo the reaction successfully. An ionic mechanism was proposed that goes through Breslow intermediate **45** that is tautomerized to the keto form **46**, followed by loss of the 3-aryl amino group to re aromatize the imidazole and to

generate ketone **47** (**Scheme 17**). Recently, Sunoj[12] and coworkers published a review on Breslow intermediates with computational work showing that a 1,2 hydride shift like what is shown in **44** is too high in energy, and a more likely pathway is a base assisted mechanism.

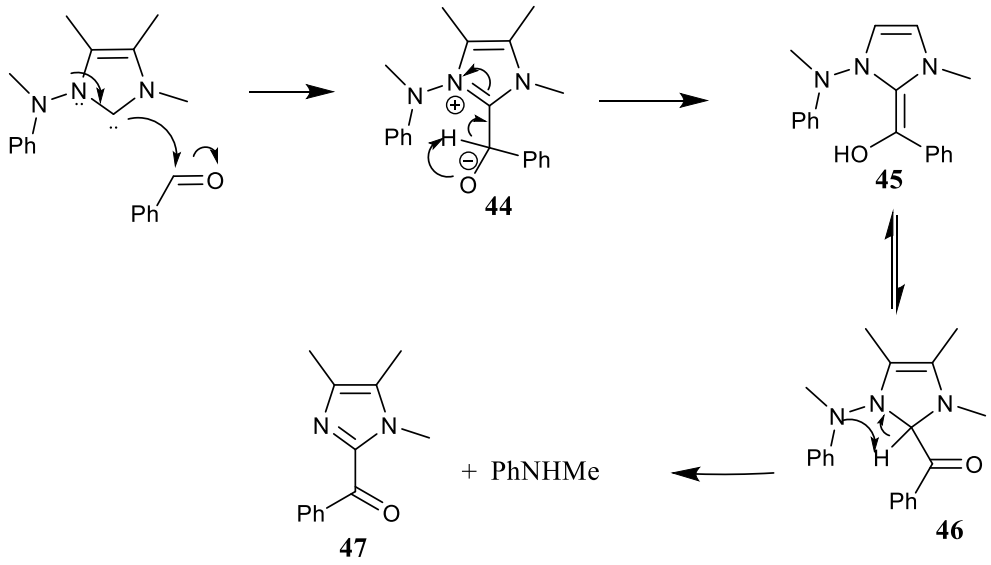

Scheme 17: Tsoleridis proposed mechanism for the 2-keto-imidazoles

Based on this, and our own work, we propose that these 2-keto-imidazoles are being formed by the mechanism shown in **Scheme 18**. Formation of **44** occurs the same way with carbene addition to the electrophilic carbon of the aldehyde, but from there the oxygen is protonated by DBU to form **44a** which is then deprotonated by DBU at the carbon adjacent to the alcohol to give the Breslow intermediate **45**. At this point we propose an N-N homolysis to give **45a**/**45b** which undergoes disproportionation to form **47**.

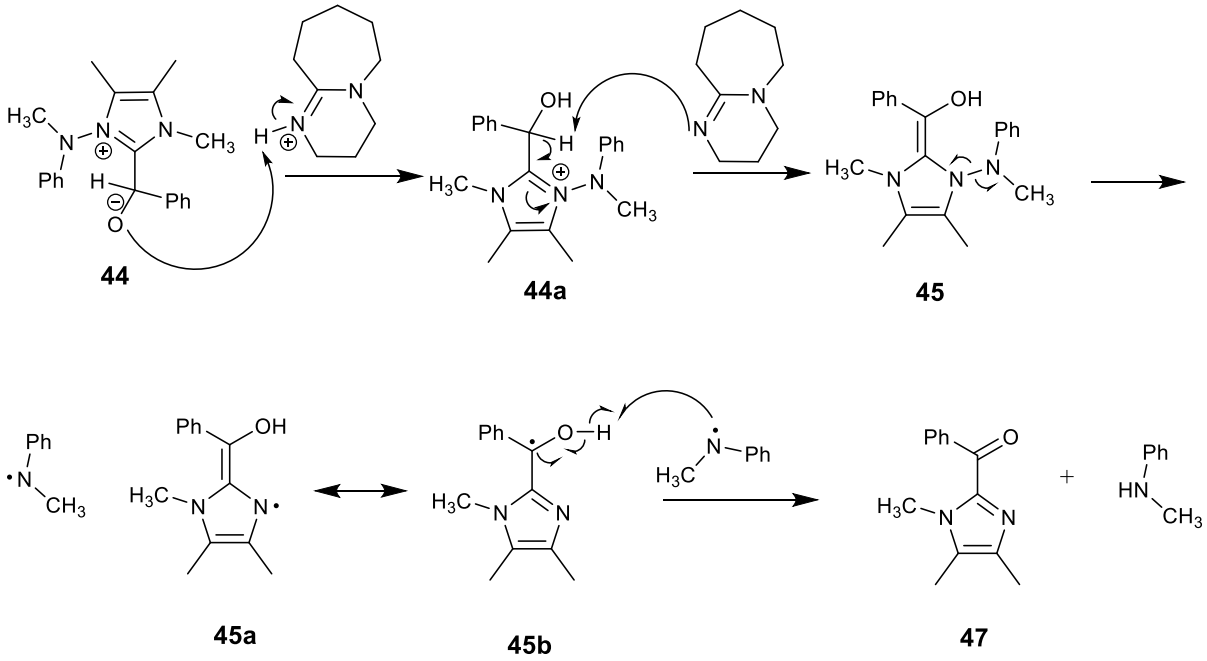

Scheme 18: McIntosh proposed mechanism for 2-keto-imidazoles

1.9 McIntosh: Radical [1,3] rearrangements of Breslow intermediates

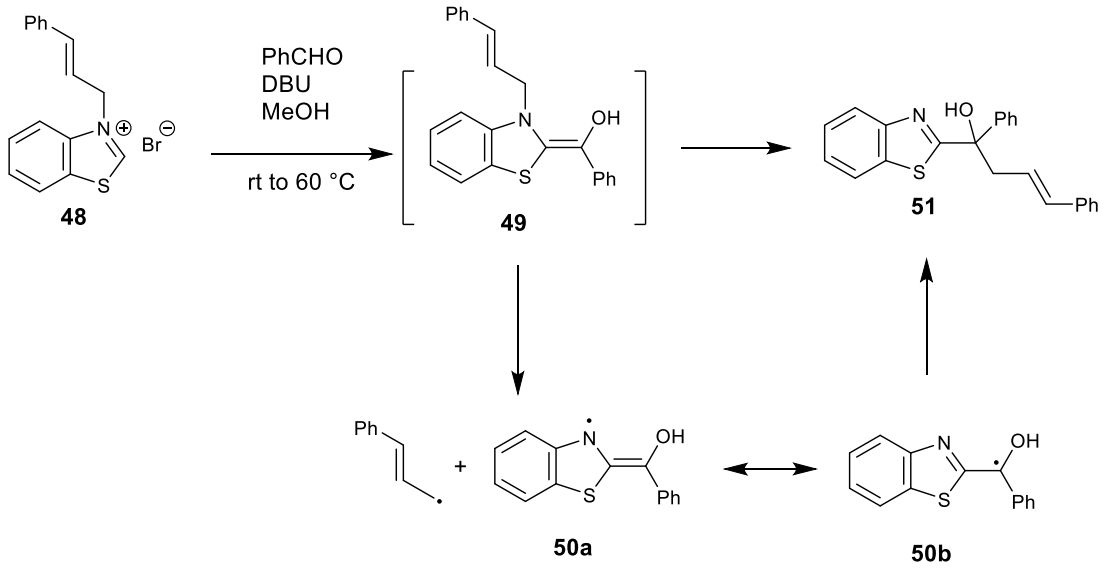

Scheme 19: Proposed radical mechanism

While capturing Breslow intermediates derived from N-allyl benzothiazolium bromide **48** and aromatic aldehydes via a Claisen rearrangement a [1,3] rearrangement product was discovered.[13] The scope of this reaction was investigated with various benzothiazoles and

thiazoles reacting with different aldehydes. The [1,3] rearrangement product **48** was proposed to be formed by a radical mechanism (**Scheme 19**). Upon generation of the Breslow intermediate **49**, the C-N bond could undergo homolysis to form **50a** and then through resonance form **50b** where the radical has moved from the nitrogen to the carbon of the alcohol. Then **50b** can recombine with the N-substituent radical to form the final product **51**. The [1,3] rearrangement product mechanism was supported by DFT calculations that showed a low enthalpy of homolysis for several of the N-substituents on the Breslow intermediates. The enthalpies of homolysis were as low as 6.6 kcal/mol for di-(4-F-phenyl)methyl **53** and only as high as 20 kcal/mol for benzyl. This is consistent with the lab results that showed benzyl being a lower yielding reaction and the di-(4-F-phenyl)methyl reaction (**Figure 4**) proceeding at room temperature. Trapping with 2,2,6,6-tetramethylpiperidine N-oxide (TEMPO) did not provide any isolable products most likely due to the reaction being a highly caged process. Additionally, EPR experiments done on the di-(4-F-phenyl)methyl thiazole with 2-methyl-2-nitrosopropane (MNP) provided hyperfine coupling constants consistent with the trapped radicals (**Figure 4** inset). The proposed radical mechanism is shown in **Figure 4**, with Breslow intermediate **53** undergoing homolysis to give radicals **54** and **54** which if combined with an MNP radical would produce **58** and **60**. This supports our proposed radical mechanism.

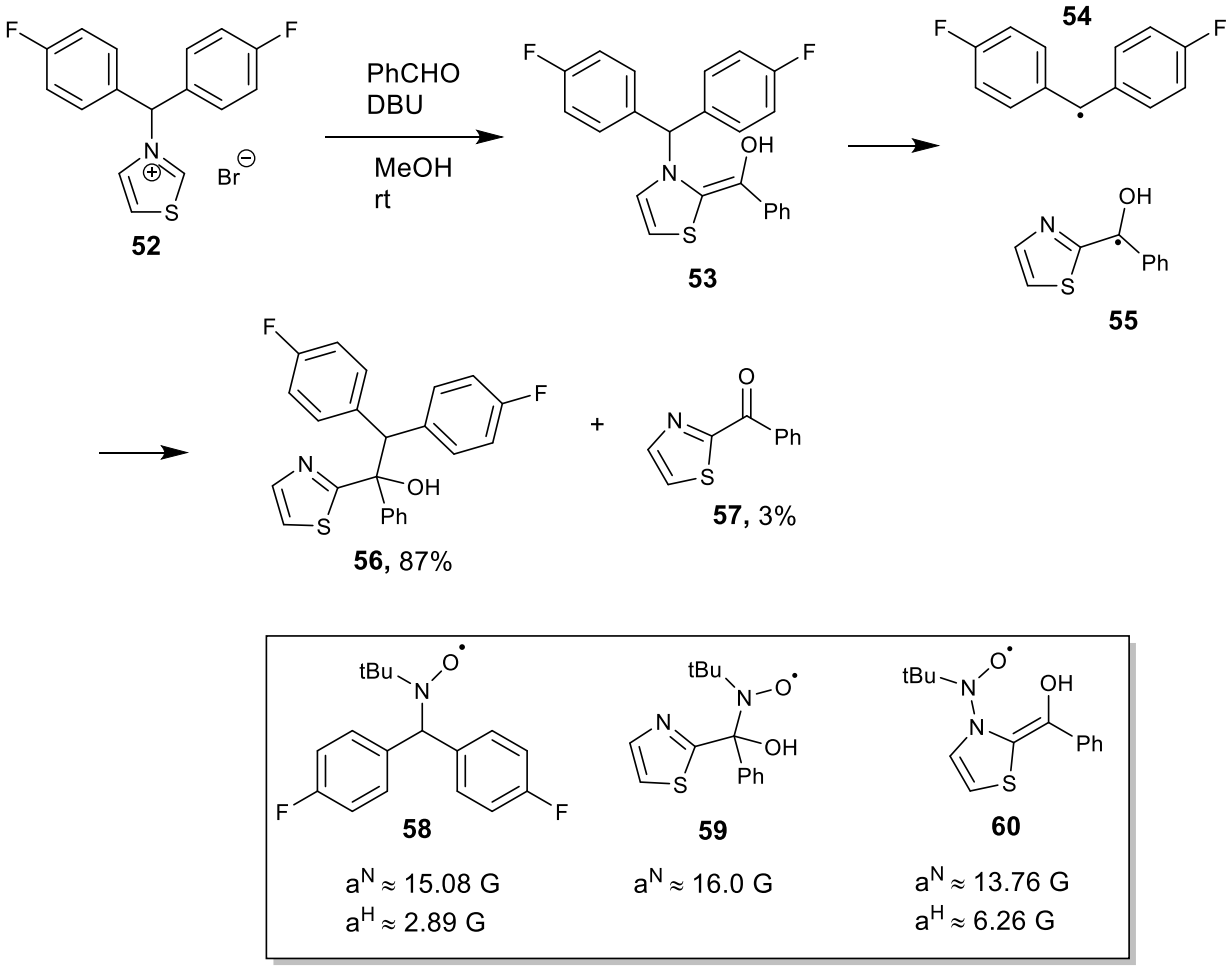

Figure 4: di-(4-F-phenyl)methyl reaction studied with EPR. (inset: EPR trapped radicals)

Chapter 2: Oka Fragmentation of the Breslow Intermediate is a Radical Process

2.1 Introduction

As you may remember from Chapter 1 (**Scheme 19**) the McIntosh group developed a new strategy to form [1,3] rearrangement products from Breslow intermediates. We propose that upon formation of the Breslow intermediates C-N homolysis occurs followed by rearrangement. This type of fragmentation was called the Oka fragmentation, by Kluger who discovered this reaction after Oka first observed this phenomenon discussed in Section 1.2. Thiamine reactions with aldehydes are known to form Breslow intermediates, just like the reactions we do in our lab with azoles. However, it is not known what mechanism Thiamine undergoes under non-enzymatic conditions. We propose that Thiamine shares a common radical mechanism via a Breslow intermediate just as with our azole chemistry (**Figure 5**).

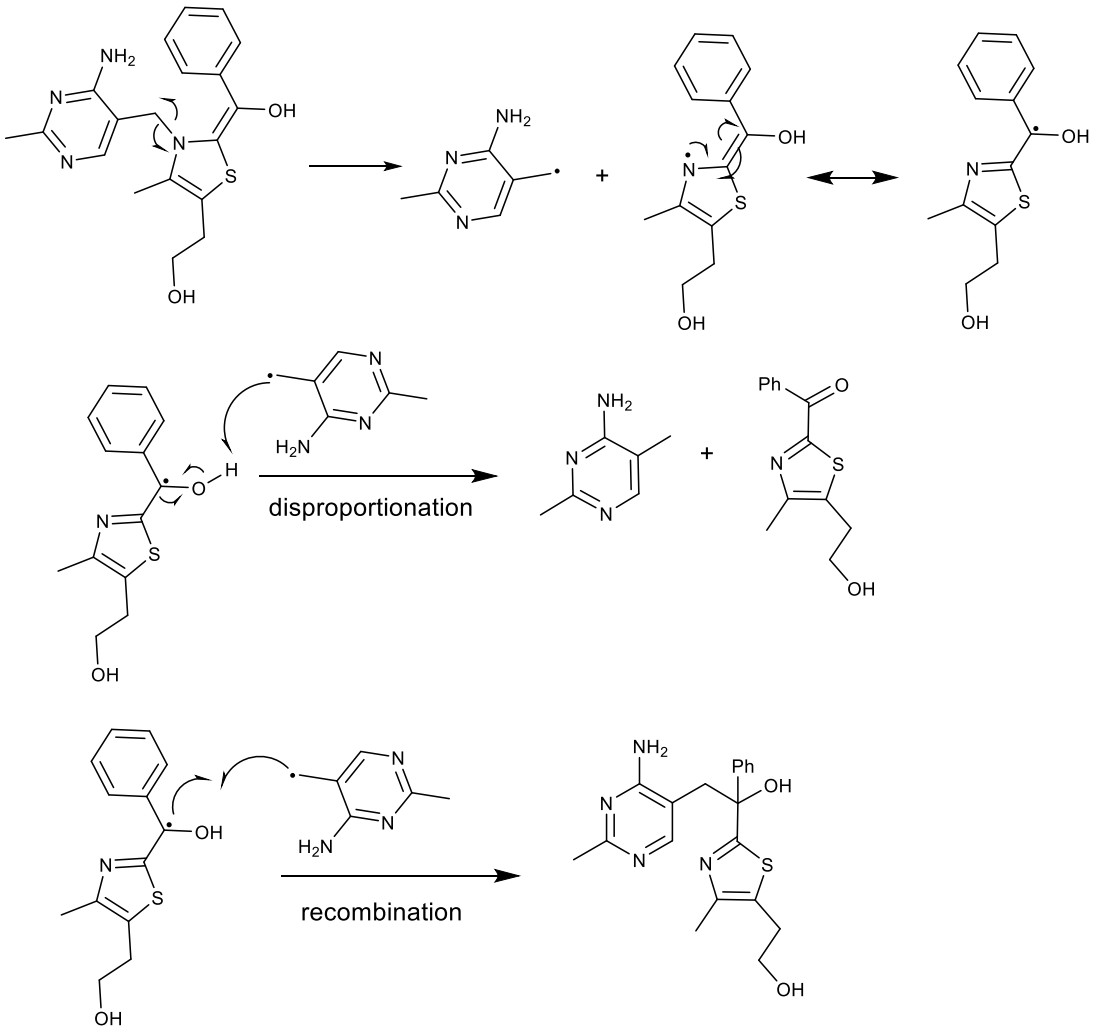

Figure 5: Proposed radical mechanism for products observed by Oka

2.2 Background and Significance

Thiamine (vitamin B1) was first identified and characterized in the 1930s.[14] It is synthesized by plants, bacteria, and fungi, but not animals. Animals do not bio synthesize thiamine and must obtain it from their diet. Thiamine is essential for the carbohydrate, fat, and protein metabolisms in the body. It is active in its phosphorylated forms of which there are five known to date; thiamine mono phosphate, thiamine di phosphate (thiamine pyrophosphate), thiamine triphosphate, adenosine thiamine diphosphate, and adenosine triphosphate. The major biological roles have been attributed to thiamine diphosphate only.[15] Biological systems can be

understood in terms of well-known organic reactions, for example, thiamine serves as a catalyst in decarboxylation to reduce the energy of the transition state in the enzyme. Thiamine in all its active forms is well known as a co factor in pathways such as ethanol fermentation, synthesis of acetyl-CoA, carbon-assimilation reactions, the citric acid cycle, and the pentose phosphate pathway.

2.2.1 The Oka Fragmentation

Thiamine can also be used to catalyze the formation of benzoin from benzaldehyde via the Breslow-intermediate.[16] In 1958 Ronald Breslow proposed an enaminol and an N-heterocyclic carbene as the intermediates in thiamine catalyzed enzymatic pathways. The heterocyclic enaminols came to be called Breslow intermediates. In 1970 Oka et al. reported a cleavage of thiamine and homologs upon reaction with aldehydes in methanol at reflux to give a rearranged alcohol along with ketone and pyrimidine products which would result from cleavage of the benzylic C-N bond (vide supra) as well as the expected benzoin product. This indicated that thiamine served as a benzoin catalyst but ultimately underwent fragmentation to an inactive form.

2.2.2 Kluger's Studies

Kluger et al. have studied thiamine and its reactions for many years.[17–20] They rediscovered the thiamine decomposition first reported by Oka and named it the Oka fragmentation. They noted that enzymes produce Breslow intermediates that do not fragment, and this process is competitive in the enzyme with the pathway that preserves the co factor and involves no fragmentation or rearrangement. They reported that the fragmentation products occurred in solutions with an alkaline pH, while no fragmentation occurred in acidic solutions.[21] Interestingly, they only recently reported the isolation of the rearrangement

product. Over the years, Kluger et al proposed several variations on an anionic polar mechanism[22] for the fragmentation leading to the products observed by our own group (**Scheme 20**). While we are confident that that Oka fragmentation in fact proceeds via a radical pathway (vide infra), Kluger's postulate led us to investigate whether the enolate version of the Breslow intermediate would be more prone to undergo fragmentation (**Scheme 20**).

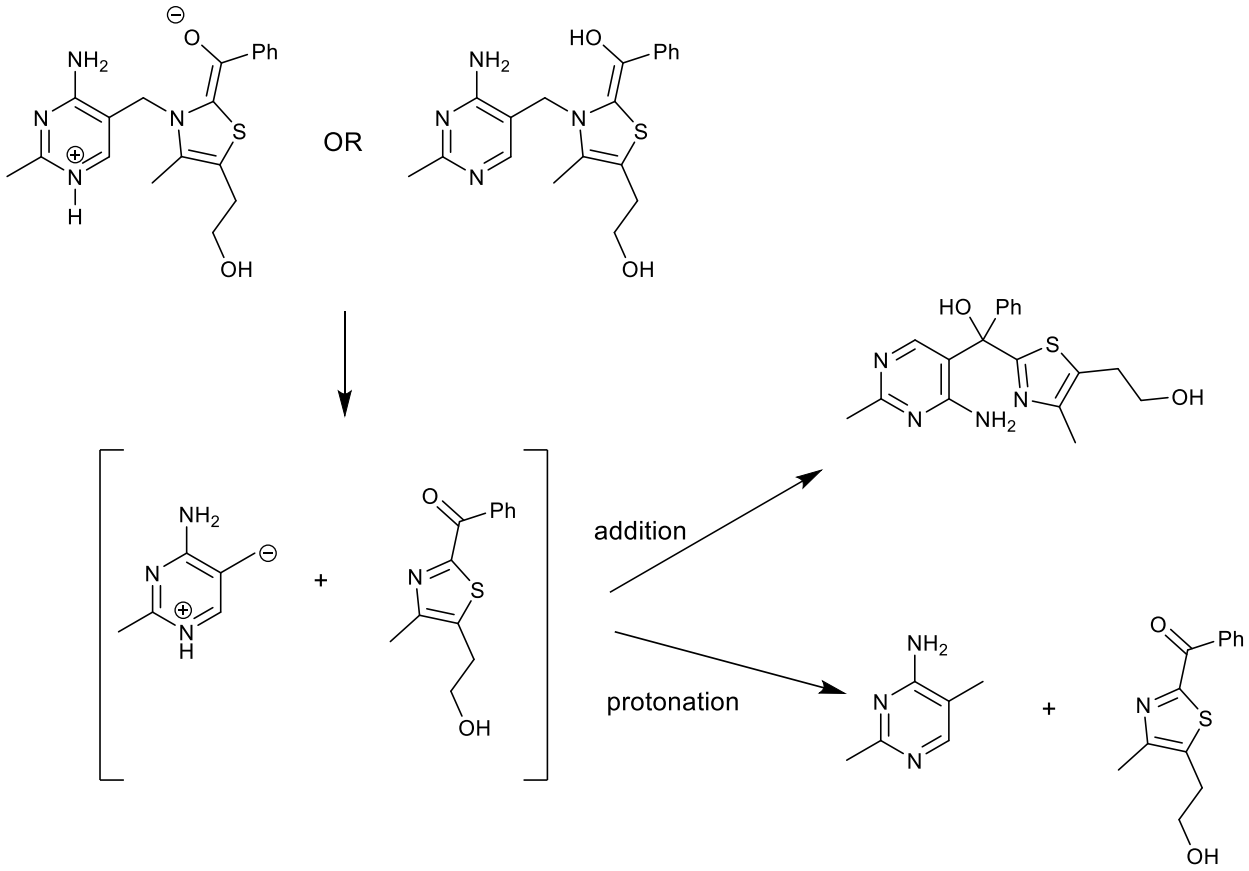

Scheme 20: Kluger's recently proposed ionic mechanism

2.3 Reaction Optimization and Scope

Several N-substituted benzothiazole and thiazole salts were synthesized to make the ketones for rearrangement (**Table 1**). Benzothiazole salts were prepared in the usual way to give generally high yields.

Table 1: Benzothiazole reaction scope with different alkyl halides

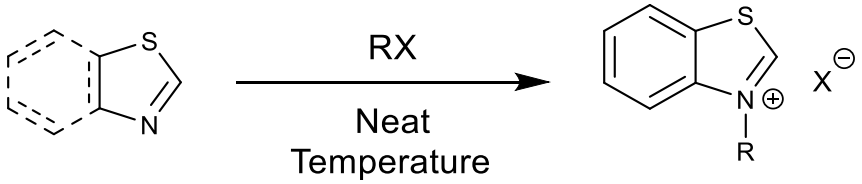

Entry	Azole	RX	Temperature °C	% Yield
1	Benzothiazole	Benzyl Bromide	60	92
2	Benzothiazole	Cinnamyl Bromide	60	78
3	Benzothiazole	Bromodiphenylmethane	65	85
4	Benzothiazole	2-bromopropane	120	88
5*	Benzothiazole	Iodomethane	70	90
6	Benzothiazole	9-bromofluorene	85	68
7	Thiazole	Benzyl Bromide	70	100
8	Thiazole	Cinnamyl Bromide	60	100
9	Thiazole	Iodomethane	60	100
10	Thiazole	Bromodiphenylmethane	50	98

*Reaction done in acetonitrile

N-Benzylbenzothiazolium ketone was chosen as a model substrate to optimize the reaction conditions due to it being easily prepared via commercially available starting materials. The benzyl group on the nitrogen was chosen as the radical stabilizing group. The best solvent screened was DMSO with the other solvents resulting in no product or biproducts (**Table 2**). The optimum base was LHMDS which gave the cleanest reaction with the best yield at one hour (entry 5). This is consistent with computations by DFT that show the lithium enolate as the lowest energy when compared to other cations or even the bare enolate. The reaction was subjected to catalytic amounts of base to determine if it was catalytic, but the reaction was not successful when catalytic amounts of base was used (entry 6). Oxygen did not hinder the reaction since degassing had no effect on the yield (entry 7). A weaker base (DBU) did not provide any of the desired product and changing the solvent to DMPU did not offer any increase in yield or decrease in biproducts.

Table 2: Reaction optimization for enolate rearrangement

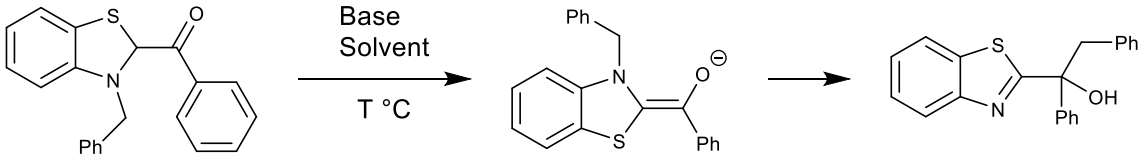

Entry	Base	Solvent	Temperature °C	Time	Yield
1	LHMDS	THF	-78-rt	1-7 h	0-6%
2	KOtBu	THF	-78-rt	1-7 h	0-6%
3	LHMDS	DMSO	rt	5 min	35-38%
4	KOtBu	THF	rt	5 min	35-38 %
5	LHMDS	DMSO	rt	1 h	51-80%
6	LHMDS**	DMSO	rt	19 h	0%
7	LHMDS*	DMSO	rt	5 min	36%
8	LHMDS	DMSO/THF	rt	1 h	0%
9	DBU	DMSO	rt	1 h	0%
10	KHMDS	DMSO	rt	1 h	0%
11	LHMDS	DMPU	rt	1 h	0%
12	LHMDS*	DMPU	rt	1 h	0%

* reactions were degassed, **reaction uses 0.2 equivalents of base and degassed

Table 3: Ketone formation with different Nitrogen substituents

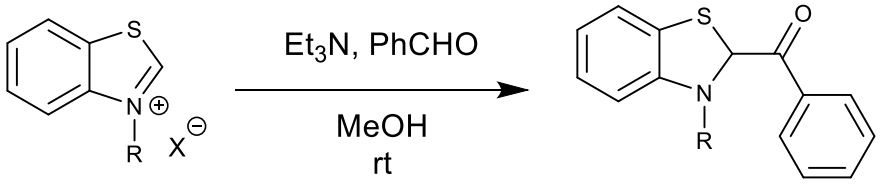

Entry	R	% Yield
1	Benzyl	91
2	Diphenyl methyl	15
3	Cinnamyl	24
4*	Methyl	10
5*	Isopropyl	22
6**	Fluourene	22

*Reactions carried out at 70 °C, **Methyl formyl-4-benzoate used as aldehyde

After successful synthesis of the thiazole salts, the scope of the ketone formation from the salts was investigated (**Table 3**). The benzyl salt gave the best yield of the ketone (entry 1) with all other analogs giving significantly less ketone product. Cinnamyl, isopropyl, and methyl were the next best with 24, 22, and 22, percent yield, respectively. The methyl ketone was only able to be synthesized with a 10% yield even with heat (entry 4). It is unclear why they yield for entry 4 was not higher.

Table 4: Scope of the enolate rearrangement reaction

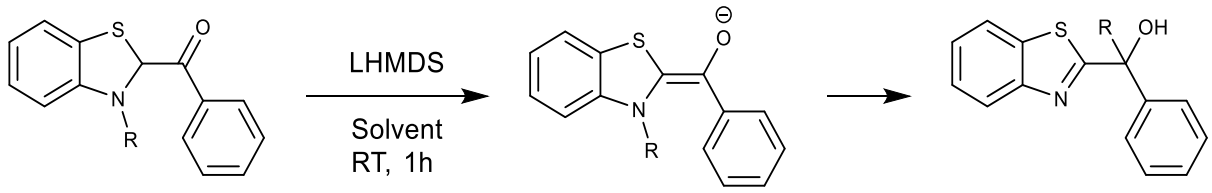

Entry	Solvent	R	Yield
1	DMSO	Fluorene	0%
2	DMSO	Cinnamyl	6-15%
3	DMSO	Diphenyl	0%
4*	DMSO	Methyl	0%
5	DMSO	Methyl	(3)
6	DMSO	Isopropyl	(3)
7	DMPU	Isopropyl	(3)
8	THF	Isopropyl	0%

*RT-45°C

With the optimized conditions in hand the scope was examined by varying groups on the nitrogen for enolate rearrangement (**Table 4**). The only other substrate to give rearrangement product under the optimized conditions was cinnamyl (entry 2). The other benzothiazolium salts gave no product or biproduct even when changing the temperature or solvent (entry 4 and 8). Thiazole ketones were synthesized, to attempt to expand the scope but unfortunately gave none of the desired ketone product **(Table 5**). In addition to the limited scope the ketones that were synthesized were not high yielding. In comparison to the previously used conditions for

rearrangement (vide supra) the enolate conditions are completed at ambient temperature and in a shorter time (7 days vs 1 hour). There were no fragmentation products observed in these reactions which is further evidence that this is radical and not ionic as suggested by Kluger. Based on these observations it seems that an enolate intermediate in the rearrangement is a viable reaction pathway, but the conditions were not applicable to a broad range of reactants (**Figure 6**). However, this still supports the hypothesis that electron rich systems are more prone to homolysis.

Table 5: Thiazole ketone formation scope

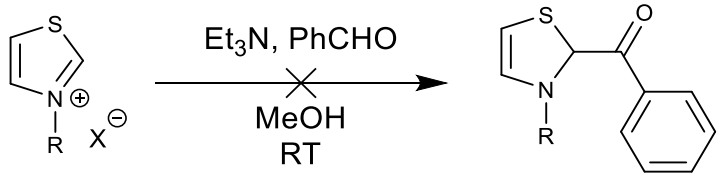

Entry	R	Product
1	Benzyl	None
2	Diphenyl methyl	Benzoin
3	Cinnamyl	Benzoin
4	Methyl	Benzoin

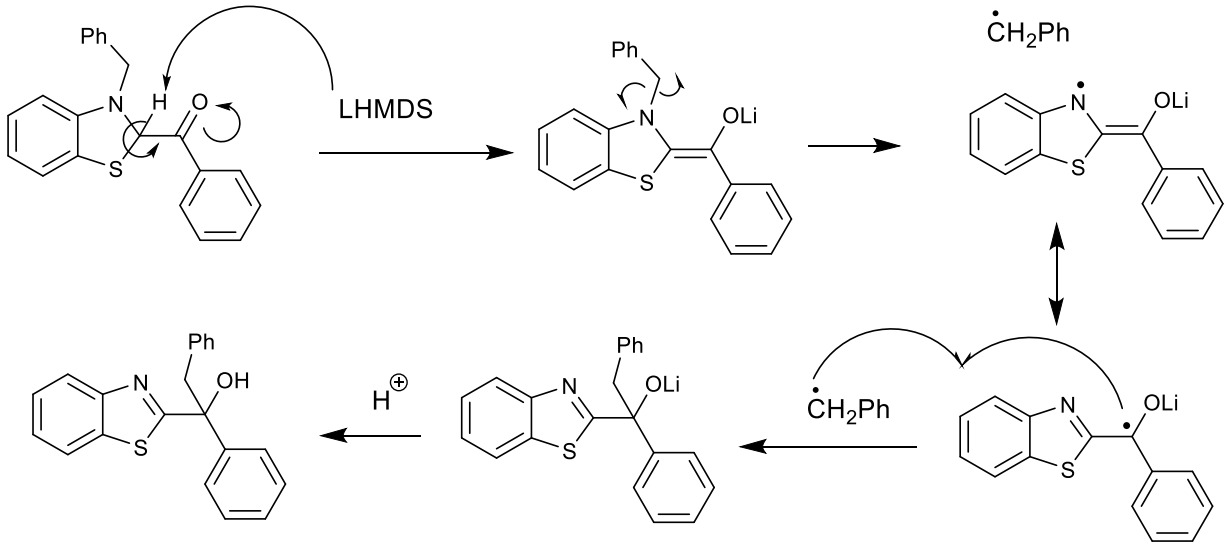

Figure 6: Proposed Radical mechanism

2.3.1 Mechanistic studies

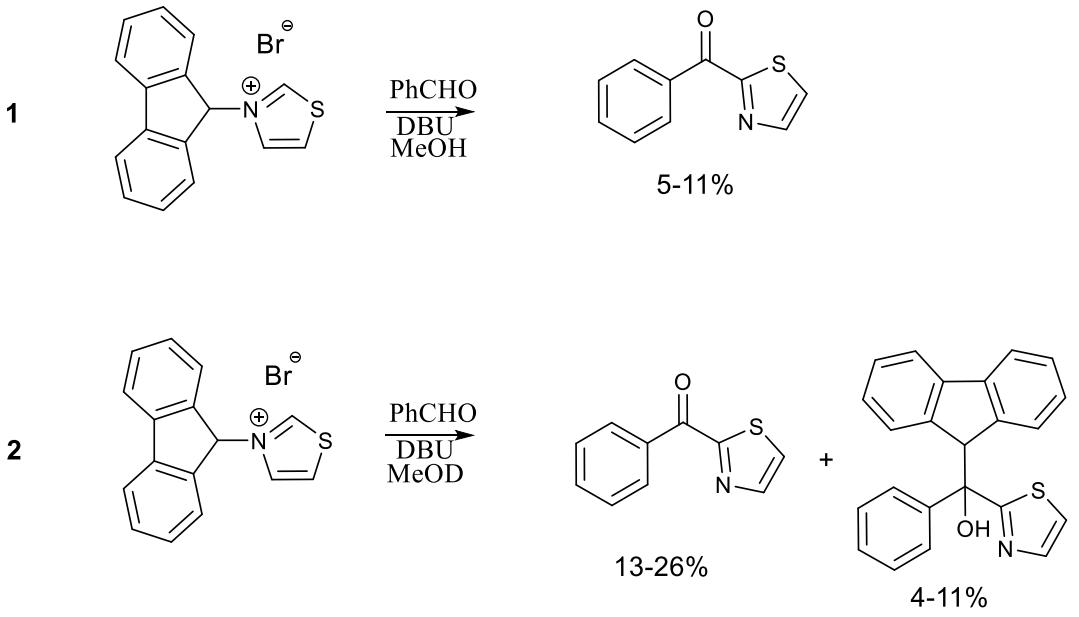

Figure 7: Deuterium exchange experiment: (**1**) in Methanol and (**2**) in Methanol-d1

If our proposed radical mechanism were correct, exchanging a hydrogen on the Breslow intermediate oxygen with a deuterium should result in a slower disproportionation relative to combination since deuterium atom abstraction would be expected to be slower. We tested this by comparing two reactions, one in methanol and one in methanol-d1 (**Figure 7**). Both reactions were run at the same temperature and under the same conditions. The result was that the reaction performed in methanol contained only disproportionation product, while the reaction performed in methanol-d1 reactions yielded both recombination and disproportionation. This supports that the deuterated solvent slowed down the formation of the disproportionation product, allowing the recombination product to appear (**Figure 8**). These results were confirmed by LC/MS. The results have the opposite k_d/k_c result gained by other lab members and needs to be explored further (Taylor Burnett Thesis).

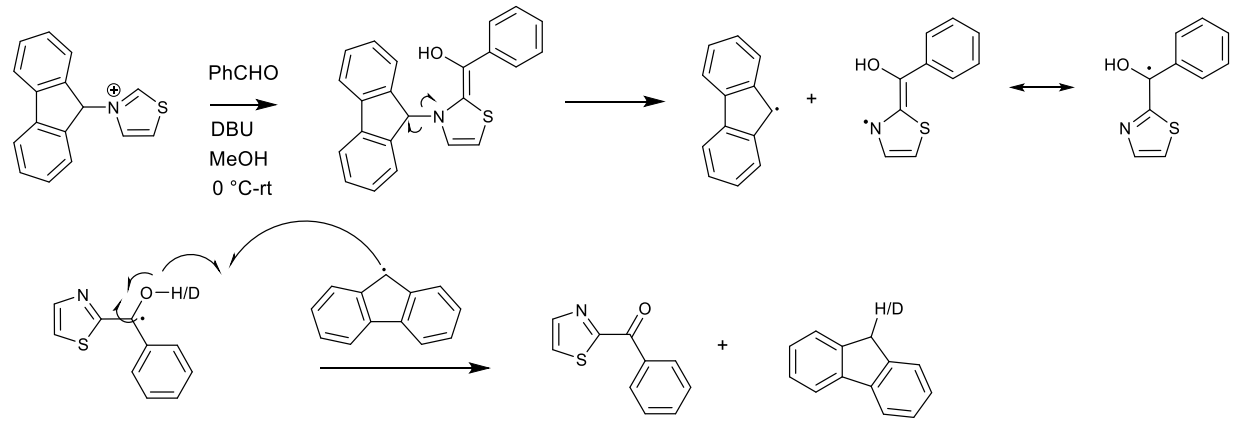

Figure 8: Proposed radical mechanism with hydrogen or deuterium

DFT calculations in water using b3lyp-631g* show that the change in energy from the Breslow intermediate of thiamine **54** to the radical fragmentation products is +16.6 kcal/mol, whereas the same difference in energy for the anionic polar mechanism proposed is +53.8 kcal/mol. Additionally, the proposed tautomer **55** of the Breslow like structure is +19.4 kcal/mol energy higher than the normal Breslow intermediate of thiamine **54** (**Figure 9**).

In addition to these calculations, Oka's reported procedure was repeated and his results were confirmed reproducible. I also subjected Thiamine to Oka's conditions using methanol-d1 to see if there would be any changes in the product ratios (**Scheme 21**). Unfortunately, the deuterated methanol reaction did not provide any conclusive results. More work needs to be done to determine why nothing conclusive came from this reaction.

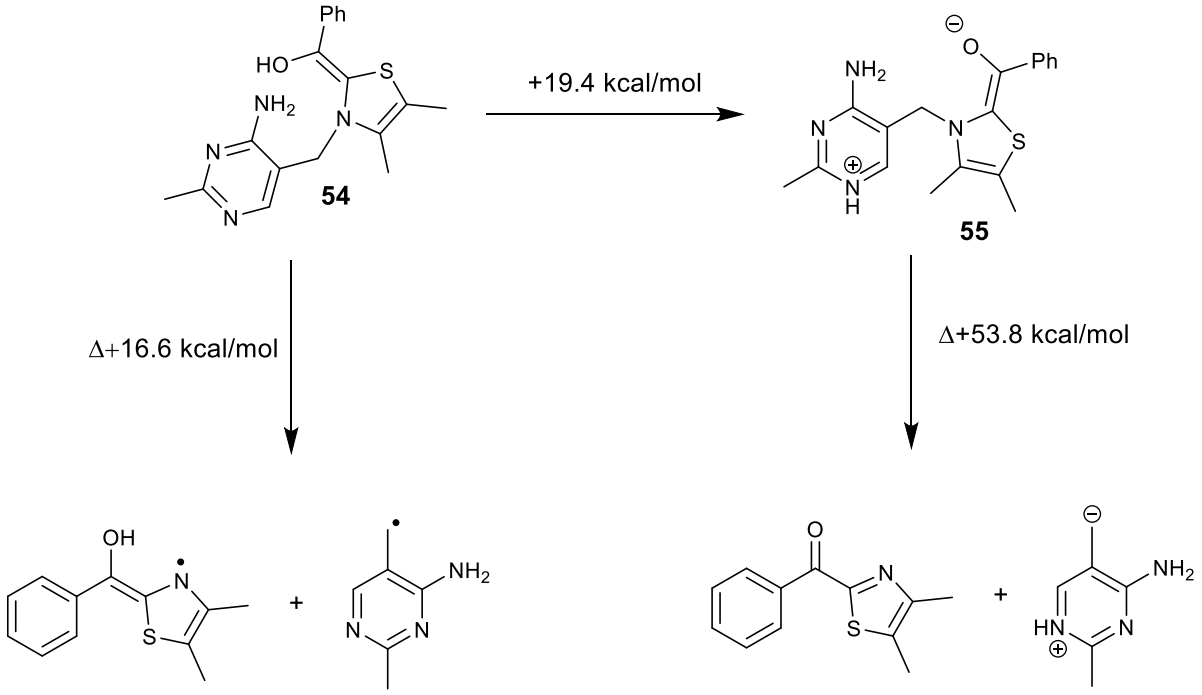

Figure 9: Homolysis enthalpies for the thiamine enol and enol

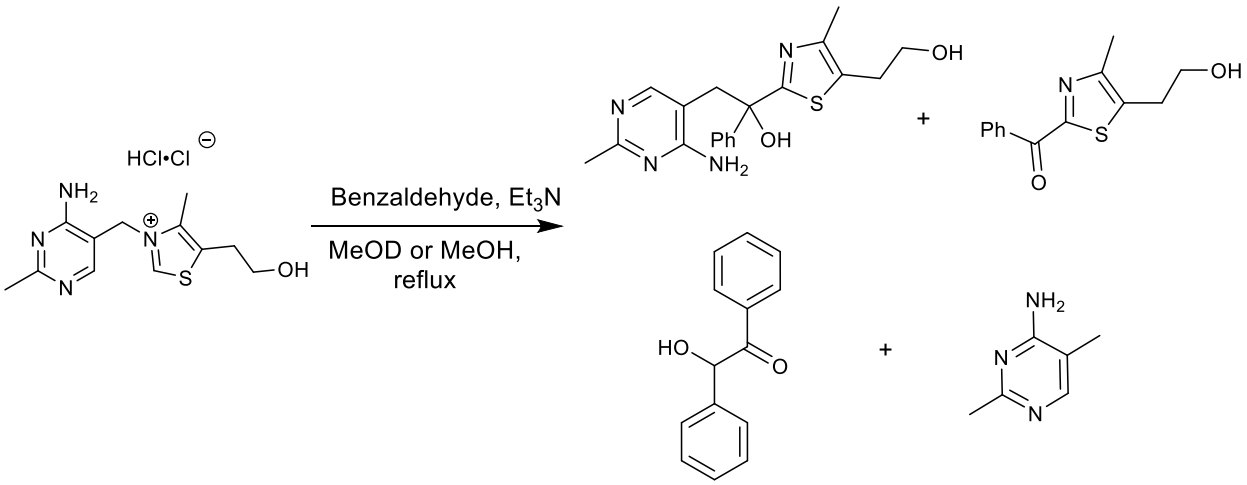

Scheme 21: Oka's procedure in methanol or methanol-d1

2.3.2 DFT Calculations

To predict what substrates would undergo homolysis, we looked at the effect of different R groups on the thiazole and calculated the energy of homolysis versus the HOMO energy (**Scheme 22**). The 4 position did not seem to show any trend in the electron richness of the R group and the energy of homolysis versus the HOMO energy, so we investigated the 5 position. This looked promising until further R groups were added (**Figure 10**).

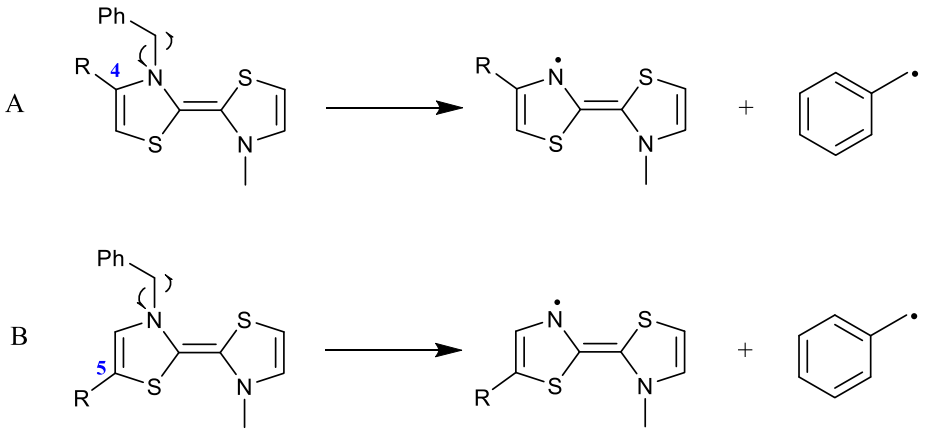

Scheme 22: Homolysis with substitution at the 4 (A) or 5 (B) positions

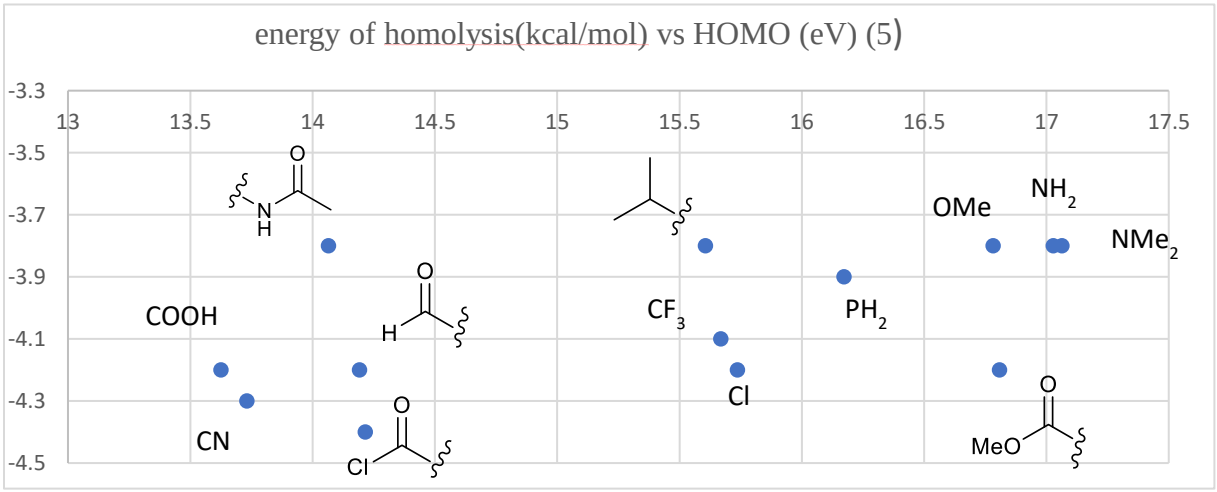

Figure 10: Energy of homolysis (kcal/mol) plotted versus the HOMO (eV)

The next attempt at predicting homolysis was the energy of homolysis versus the energy of electron transfer. This showed somewhat of a trend but fell apart with more groups added just like the previous attempt. This resulted in a new approach which was to look at the electrostatic charge on the atoms involved in the homolysis. The idea was that if the mechanism were radical

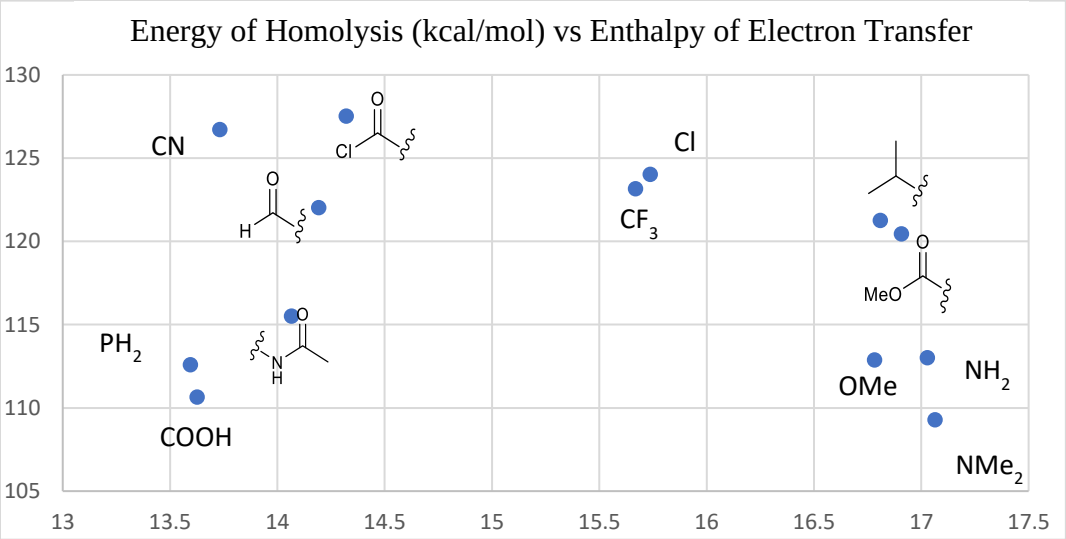

Figure 11: Energy of homolysis (kcal/mol) versus the enthalpy of electron transfer

there would be little to no charge on the atoms in the homolysis, whereas if the mechanism were ionic, you would see a charge

Our next attempt at predicting homolysis involved the same R groups, but this time comparing the energy of homolysis to the enthalpy of electron transfer (**Figure 11**). This like the previous attempt did not show any specific trend in the electron withdrawing or electron donating ability of the R groups.

The next hypothesis was that if we calculated the electrostatic charge of each of the red Carbons and Nitrogen's for the radical pathway and the ionic pathway and compared both to the electrostatic charge if you stretch the bond by 1 Angstrom, the difference could tell us if one was favored (**Figure 12**). If the difference between the radical electrostatic charge and the stretched

bond were small that would indicate the stretched bond most likely going by a radical mechanism as opposed to an ionic one. There was a small difference between the radical and the stretched bond electrostatic charges, supporting our radical mechanism **(Figure 13)**.

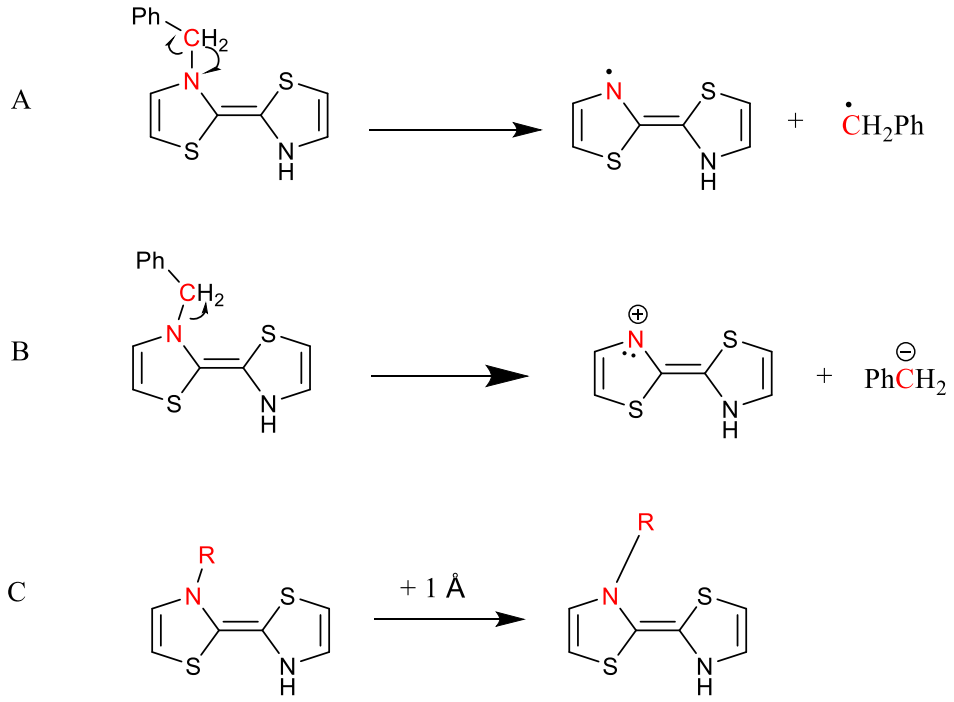

Figure 12: (A) homolysis of equilibrium C-N bond. (B) Ionic breaking of C-N bond. (C) Stretched C-N bond homolysis

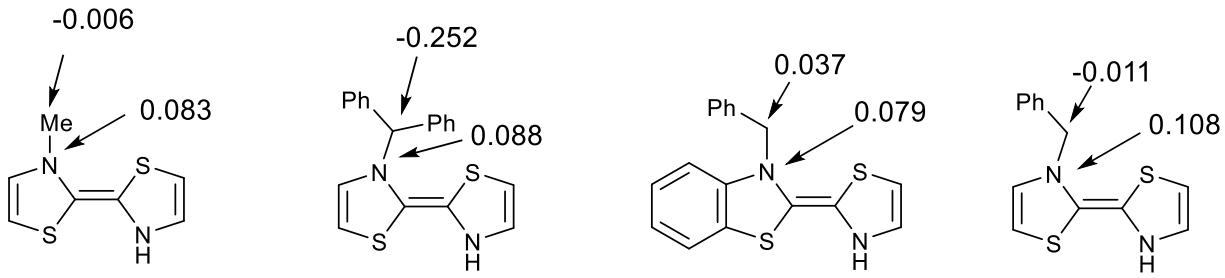

Figure 13: Calculated electrostatic charges for carbon and nitrogen for various N-substituents

Chapter 3: Synthesis of Pyridine analogs by C-N sigma bond homolysis and recombination

3.1 Introduction

Only a few examples of low temperature C-N homolysis have been discussed in Chapter 1 (vide supra). Beyond those examples there are very few in the literature. Yet, substituted pyridines can form Breslow-like intermediates or enamines that serve as electron rich alkenes and could undergo rearrangement. This represents an underexplored area that could be exploited to undergo the same [1,3] rearrangement reaction.

3.2 Background and significance

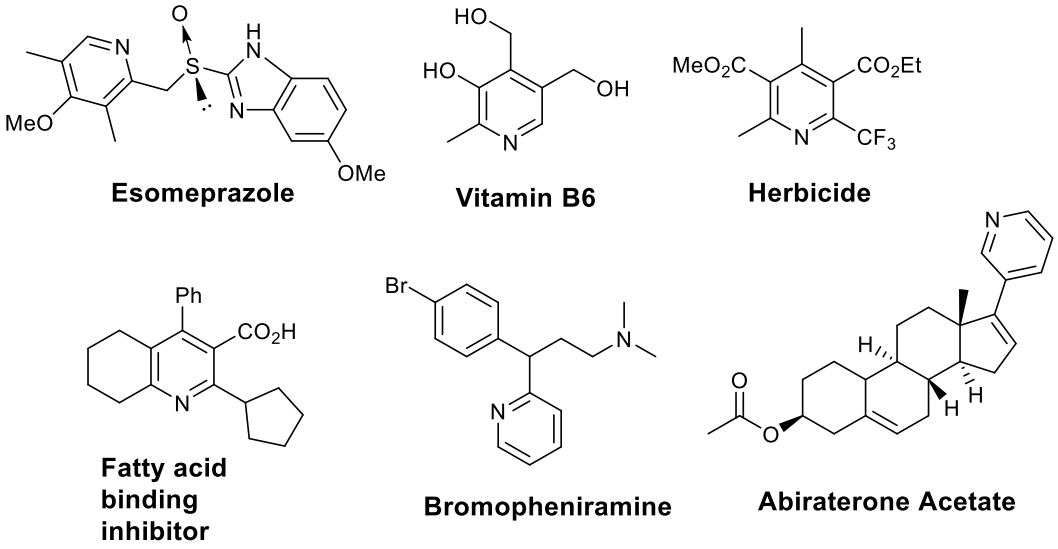

Figure 14: Selected examples of pyridine applications

Pyridine motifs are found in many biologically active molecules.[23] Pyridines are the most commonly used aromatic heterocycle among the FDA approved pharmaceuticals with most of them being C2 substituted.[24] Some of the classes of drugs containing pyridines include antihistamines such as bromopheniramine, anti-cancer drugs like the prostate cancer treatment prodrug abiraterone acetate, vitamin B6, proton pump inhibitors that treat excess stomach acid

(Esomeprazole), fatty acid binding inhibitors, and herbicides (**Figure 14**). Substituted pyridines are generally synthesized via Grignards,[25] alkyl lithiums,[26,27] using transition metal catalysts[28] or from the N-oxide by using boryl alkanes.[29] These often employ harsh conditions and cryogenic temperatures (**Figure 15**).

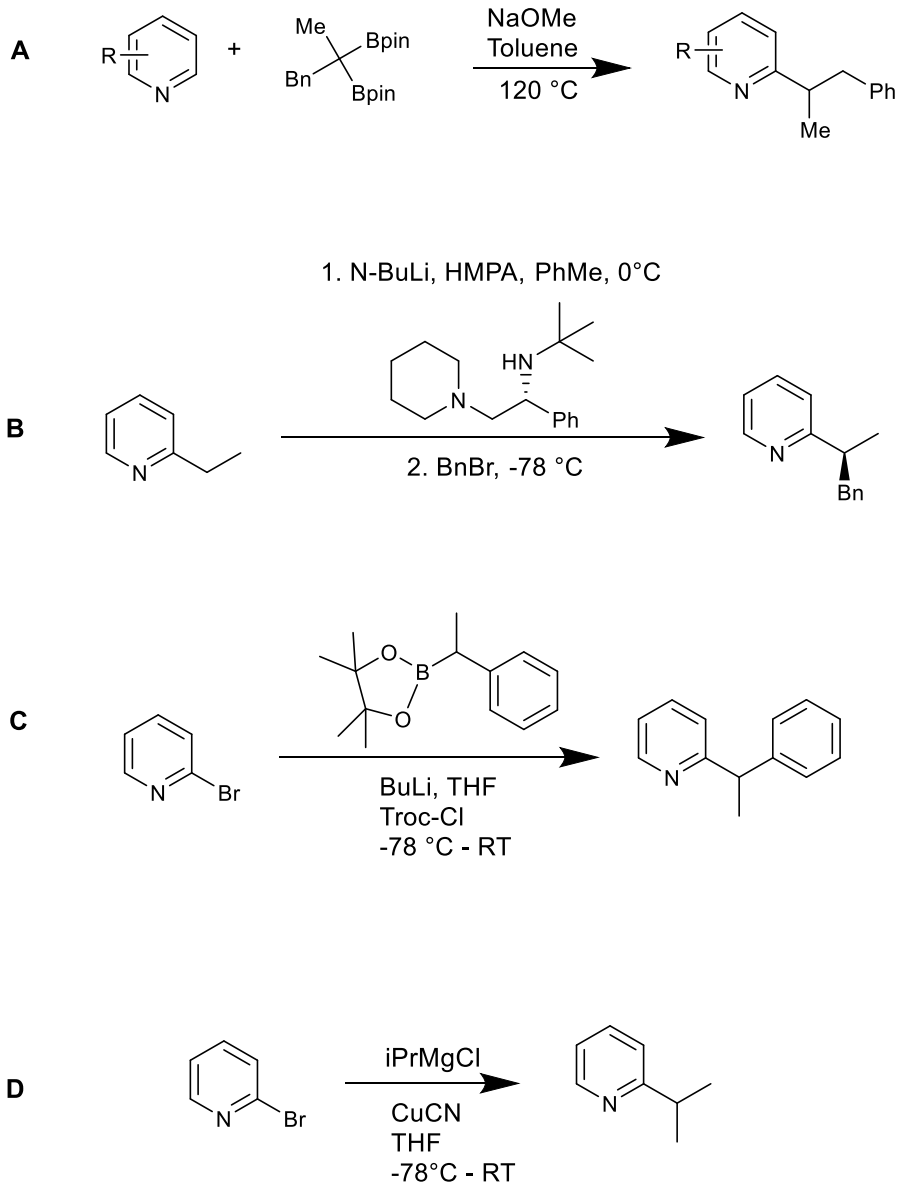

Figure 15: Different examples of how to make 2-substituted pyridines

3.3 Results and discussion

Table 6: Enamine optimization

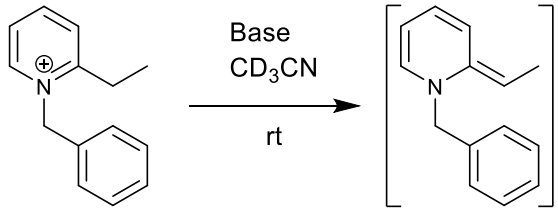

Base	Enamine
DBU	No
K_2CO_3	No
NaH	Yes

Given that an enamine is an electron rich double bond, just like a Breslow intermediate, we wanted to see if the same type of rearrangement could occur. Computations showed that the homolysis of the C-N bond after enamine formation (**Table 6**) was +29 kcal/mol. This is higher than previously published Breslow intermediate rearrangements by about 16 kcal/mol. The higher enthalpy of homolysis made the possibility of observing the enamine intermediate by NMR a possibility, since this reaction would need a higher temperature in order to rearrange. Based on the computational evidence we decided to pursue this reaction to potentially expend the scope of motifs that undergo [1,3] rearrangements, and determine if the enamine could be observed in situ.

N-benzyl alkylated 2-ethyl pyridine was chosen as a model substrate to optimize the reaction conditions. Benzyl is a well-known radical stabilizing group and therefore was an appropriate choice to start the alkyl isopyridine homolysis optimization. The enamine needs to be formed first before any rearrangement could occur. Sodium hydride turned out to work the best with the enamine forming in 30 minutes, while the other bases did not result in any formation even with heat (**Table 6**). Once the enamine could be formed, we looked at optimizing the rearrangement

(**Table 7**). Lower temperatures did not generate any rearrangement product, so higher boiling solvents such as like DMF and Toluene were used. Toluene produced the product but only in modest yield (entries 3-5), while DMF gave a much higher yield of 35% at 4 hours (entry 7). Increasing the reaction scale to 0.5 g (of salt) did not cause a decrease in yield (entry 8). Oxygen seemed to inhibit the reaction because degassing improved the yield (entry 9 vs 10). The optimized conditions seemed to be 16 hours and degassed giving the best yield of 56% (entry 10).

Table 7: Pyridine rearrangement optimization

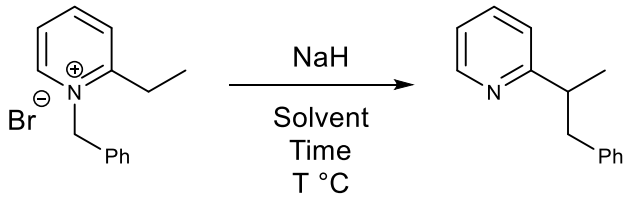

Entry	Solvent	T (°C)	Time (h)	Degassed	Yield (%)
1	MeCN	65	5 h	No	0%
2	MeCN	100	0.5 h	“	0%
3	Toluene	165	1 h	“	Trace
4	Toluene	165	4 h	“	12%
5*	Toluene	165	4 h	“	11%
6	DMF	165	1 h	“	Trace
7	DMF	165	4 h	“	35%
8**	DMF	165	4 h	“	48%
9	DMF	165	16 h	“	14%
10	DMF	165	16 h	Yes	56%

*different workup. **0.5g scale

With the optimized reaction conditions, many salts were synthesized using a previously published procedure[30] to expand the scope of the rearrangement (**Figure 16**). Many functional groups were tolerated in the salt formation, including halogens, nitro substituents, aromatics and heteroatomatics. Both ortho and para substitution on the aromatic ring was tolerated. Many different N-heterocycles were functionalized, including pyridine, pyrazine (**56j**), methyl

pyridines (**56i, 56k, 56p**), tetrahydroquinoline (**56z**), and ones with unprotected alcohols (**56o, 56x, 56ab**) with modest to good yields.

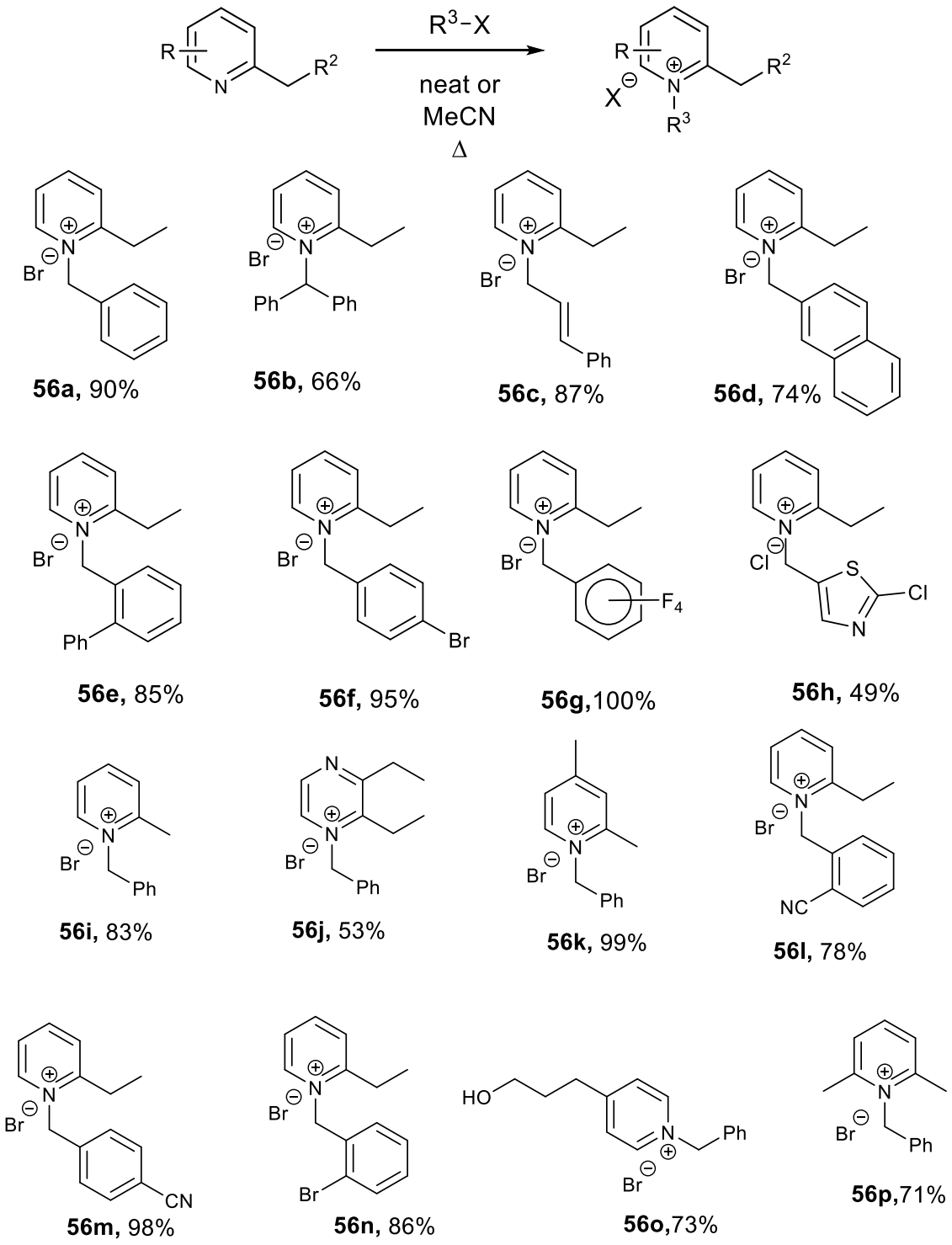

Figure 16: Scope of salt formation

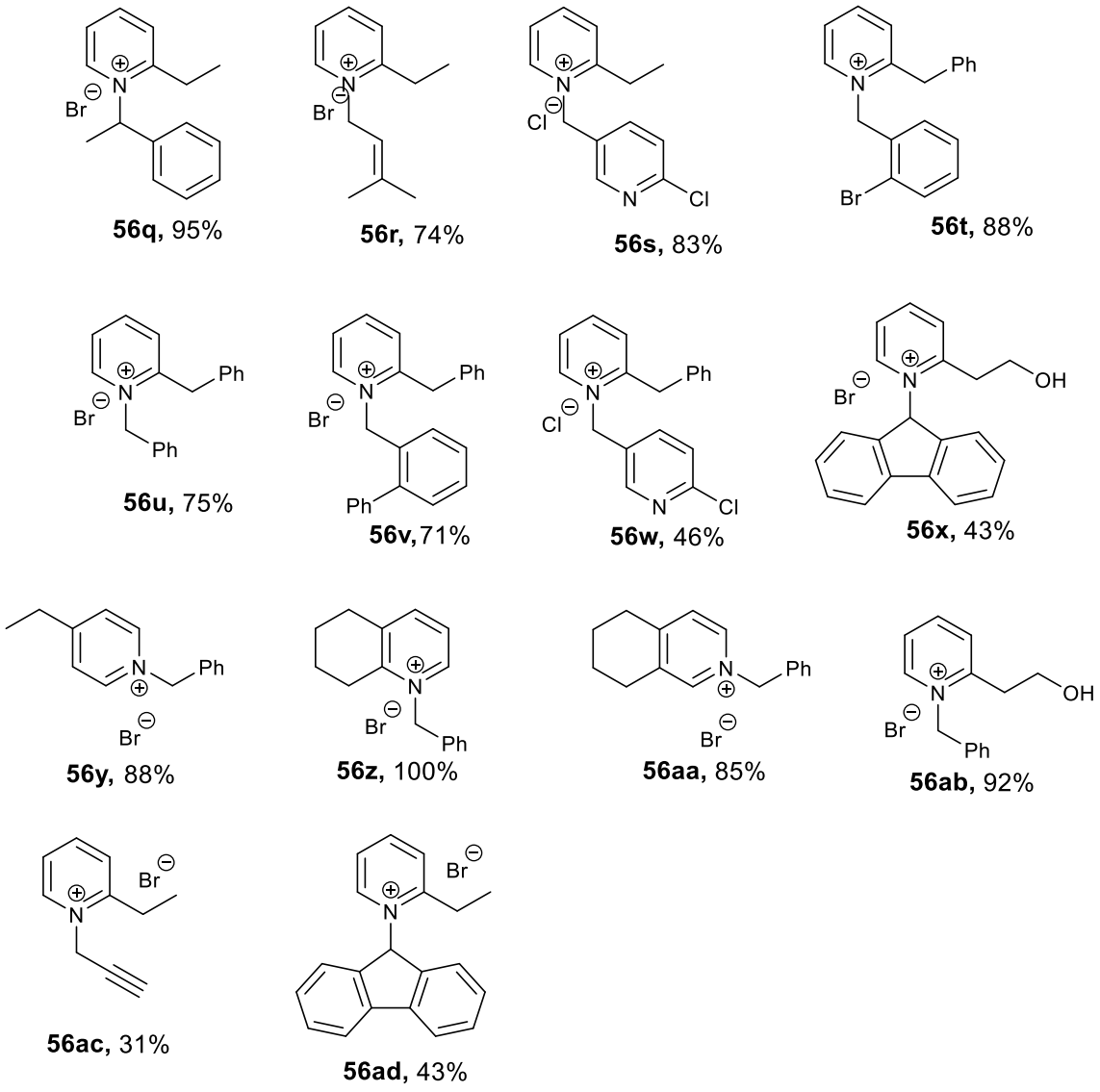

Figure 16 Cont.: Scope of salt formation

Next, the scope of the enamine formation was examined since the enamine is the intermediate precursor to the rearrangement (**Table 8**). Sodium hydride in deuterated acetonitrile was used to observe the enamines in situ by proton NMR. Some substrates required the addition of DBU (1 equivalent) and the sodium hydride for the enamine to form completely in a reasonable amount of time. Some substrates did not exhibit any enamine formation by 1H-NMR analysis even with

the addition of the additive. The N-fluorenyl structures have acidic protons at C9 of the fluorene, which potentially interfered with the formation of the enamine since deprotonation at C9 would result in an ylide and none of the desired enamine precursor (**56x, 56ad**). Oddly, the N-propargyl structure showed nothing interpretable in the 1H-NMR and subjecting the reaction to the rearrangement conditions did not result in any product (**56ac**). The N-cinnamyl salt did not form an enamine, but instead the benzylic position next to the Nitrogen was deprotonated to form the ylide (**56c**). The N-cinnamyl ylide was purified from the crude reaction mixture and identified by 1H-NMR.

Table 8: Enamine formed with 2-ethylpyridines

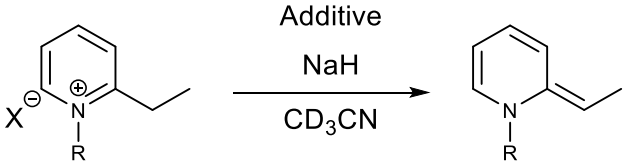

Entry	R	Additive
1	Benzyl	
2	Diphenyl methyl	
3	(2-napthyl)benzyl	
4	4-bromobenzyl	
5	dimethylallyl	
6	2-phenylbenzyl	
7	alpha-methylbenzyl	DBU
8	2-chlorothiazole	DBU
9	pentafluorobenzyl	DBU
10	2-cyanobenzyl	DBU
11	4-cyanobenzyl	DBU
12	2-bromobenzyl	

Table 9: Rearrangement reaction scope with 2-ethyl pyridines

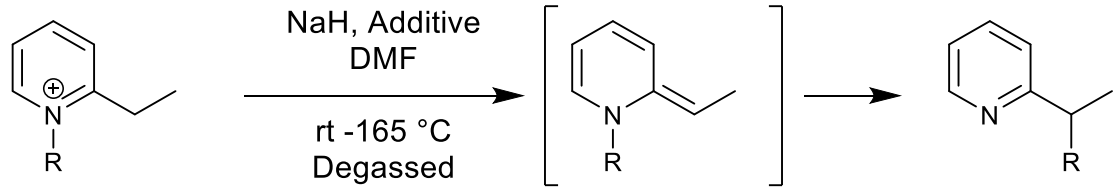

Entry	R	Additive	Yield
1*	Cinnamyl	-	0%
2	Diphenyl methyl	-	33%
3	4-bromobenzyl	-	52%
4	2-phenylbenzyl	-	74%
5	alpha-methylbenzyl	-	7%
6	(2-napthyl)benzyl	-	37%
7	2-bromobenzyl	-	45%
8	pentafluorobenzyl	DBU	4%
9	2-chlorothiazole	DBU	0%
10	2-cyanobenyl	DBU	23%
11**	4-cyanobenzyl	DBU	17%
12***	benzyl	-	51%

*product was ylide only, **120 °C. ***NaOH instead of NaH was used.

The cinnamyl substituent gave the ylide as the only isolated product (**Table 9** entry 1). A phenyl substitution was easily tolerated giving the best yield of 74% (entry 4). The alpha-methyl benzyl derivative gave a poor yield along with the pentafluorobenzyl which needed the addition of DBU to form the enamine. The thiazole derivative **56h** did not give any rearrangement product (entry 9), while the cyano-substituted benzyls gave a modest yield of 17% and 23% for the para (**56m**) and ortho (**56l**) substituted, respectively. Both bromo-substituted benzyls were tolerated well, with the ortho substituted (**56n**) giving a 45% yield, and the para substituted (**56f**) giving a 52% yield. The diphenyl and napthyl substituents gave only modest yields (entry 2 and entry 6). Sodium hydroxide was also explored as a potential base option and gave 51% yield (entry 12), but further work is needed to optimize these conditions. Further optimization with other pyridines showed that the [1,3] rearrangement reaction was tolerated well my many functional groups (**Table 10**). Notably, the 4-propanolpyridine derivative with an unprotected alcohol smoothly afforded the product in 47% yield (entry 13). Pyridine derivatives with a benzyl substituted in the 2-position needed DBU added to the reaction for better product yield. Degassing increased the yield by 15% for the 2-bromobenzyl derivative (entry 1 and 2). The methyl substituted pyridines both worked smoothly with good yield in the 2-methylpyridine and modest yield for the disubstituted pyridine (entries 10 and 11). The 2,4-dimethylpyridine gave an overall yield of 56%, but that is of 2 products. One where the rearrangement occurred on the 2 position, and the other rearranged at the 4 position (entry 12). Tetrahydroquinoline gave a good yield of 65% (entry 9). The isoquinonline isomer resulted in 20% of the expected rearranged product, but with 11% of the dibenzyl substituted product (entry 8). This is most likely due to radicals escaping from the solvent cage.

Table 10: Rearrangement scope with other substituted pyridines

Entry	Pyridine Salt	Product	Additive	Yield	Enamine
1**	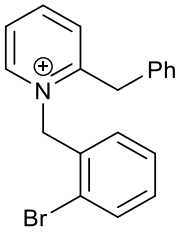	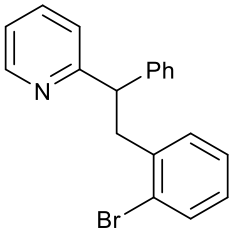		36%	Yes
2*	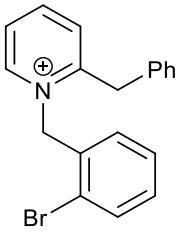	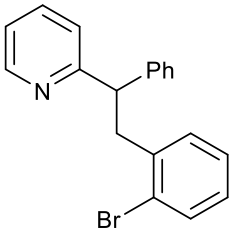		21%	Yes
3	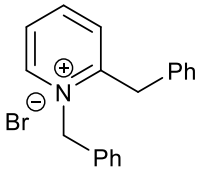	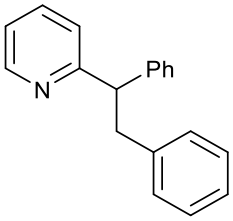	DBU	45%	Yes
4**	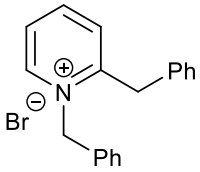	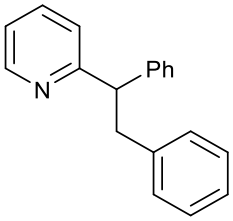		25%	Yes
5	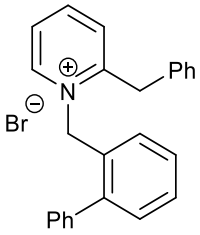	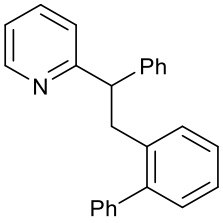	DBU	32%	Yes
	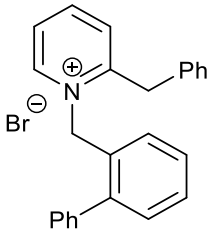	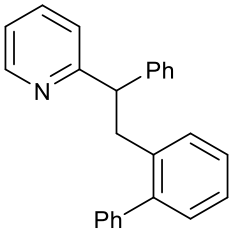		26%	Yes
7	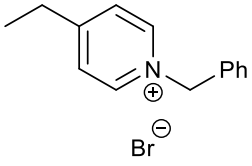	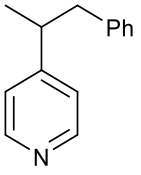		51%	Yes

Table 10 Cont.: Rearrangement scope with other substituted pyridines

8***	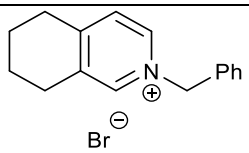	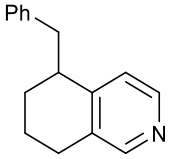	20%	Yes
9	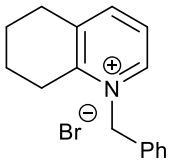	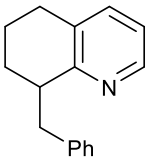	65%	Yes
10	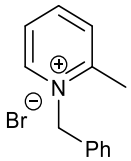	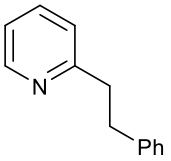	45%	Yes
11	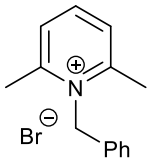	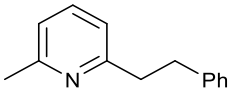	29%	Yes
12****	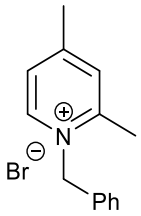	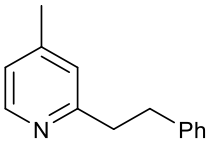	56%	Yes
13	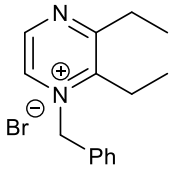	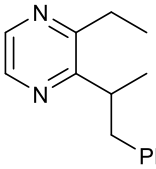	0%	Complex mixture
14	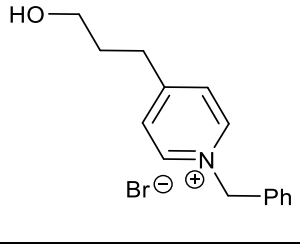	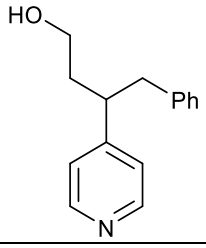	47%	Yes

*not degassed/4h **4h instead of overnight. ***11% disubstituted product.
****combined yield with rearrangement at the 4 position.

3.4 Mechanistic studies

To gain more evidence for a radical mechanism the N-methyl 2-ethylpyridine was synthesized and taken on to see if rearrangement occurred. An anionic mechanism should have

no problem with methyl as the nitrogen substituent, but a radical mechanism would not be as likely (**Figure 17**).

The reaction was run under the standard conditions after confirming the formation of the enamine, and no rearrangement product was observed (**Scheme 23**). This is supportive of the proposed radical mechanism.

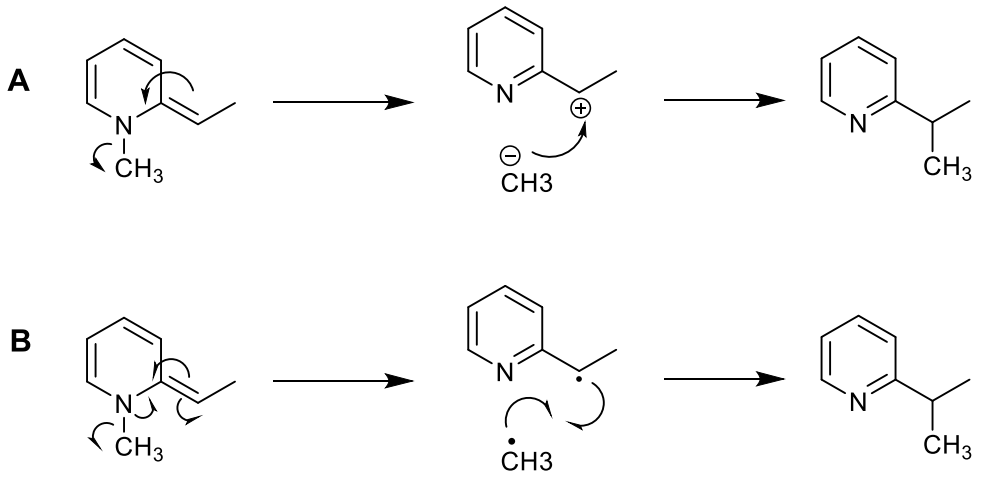

Figure 17: (A) anionic mechanism. **(B)** radical mechanism

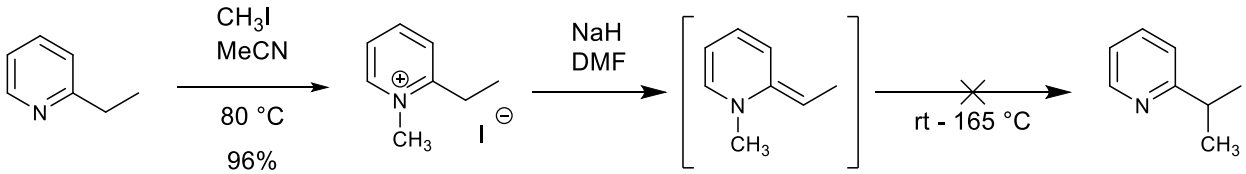

Scheme 23: Methyl rearrangement reaction

In addition to the N-methyl salt, the N-dimethylallyl salt was synthesized, since it would provide unique products for both a [1,3] and a [3,3]-rearrangement (**Scheme 24**). After confirmation that the enamine can form, the reaction was subjected to the standard rearrangement conditions which afforded both the [1,3] and the [3,3] products by crude 1H NMR in a 2:1 ratio. This seems to support a radical mechanism, since both products were observed instead of just the [3,3] product

which could have been from an ionic mechanism. Given this result, more work is needed to determine if more than just a radical mechanism is responsible for the products.

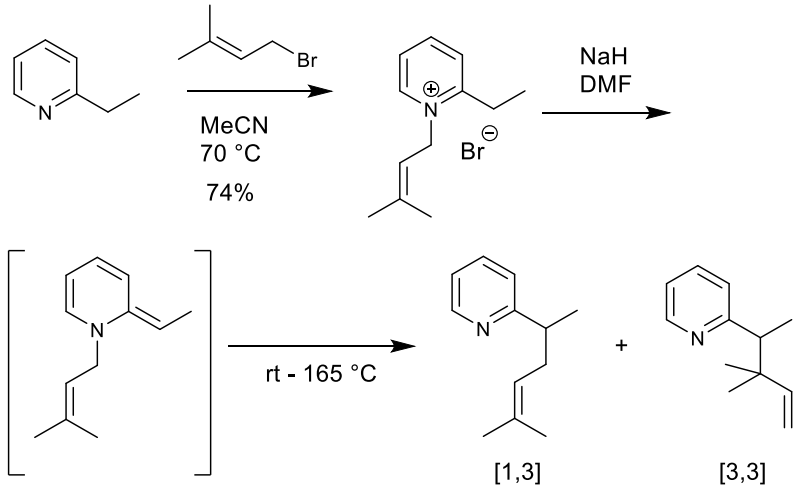

Scheme 24: Dimethylallyl rearrangement reaction

We attempted to trap any radicals with TEMPO with the N-Benzyl 2-ethyl pyridine salt under the standard rearrangement conditions, but nothing productive was observed. Additionally, the acidity of the protons in the salt was investigated using a deuterium exchange experiment (**Scheme 25**). The proton at the carbon of the ethyl pyridine was found to exchange at about the same rate as the aromatic hydrogen ortho to the Nitrogen of the ring, and none of the benzylic hydrogens adjacent to the Nitrogen exchanged in this case. This suggests that deprotonation is possible based on acidity.

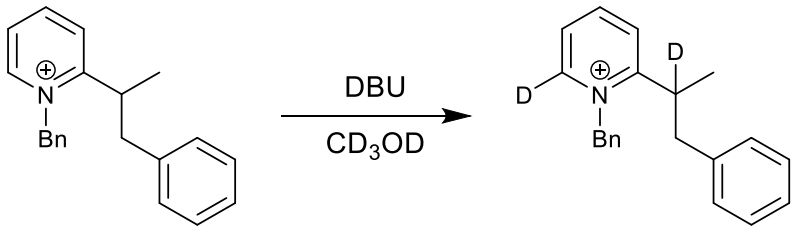

Scheme 25: Deuterium exchange experiment

3.5 Other directions

Many different conditions were tried to rearrange a benzyl group a second time to increase product diversity (**Table 11**). The addition of DBU to NaH did not form the enamine, nor did the addition of heat (entries 2 and 3). Different base combinations including, NaOH/TBACl and t-BuOH/NaH (entries 4 and 5) did not result in the formation of the enamine either. LHMDS was tried on a preparatory scale with heat and degassed to see if rearrangement product could be observed, but there was no evidence in the crude reaction mixture or after purification of the enamine or any rearrangement product. Computational work showed that the lowest energy conformation puts the desired hydrogen for deprotonation under allylic strain, so this along with experimental evidence suggests a potential reason for the lack of enamine formation.

Table 11: Reaction optimization for enamine formation of second rearrangement

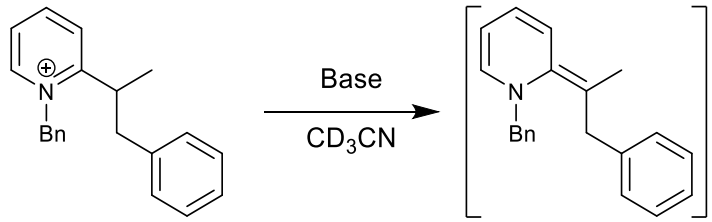

Entry	Conditions	Enamine
1	NaH	No
2	NaH, DBU	No
3	NaH, rt-60 °C	No
4	NaH, t-BuOH	No
5	NaOH, TBACl, rt – 80 °C	No
6*	LHMDS, Tol, 0 – 115 °C, degassed	No

*no rearranged product observed.

Computational work shows that the addition of a Lewis Acid coordinating to the Nitrogen of the pyridine would lower the energy of homolysis significantly. This led to the investigation of adding Lewis acids into the rearrangement reaction conditions to see if the rearrangement could

be done at a lower temperature (**Table 12**). Entry 1 shows that no reaction occurs without the base. Trimethylborate took the reaction back to the salt after the enamine formed with sodium hydride, indicating the moisture sensitivity of the enamine (entries 2 and 3). Titanium isopropoxide did not afford any product even with heat (entry 3). The borane morpholine complex did not result in any rearrangement even with heat (entry 3).

Table 12: Lewis Acid rearrangement optimization

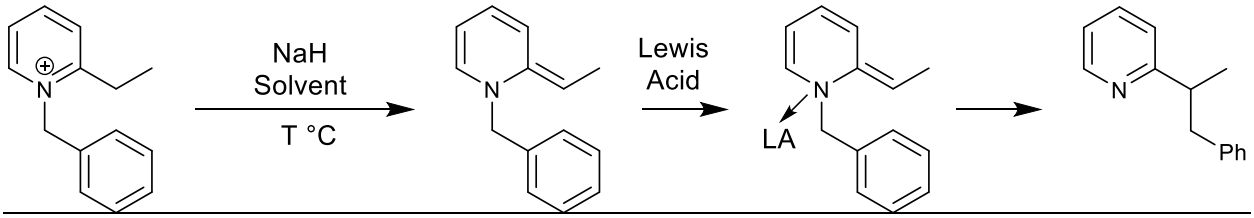

Entry	Solvent	Lewis Acid	T °C	Product
1*	CD_3CN	$B(OCH_3)_3$	rt	No reaction
2	CD_3CN	$B(OCH_3)_3$ (distilled)	rt - 70	Salt
3	CD_3CN	$Ti(O\textit{i}\text{-}Pr)_4$	rt - 65	No
4	CD_3CN	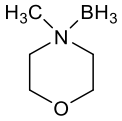	rt	Borane + enamine
5	CD_3CN	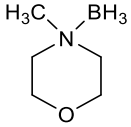	rt - 60	No
6	CH_3CN	BF_3OEt_2	rt - 50	No
7**	CH_3CN	BF_3OEt_2	rt - 50	Isomer

*reaction done with out NaH as control. **reaction degassed and identified by LCMS

Table 13: DFT calculations of homolysis enthalpy with Lewis Acid coordination

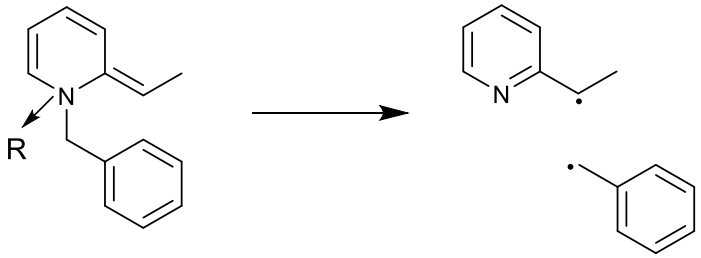

Entry	R	Homolysis Enthalpy
1	-	29 kcal/mol
2	H^+	15 kcal/mol
3	BH_3	4.1 kcal/mol

(DFT B3lyp- 631g* polar solvent)

Borane 4-methyl-morpholine complex only gave the starting material borane and enamine when added at room temperature (entry 4), and none of the desired product when heated (entry 5). Boron trifluoride dietherate gave an unknown oxidation product (entry 6). Degassing the boron trifluoride dietherate gave an unknown isomer of the desired product based on 1H NMR and Mass spectrometry (Entry 7). The product formation at a lower temperature aligns with the computations done in DFT, in which a coordinating acid lowered the homolysis enthalpy by about 10-25 kcal/mol (**Table 13**).

To expand the scope of the rearrangement other reaction conditions were employed to see if a rearrangement product could be observed, thus potentially expanding the scope of the reaction (**Figure 18** inset). This procedure allows for the generation of the base in situ, so there is no intermediate step required for synthesizing the salt, and the rearrangement product could be made in one step. The 2-methylpyridine was reacted with 2-phenyloxirane and heat to generate the alkylated Nitrogen, with a negatively charged oxygen from the opened epoxide which could serve as an internal base. The internal base could deprotonate the one of the protons from the methyl and form the enamine which could then undergo homolysis and recombination like

previously seen (**Figure 18**)

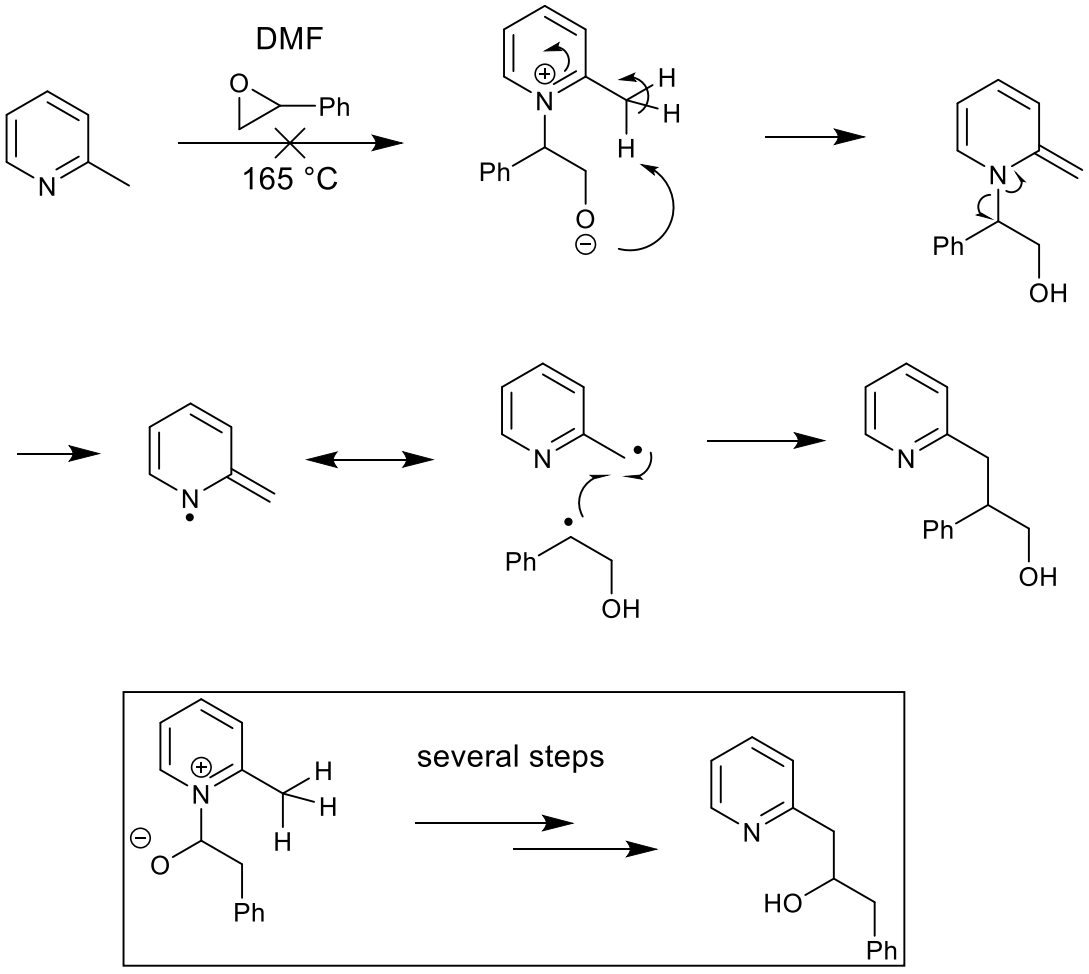

Figure 18: Other potential reaction conditions for radical rearrangement

3.6 Future work

We have strong evidence for our hypothesis that electron rich alkenes undergo homolysis easier, but more work is needed to be able to predict when homolysis will occur. We will continue this project to be able to predict C-N homolysis via experimenting with different computational methods and looking at other factors that could influence homolysis. Optimizing

and expanding the scope of this rearrangement to more diverse pyridines and alkyl halides is also an ongoing effort in the lab. Further work is needed to obtain a successful second rearrangement, but this would open the door to many more structurally diverse products via a [1,3] rearrangement reaction. The conditions for Lewis Acid assisted rearrangement are also ongoing. Currently, mechanistic studies are being done on Thiamine and related compounds to further support a radical mechanism, and better understand how the enzyme avoids fragmentation.

4. References

(1) Chatgilialoglu, C.; Studer, A. *Encyclopedia of Radicals in Chemistry, Biology and Materials*; John Wiley & Sons: Chichester, West Sussex, 2012; Vol. 1.

(2) Oka, Y.; Kishimoto, S.; Hirano, H. Studies on Vitamin B₁ and Related Compounds. CX. Rearrangements of α-Hydroxybenzylthiamin and Its Homologues. *Chem. Pharm. Bull. (Tokyo)* **1970**, *18* (3), 534–541. https://doi.org/10.1248/cpb.18.534.

(3) Jefcoate, C. R.; Ghisla, S.; Hemmerich, P. Studies in the Flavin Series. Part XVI. Alkylation and Rearrangement Reactions of Dihydroalloxazines. *J. Chem. Soc. C Org.* **1971**, No. 0, 1689–1694. https://doi.org/10.1039/J39710001689.

(4) Baldwin, J. E.; Walker, J. A. Competing [1-3]- and [3,3]-Sigmatropic Rearrangements of Electron-Rich Olefins. *J. Am. Chem. Soc.* **1974**, *96* (2), 596–597. https://doi.org/10.1021/ja00809a053.

(5) Baldwin, J. E.; Branz, S. E.; Walker, J. A. The Radical Nature of the [1,3]-Sigmatropic Rearrangements of Electron-Rich Olefins. *J. Org. Chem.* **1977**, *42* (25), 4142–4144. https://doi.org/10.1021/jo00445a034.

(6) Lown, J. W.; Akhtar, M. H.; McDaniel, R. S. Stereochemistry and Mechanism of the Thermal [1,3] Alkyl Shift of Stable 1,4-Dialkyl-1,4-Dihydropyrazines. *J. Org. Chem.* **1974**, *39* (14), 1998–2006. https://doi.org/10.1021/jo00928a004.

(7) Çetinkaya, B.; Çetinkaya, E.; Chamizo, J. A.; Hitchcock, P. B.; Jasim, H. A.; Küçükbay, H.; Lappert, M. F. Synthesis and Structures of 1,3,1J,3J-Tetrabenzyl-2,2J-Biimidazolidinylidenes (Electron-Rich Alkenes), Their Aminal Intermediates and Their Degradation Products. **1998**, 8.

(8) Çetinkaya, E.; Hitchcock, P. B.; Küçükbay, H.; Lappert, M. F.; Al-Juaid, S. Carbene Complexes: XXIV22For Part XXIII, See Ref. 1. No Reprints Available.. Preparation and Characterization of Two Enetetramine-Derived Carbenerhodium(I) Chloride Complexes RhCl(LR)3 and [RhCl(COD)LR] and the Preparation and X-Ray Structures of the Enetetramine L2R and Its Salt [L2R][BF4]2. *J. Organomet. Chem.* **1994**, *481* (1), 89–95. https://doi.org/10.1016/0022-328X(94)85013-5.

(9) Cetinkaya, E.; Hitchcock, P. B.; Jasim, H. A.; Lappert, M. F.; Spyropoulos, K. Synthesis and Characterisation of Unusual Tetraaminoalkenes (Enetetramines). *J. Chem. Soc. Perkin 1* **1992**, No. 5, 561. https://doi.org/10.1039/p19920000561.

(10) Holtgrewe, C.; Diedrich, C.; Pape, T.; Grimme, S.; Hahn, F. E. Rearrangement of Electron-Rich N-Allyldibenzotetraazafulvalenes –An Experimental and Theoretical Study. *Eur. J. Org. Chem.* **2006**, *2006* (14), 3116–3124. https://doi.org/10.1002/ejoc.200600087.

(11) Zarganes-Tzitzikas, T.; Neochoritis, C. G.; Stephanidou-Stephanatou, J.; Tsoleridis, C. A. Synthesis of 2-Keto-Imidazoles Utilizing N-Arylamino-Substituted N-Heterocyclic Carbenes. *J. Org. Chem.* **2011**, *76* (5), 1468–1471. https://doi.org/10.1021/jo102244x.

(12) Pareek, M.; Reddi, Y.; Sunoj, R. B. Tale of the Breslow Intermediate, a Central Player in N-Heterocyclic Carbene Organocatalysis: Then and Now. *Chem. Sci.* **2021**, 10.1039.D1SC01910D. https://doi.org/10.1039/D1SC01910D.

(13) Alwarsh, S.; Xu, Y.; Qian, S. Y.; McIntosh, M. C. Radical [1,3] Rearrangements of Breslow Intermediates. *Angew. Chem. Int. Ed.* **2016**, *55* (1), 355–358. https://doi.org/10.1002/anie.201508368.

(14) Chaitanya, K. V. Role of Thiamine in Human Metabolism – A Review. *J. Pharm. Res.* **2012**, No. 11, 6.

(15) Bunik, V. I.; Tylicki, A.; Lukashev, N. V. Thiamin Diphosphate-Dependent Enzymes: From Enzymology to Metabolic Regulation, Drug Design and Disease Models. *FEBS J.* **2013**, *280* (24), 6412–6442. https://doi.org/10.1111/febs.12512.

(16) Breslow, R. On the Mechanism of Thiamine Action. IV. [1] Evidence from Studies on Model Systems. *J. Am. Chem. Soc.* **1958**, *80* (14), 3719–3726. https://doi.org/10.1021/ja01547a064.

(17) Kluger, R.; Moore, I. F. Destruction of Vitamin B1 by Benzaldehyde. Reactivity of Intermediates in the Fragmentation of *N* 1‘-Benzyl-2-(1-Hydroxybenzyl)Thiamin. *J. Am. Chem. Soc.* **2000**, *122* (26), 6145–6150. https://doi.org/10.1021/ja000194i.

(18) Kluger, R.; Lam, J. F.; Pezacki, J. P.; Yang, C.-M. Diverting Thiamin from Catalysis to Destruction. Mechanism of Fragmentation of N(1’)-Methyl-2-(1-Hydroxybenzyl)Thiamin. *J. Am. Chem. Soc.* **1995**, *117* (46), 11383–11389. https://doi.org/10.1021/ja00151a001.

(19) Kluger, R.; Tittmann, K. Thiamin Diphosphate Catalysis: Enzymic and Nonenzymic Covalent Intermediates. *Chem. Rev.* **2008**, *108* (6), 1797–1833. https://doi.org/10.1021/cr068444m

(20) Hu, Q.; Kluger, R. Reactivity of Intermediates in Benzoylformate Decarboxylase: Avoiding the Path to Destruction. *J. Am. Chem. Soc.* **2002**, *124* (50), 14858–14859. https://doi.org/10.1021/ja027976r.

(21) Kluger, R.; Lam, J. F.; Kim, C. S. Decomposition of 2-(1-Hydroxybenzyl)Thiamin in Neutral Aqueous Solutions: Benzaldehyde and Thiamin Are Not the Products. *Bioorganic Chem.* **1993**, *21* (3), 275–283. https://doi.org/10.1006/bioo.1993.1023.

(22) Bielecki, M.; Kluger, R. The Need for an Alternative to Radicals as the Cause of Fragmentation of a Thiamin-Derived Breslow Intermediate. *Angew. Chem. Int. Ed.* **2017**, *56* (22), 6321–6323. https://doi.org/10.1002/anie.201702240.

(23) Uredi, D.; Motati, D. R.; Watkins, E. B. A Simple, Tandem Approach to the Construction of Pyridine Derivatives under Metal-Free Conditions: A One-Step Synthesis of the Monoterpene Natural Product, (−)-Actinidine. *Chem. Commun.* **2019**, *55* (22), 3270–3273. https://doi.org/10.1039/C9CC01097A.

(24) Vitaku, E.; Smith, D. T.; Njardarson, J. T. Analysis of the Structural Diversity, Substitution Patterns, and Frequency of Nitrogen Heterocycles among U.S. FDA Approved Pharmaceuticals: Miniperspective. *J. Med. Chem.* **2014**, *57* (24), 10257–10274. https://doi.org/10.1021/jm501100b.

(25) Rappenglück, S.; Sichler, S.; Höfner, G.; Wein, T.; Niessen, K. V.; Seeger, T.; Paintner, F. F.; Worek, F.; Thiermann, H.; Wanner, K. T. Synthesis of a Series of Structurally Diverse MB327 Derivatives and Their Affinity Characterization at the Nicotinic Acetylcholine Receptor. *ChemMedChem* **2018**, *13* (17), 1806–1816. https://doi.org/10.1002/cmdc.201800325.

(26) Llaveria, J.; Leonori, D.; Aggarwal, V. K. Stereospecific Coupling of Boronic Esters with N-Heteroaromatic Compounds. *J. Am. Chem. Soc.* **2015**, *137* (34), 10958–10961. https://doi.org/10.1021/jacs.5b07842.

(27) Gladfelder, J. J.; Ghosh, S.; Podunavac, M.; Cook, A. W.; Ma, Y.; Woltornist, R. A.; Keresztes, I.; Hayton, T. W.; Collum, D. B.; Zakarian, A. Enantioselective Alkylation of 2-Alkylpyridines Controlled by Organolithium Aggregation. *J. Am. Chem. Soc.* **2019**, *141* (38), 15024–15028. https://doi.org/10.1021/jacs.9b08659.

(28) Wang, Y.; Li, X.; Leng, F.; Zhu, H.; Li, J.; Zou, D.; Wu, Y.; Wu, Y. One-Pot Double Benzylation of 2-Substituted Pyridines Using Palladium-Catalyzed Decarboxylative Coupling of Sp2 and Sp3 Carbons. *Adv. Synth. Catal.* **2014**, *356* (16), 3307–3313. https://doi.org/10.1002/adsc.201400311.

(29) Hwang, C.; Jo, W.; Cho, S. H. Base-Promoted, Deborylative Secondary Alkylation of N-Heteroaromatic N-Oxides with Internal Gem-Bis[(Pinacolato)Boryl]Alkanes: A Facile Derivatization of 2,2′-Bipyridyl Analogues. *Chem. Commun.* **2017**, *53* (54), 7573–7576. https://doi.org/10.1039/C7CC03731G.

(30) Alwarsh, S.; Ayinuola, K.; Dormi, S. S.; McIntosh, M. C. Intercepting the Breslow Intermediate via Claisen Rearrangement: Synthesis of Complex Tertiary Alcohols without Organometallic Reagents. *Org. Lett.* **2013**, *15* (1), 3–5. https://doi.org/10.1021/ol303053c.

5. Appendix

5.1 General procedure for the preparation of pyridine salts

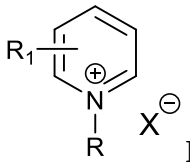

Method A: Alkyl pyridine was mixed neat with a slight excess of alkyl halide (1.1 eq) in a pressure tube and the mixture maintained at 80 °C until the reaction mixture solidified (1-14 h). The resulting salt was dissolved in a minimal amount of methanol and triturated with diethyl ether. The solvent was decanted and the solid dried in vacuo.

Method B: Alkyl pyridine was mixed in acetonitrile with a slight excess of alkyl halide (1.1 eq) in a pressure tube and the mixture maintained at 80 °C until the starting material was consumed by TLC (4-16 h). The resulting liquid was poured into a round bottom and triturated with diethyl ether. The solvent was decanted and the solid dried in vacuo.

5.1.2 General procedure for the preparation of pyridine rearrangements

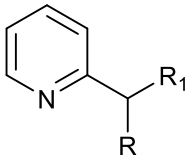

Method A: The pyridine salt was placed into a pressure tube followed by DMF and NaH. The reaction mixture was allowed to stir for 20-45 min and then a vacuum cap was sealed with a plunger tube cap and degassed three times by the freeze pump thaw method, on the last pump the pressure tube was sealed under vacuum and the reaction was allowed to come up to room temperature before being placed in a 165 °C oil bath for 16-20 h. The reaction mixture was cooled and quenched with saturated ammonium chloride solution, then extracted with DCM 3x, dried with $MgSO_4$, filtered, and concentrated. Reactions were purified by preparatory TLC or flash chromatography in hexanes/ethyl acetate.

Method B: Same as method A but DBU was added before the NaH.

5.2 Procedure for N-benzyl benzothiazole ketone:

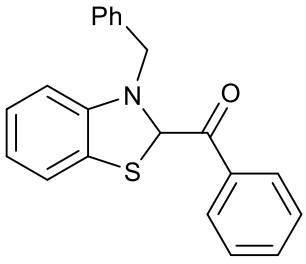

A 0.15M methanolic solution of benzothiazole salt was added to a neat

solution of benzaldehyde (2 eq) and triethylamine (2 eq) dropwise over 20-25 minutes at rt. The reaction was stirred at room temperature for 4 days and then the reaction was evaporated and purified by column chromatography. Product was a bright yellow oil. 30% yield.

(3-benzyl-2,3-dihydrobenzo[d]thiazol-2-yl)(phenyl)methanone: ^{1}H NMR (400 MHz, CDCl3) δ 4.33 (d, 1H, J=14.98 Hz), 4.82 (d, 1H, J=14.99 Hz), 6.10 (s, 1H), 6.58 (d, 1H, J=7.91 Hz), 6.71 (t, 1H, J=7.51 Hz), 7.03 (m, 2H), 7.32-7.39 (m, 5H), 7.46 (t, 2H, J=7.88 Hz), 7.59 (t, 1H, J=7.40 Hz), 7.80 (d, 2H, J=7.42 Hz). 13C NMR (300 MHz, CDCl3) δ 29.7, 51.4, 68.8, 107.6, 119.1, 122.1, 126.6, 127.7, 128.1, 128.5, 128.7, 128.8, 133.5, 136.5, 147.4, 190.5.

5.2.1 Procedure for N-benzyl benzothiazole enolate rearrangement:

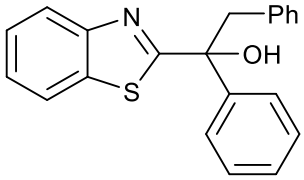

The N-benzyl ketone from the previous step was dissolved in dry DMSO under N2 and then LHMDS (2.2 eq) was syringed in. The reaction turned a dark red and was stirred for 1 hour under N2 at rt. After one hour the reaction was quenched with acetic acid and then sodium bicarbonate was added and the solution was extracted with diethyl ether 4 times, dried over MgSO4, filtered, and evaporated. The crude pale yellow oil was purified by a prep plate ran in 1:9 ethyl acetate to Hexanes to give a pale yellow solid in 79% yield.
***α*-phenyl-*α*-(phenylmethyl)-2-Benzothiazolemethanol:** 1H NMR (400 MHz, CDCl3) δ 3.37 (s, 1H), 3.59 (d, 1H, J=13.6 Hz), 4.13 (d, 1H, J=13.6 Hz), 7.12 (m, 2H), 7.21 (m, 3H), 7.30 (m, 2H), 7.38 (m, 3H), 7.50 (td, 1H, J=1.1 Hz), 7.77 (d, 2H, J=7.36 Hz), 7.83 (d, 1H, J=7.88 Hz), 8.08 (d, 1H, J=8.16 Hz).13C NMR (300 MHz, CDCl3) δ 48.4, 78.7, 121.7, 123.2, 124.9, 125.5, 125.9, 127.3, 127.6, 128.3, 128.4, 130.8, 134.9, 135.6, 143.6, 153.1, 178.1.
Matched previously published data: Alwarsh, Sefat et al. *Angew. Chem. Int. Ed.* **2016**, 355-358.

5.3 Alkyl pyridine experimental

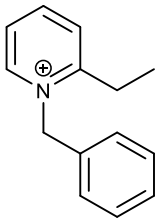

2-ethyl-1-(phenylmethyl)-pyridinium bromide: Synthesized using Salt method A. The product was obtained as a tan solid in 82% yield. ^{1}H NMR (400 MHz, $CDCl_3$) δ 1.36 (t, 3H, J=8.01), 3.26 (q, 2H, J=8.01) 6.31 (s, 2H), 7.30 (m, 2H), 7.38 (m, 2H), 7.89 (d, 1H, J=8.01 Hz), 7.99 (t, 1H, J=7.20 Hz), 8.472 (t, 1H, J=7.80 Hz), 9.77 (d, 1H, J=6.4 Hz). ^{13}C NMR (400 MHz, $CDCl_3$) δ 11.8, 26.3, 61.2, 125.9, 127.5, 127.8, 129.3, 129.4, 129.5, 129.6, 132.3, 145.8, 147.2, 159.6. Characterized previously by mass spec.

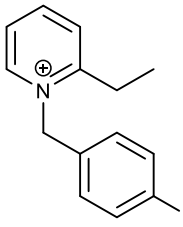

2-ethyl-1-(4-bromophenylmethyl)-pyridinium bromide: Synthesized using Salt method A. The product was obtained as a tan solid in 95% yield. ^{1}H NMR (400 MHz, $CDCl_3$) δ 1.39 (t, 3H, J=7.24), 3.28 (q, 2H, J=7.39) 6.41 (s, 2H), 7.30 (m, 2H), 7.51 (d, 2H, J=7.88 Hz), 7.85 (d, 1H, J=8.02 Hz), 7.97 (t, 1H, J=6.89 Hz), 8.43 (t, 1H, J=7.80 Hz), 9.92 (d, 1H, J=6.15 Hz). ^{13}C NMR (400 MHz, $CDCl_3$) δ 11.7, 26.3, 60.5, 123.6, 225.8, 127.4, 129.9, 131.3, 132.7, 145.4, 147.7, 160.13.

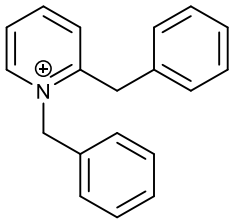

1,2-bis(phenylmethyl)-pyridinium bromide: Synthesized using Salt method A. The product was obtained as a light white solid in 75% yield. ^{1}H NMR (400 MHz, $CDCl_3$) δ 1.39 (t, 3H, J=7.24), 3.28 (q, 2H, J=7.39) 6.41 (s, 2H), 7.30 (m, 2H), 7.51 (d, 2H, J=7.88 Hz), 7.85 (d, 1H, J=8.02 Hz), 7.97 (t, 1H, J=6.89 Hz), 8.43 (t, 1H, J=7.80 Hz), 9.92 (d, 1H, J=6.15 Hz). ^{13}C NMR (300 MHz, $CDCl_3$) δ 39.1, 61.5, 126.1, 128.3, 129.4, 129.5, 129.6, 129.7, 131.9, 133.1, 145.2, 147.2, 158.1. Data matched that reported by Qu, Bo et al. *Org. Lett.* **2016**, 4920-4923.

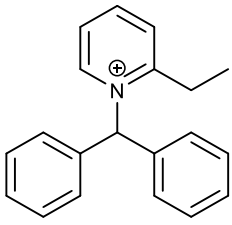

1-(diphenylmethyl)-2-ethylpyridinium bromide: Synthesized using Salt method A. The product was obtained as an off-white solid in 66% yield. ^{1}H NMR (400 MHz, $CDCl_3$) δ 1.35 (t, 3H, J=7.26 HZ), 3.57 (q, 2H, J=7.25 Hz), 7.30 (m, 4H), 7.46 (m, 6H), 7.90 (t, 1H, J=6.71 Hz), 8.04 (s, 1H), 8.12 (d, 1H, J=8.08 Hz), 8.29 (d, 1H, J=6.43 Hz), 8.55 (t, 1H, J=7.74 Hz). ^{13}C NMR (300 MHz, $CDCl_3$) δ-11.8, 27.3, 72.9, 125.3, 128.8, 129.2, 129.8, 129.9, 134.9, 142.6, 145.9, 162.1.

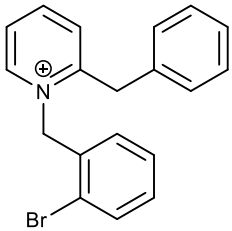

1-(2-bromophenylmethyl) 2-(phenylmethyl)pyridinium bromide: Synthesized using Salt method A. The product was obtained as an off-white solid in 88% yield.

^{1}H NMR (400 MHz, $CDCl_3$) δ 4.78 (s, 2H), 6.35 (s, 2H), 7.32 (m, 2H), 7.40 (m, 4H), 7.48 (d, 1H, J=), 7.66 (d, 2H, J=), 7.85 (m, 2H), 8.33 (t, 1H, J=7.20 Hz), 8.74 (d, 1H, J=7.62 Hz).^{13}C NMR (300 MHz, $CDCl_3$) δ 39.5, 60.9, 124.8, 125.9, 128.3, 129.6, 129.7, 129.8, 131.9, 132.8, 133.0, 144.8, 145.3, 158.0.

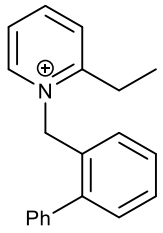

1-([1,1'-biphenyl]-2-ylmethyl)-2-ethylpyridin-1-ium bromide: Synthesized using Salt method B. The product was obtained as an off-white solid-in 85% yield.-^{1}H NMR (400 MHz, $CDCl_3$) δ 1.09 (t, 3H, J=7.42 Hz), 2.66 (q, 2H, J=7.40 Hz), 6.20 (s, 2H), 7.20 (dd, 2H, J1=7.44 Hz, J2=5.4 Hz), 7.34 (d, 1H, J=7.12 Hz), 7.42 (m, 6H), 7.67 (d, 1H, J=7.96 Hz), 7.83 (t, 1H, J=6.86 Hz), 8.32 (t, 1H, J=7.78 Hz), 9.54 (d, 1H, J=6.04 Hz). ^{13}C NMR (300 MHz, $CDCl_3$) δ 11.6, 25.9, 59.4, 125.4, 127.4, 128.2, 128.7, 128.8, 128.9, 129.3, 129.6, 129.8, 130.8, 129.1, 142.1, 145.4, 147.1.

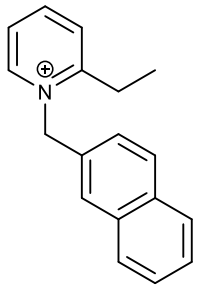

2-ethyl-(2-napthalenylmethyl)pyridinium bromide: Synthesized using Salt method B. The product was obtained as a brown solid-in 74% yield.^{1}H NMR (400 MHz, $CDCl_3$) δ 1.41 (t, 3H, J=7.04 Hz), 3.32 (q, 2H, J=7.38), 6.50 (s, 2H), 7.40 (d, 1H, J=), 7.54 (t, 2H, J=8.48 Hz), 7.77 (s, 1H), 7.85 (m, 3H), 7.97 (t, 1H, J=6.59 Hz), 8.41 (t, 1H, J=7.57 Hz), 9.81 (d, 1H, J=5.68 Hz). ^{13}C NMR (300 MHz, $CDCl_3$) δ 11.8, 26.5, 61.3, 124.7, 125.8, 127.0, 127.1, 127.6, 127.7, 128.1, 129.6, 129.7, 133.0, 133.1, 145.7, 146.1, 147.1, 159.9.

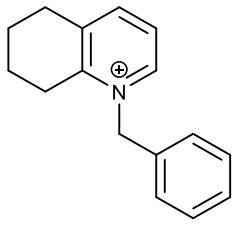

5,6,7,8-tetrahydro-1-(phenylmethyl)quinolinium bromide: Synthesized using Salt method B. The product was obtained as a dark yellow solid in 98% yield.^{1}H NMR (400 MHz, $CDCl_3$) δ 1.83 (m, 2H), 1.97 (m, 2H), 2.98 (t, 2H, J=6.13 Hz), 3.22 (t, 2H, J=6.32 Hz), 6.22 (s, 2H), 7.29 (m, 2H), 7.37 (m, 3H), 7.86 (t, 1H, J=7.04), 8.15 (d, 1H, J=7.86 Hz), 9.52 (d, 1H, J=6.04 Hz). ^{13}C NMR (400 MHz, $CDCl_3$) δ20.4, 21.4, 27.7, 29.0, 61.2, 124.7, 127.9, 129.2, 129.5, 132.1, 139.6, 145.3, 145.5, 154.6.

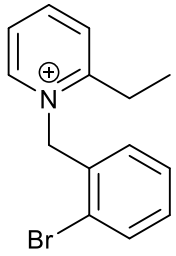

1-(2-bromobenzyl)-2-ethylpyridinium bromide: Synthesized using Salt method B. The product was obtained as a light tan solid in 86% yield. ^{1}H NMR (400 MHz, $CDCl_3$) δ 1.50 (t, 1H, J=), 3.33 (m, 2H), 6.30 (s, 2H), 7.36 (d, 1H, J=6.77 Hz), 7.44 (m, 1H), 7.67 (d, 2H, J=7.84 Hz), 7.93 (m, 2H), 8.48 (m, 1H), 9.03 (m, 1H).^{13}C NMR (300 MHz, $CDCl_3$) δ 11.9, 26.6, 60.4, 124.1, 125.8, 127.9, 128.9, 131.1, 131.6, 131.9, 133.6, 145.6, 145.9.

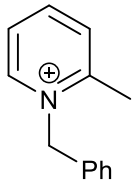

1-benzyl-2-methylpyridinium bromide: Synthesized using Salt method B. The product was obtained as a light brown solid in 83% yield. ^{1}H NMR (400 MHz, $CDCl_3$) δ 2.96 (s, 3H), 6.28, (s, 2H), 7.34 (m, 5H), 7.95 (m, 2H), 8.41 (t, 1H, J=7.73 Hz), 9.68, (d, 1H, J=4.81 Hz). ^{13}C NMR (400 MHz, $CDCl_3$) δ 21.5, 61.7, 126.0, 128.2, 129.4, 129.6, 130.5, 131.8, 145.4, 146.8, 155.8. Data matched that reported by Qu, Bo et al. *Org. Lett.* **2016**, 4920-4923.

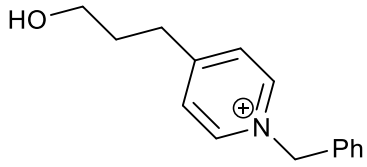

1-benzyl-4-(3-hydroxypropyl)pyridin-1-ium bromide: Synthesized using Salt method B. The product was obtained as a brown solid in 73% yield. ^{1}H NMR (400 MHz, MeOD-d4) δ 1.97 (m, 2H), 3.04 (t, 2H, J=7.6 Hz), 3.63 (t, 2H, J=6.10 Hz), 4.85 (s, 1H), 5.82 (s, 2H), 7.46 (m, 2H), 7.48 (m, 2H), 7.53 (m, 2H), 8.01 (d, 2H, J=6.40 Hz), 8.95 (d, 2H, J=6.55 Hz).^{13}C NMR (300 MHz, MeOD-d4) δ 31.8, 60.2, 63.5, 128.1, 128.7, 129.3, 129.5, 133.5, 143.7, 164.1

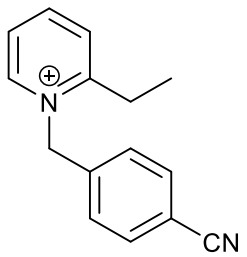

1-(4-cyanobenzyl)-2-ethylpyridinium bromide: Synthesized using Salt method B. The product was obtained as a light tan solid in 98% yield. ^{1}H NMR (400 MHz, $CDCl_3$) δ 1.35 (t, 2H, J=7.33 Hz), 3.24 (q, 2H, J=7.32), 6.67 (s, 2H), 7.53 (d, 2H, J=8.11 Hz), 7.66 (d, 2H, J=8.16 Hz), 7.90 (d, 1H, J=7.96 Hz), 8.02 (t, 1H, J=6.78 Hz), 8.49 (t, 1H, J=7.75

Hz), 10.09 (d, 1H J=6.02 Hz). ^{13}C NMR (300 MHz, $CDCl_3$) δ 11.8, 26.4, 60.2, 113.0, 117.9, 126.1, 127.8, 128.7, 133.2, 137.8, 146.1, 147.6, 160.3.

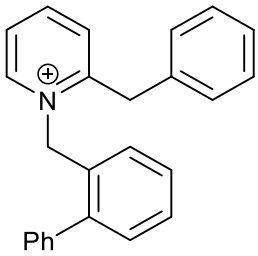

1-([1,1'-biphenyl]-2-ylmethyl)-2-benzylpyridin-1-ium bromide: Synthesized using Salt method B. The product was obtained as a brown solid in 95% yield. ^{1}H NMR (400 MHz, $CDCl_3$) δ ^{13}C NMR (300 MHz, $CDCl_3$) δ 38.6, 59.7, 125.8, 126.9, 128.2, 128.3, 128.5, 128.8, 128.9, 129.1, 129.2, 129.4, 129.5, 129.7, 129.8, 131.1, 132.6, 139.1, 142.2, 145.2, 146.9, 157.4.

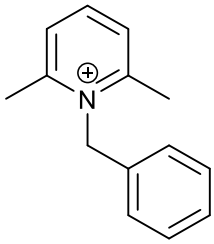

1-benzyl-2,6-dimethylpyridinium bromide: Synthesized using Salt method B. The product was obtained as an off-white solid in 70% yield. ^{1}H NMR (400 MHz, $CDCl_3$) δ 2.95 (s, 6H), 6.16 (s, 2H), 6.93 (d, 2H, J=5.86 Hz), 7.39 (m, 3H), 7.89 (d, 2H, J=7.90 Hz), 8.34 (t, 1H, J=7.88 Hz).^{13}C NMR (300 MHz, $CDCl_3$) δ 22.3, 57.4, 125.0, 125.1, 128.5, 128.8, 129.7, 131.1, 145.4, 155.5.

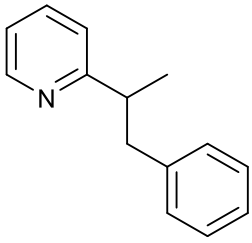

2-(1-methyl-2-phenylethyl) pyridine: Synthesized using Method A. The product was obtained as a yellow oil in 56% yield. ^{1}H NMR (400 MHz, $CDCl_3$) δ 1.30 (d, 3H, J=6.72 Hz), 2.86 (dd, 1H, J=7.72, 7.76 Hz), 3.15 (m, 2H), 7.04 (d, 1H, J=7.84 Hz), 7.10 (d, 3H, J=7.00 Hz), 7.17 (d, 1H, J=7.20 Hz), 7.24 (m, 2H), 7.54 (td, 1H, J=7.56, 7.60 Hz), 8.59 (d, 1H, J=4.08 Hz). ^{13}C NMR (300 MHz, $CDCl_3$) δ 20.0, 43.3, 43.8, 121.2, 121.9, 125.8, 128.1, 129.1, 136.2, 140.6, 149.2, 165.5. Data matched that reported by Hwang, C.; Jo, W.; Cho, S. *Chem. Commum.* **2017**, 7573-7573.

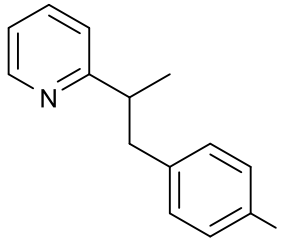

2-(1-(4-bromophenyl)propan-2-yl)pyridine: Synthesized using Method A. The product was obtained as a yellow oil in 52% yield. ^{1}H NMR (400 MHz, $CDCl_3$) δ 1.29 (d, 3H, J=6.71 Hz), 2.81 (dd, 1H, J=7.33, 7.35 Hz), 3.09 (m, 2H), 6.93 (d, 2H, J=8.16 Hz), 6.98 (d, 1H, J=7.93 Hz), 7.08 (t, 1H, J=6.06 Hz), 7.31 (d, 2H, J=8.17 Hz), 7.52 (t, 1H, J=7.67 Hz), 8.57 (d, 1H J=4.16 Hz).^{13}C NMR (400 MHz, $CDCl_3$) δ 20.1, 42.6, 43.6, 119.6, 121.3, 122.0, 130.8, 131.2, 136.2, 139.6. Elemental analysis calculated for $C_{14}H_{14}BrN$: C 60.89; H 5.11; N 5.07 found C 60.87; H 5.16; N 4.99.

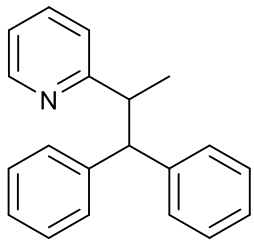

2-(1,1-diphenylpropan-2-yl)pyridine: Synthesized using Method A. The product was obtained as a yellow solid in 35% yield. ^{1}H NMR (400 MHz, $CDCl_3$) δ 1.28 (d, 3H, J=6.76 Hz), 3.78 (dd, 1H, J=4.83, 11.4 Hz), 4.39 (d, 1H, J=11.53 Hz), 6.95-7.01 (m, 3H), 7.07 (t, 2H, J=7.58 Hz), 7.21 (m, 3H), 7.34 (t, 2H, J=7.60 Hz), 7.41 (m, 1H), 7.46 (d, 2H, J=7.47 Hz), 8.51 (d, 1H, J=4.15 Hz). ^{13}C NMR (300 MHz, $CDCl_3$) δ 20.7, 46.3, 57.8, 121.0, 123.0, 125.7, 126.3, 128.0, 128.1, 128.4, 128.6, 126.0, 143.9, 144.0, 149.1, 164.8. Elemental analysis calculated for $C_{20}H_{19}N$: C 87.87, H 7.01, N 5.12 found C 86.11, H 7.23, N 4.75.

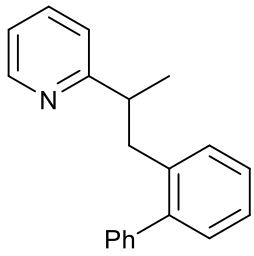

2-(1-([1,1'-biphenyl]-2-yl)propan-2-yl)pyridine: Synthesized using Method A. The product was obtained as a yellow-orange oil in 74% yield. ^{1}H NMR (400 MHz, $CDCl_3$) δ 1.18 (d, 3H, J=6.50 Hz), 2.95 (m, 2H), 3.16 (d, 1H, J=6.56 Hz), 6.70 (d, 1H, J=7.87 Hz), 7.04 (t, 1H, J=), 7.19 (t, 1H, J=6.06 Hz), 7.24 (m, 3H), 7.32, (d, 2H, J=6.96 Hz), 7.39 (d, 1H, J=7.00 Hz), 7.44 (m, 3H), 8.52 (d, 1H, J=4.43 Hz).^{13}C NMR (400 MHz, $CDCl_3$) δ 19.8, 40.5, 42.9, 121.1, 122.1, 125.9, 126.8, 127.1, 128.1, 129.3, 130.0, 130.2, 136.0, 138.1, 142.1, 124.3, 149.1, 165.4. Elemental analysis calculated for $C_{20}H_{19}N$: C 87.87; H 7.01; N 5.12 found C 87.79; H 6.94; N 5.01.

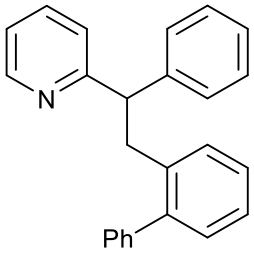

2-(2-([1,1'-biphenyl]-2-yl)-1-phenylethyl)pyridine: Synthesized using Method B. The product was obtained as a yellow oil in 32% yield. ^{1}H NMR (400 MHz, $CDCl_3$) δ 3.43 (dd, 1H, J=7.28, 7.27 Hz), 3.66 (dd, 1H, J=7.99, 7.99 Hz), 4.14 (t, 1H, J=7.58 Hz), 6.88 (d, 1H, J=7.81 Hz), 7.04 (d, 3H, J=6.50 Hz), 7.13 (m, 3H), 7.17 (m, 4H), 7.26 (d, 2H, J=6.77 Hz), 7.41 (m, 4H), 8.55 (d, 1H, J=4.03 Hz).^{13}C NMR (400 MHz, $CDCl_3$) δ 38.7, 54.3, 121.2, 123.2, 125.9, 126.2, 126.8, 127.0, 128.0, 128.1, 128.2, 129.3, 129.9, 130.2, 136.1, 137.6, 141.9, 142.2, 143.3, 149.1, 162.7. Elemental analysis calculated for $C_{25}H_{21}N$: C 89.51, H 6.31, N 4.18 found C 88.53, H 6.38, N 4.05.

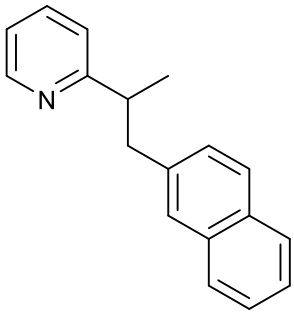

2-(1-(naphthalen-2-yl)propan-2-yl)pyridine: Synthesized using Method A. The product was obtained as an orange oil in 37% yield. ^{1}H NMR (400 MHz, $CDCl_3$) δ 1.37 (d, 3H, J=6.19 Hz), 3.04 (dd, 1H, J=10.2, 10.32 Hz), 3.32 (m, 2H), 7.06 (d, 1H, J=7.88 Hz), 7.11 (dd, 1H, J=7.33, 6.65 Hz), 7.28 (d, 1H, J=8.40 Hz), 7.44 (t, 2H, J= 5.73 Hz), 7.55 (m, 2H), 7.75 (t, 2, J=7.42 Hz), 7.80 (d, 1H, J=8.60 Hz), 8.63 (d, 1H, J=4.42 Hz). ^{13}C NMR (400 MHz, $CDCl_3$) δ 20.1, 43.5, 43.8, 121.3, 122.0, 125.1, 125.8, 127.4, 127.5, 127.6, 127.7, 127.8, 132.0, 133.5, 136.3, 138.2, 149.3, 165.4. Elemental analysis calculated for $C_{18}H_{17}N$: C 87.41, H 6.93, N 5.66 found C 87.17, H 7.07, N 5.43.

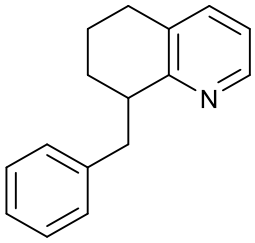

8-benzyl-5,6,7,8-tetrahydroquinoline: Synthesized using Method A. The product was obtained as a light yellow oil in 65% yield. ^{1}H NMR (400 MHz, $CDCl_3$) δ 1.67 (m, 2H), 1.77 (m, 1H), 1.88 (m, 1H), 2.69 (dd, 1H, J=24.2 ,2.23 Hz), 2.75 (m, 2H), 3.20 (m, 1H), 3.60 (dd, 1H, J=17.3, 9.74 Hz), 7.06 (dd, 1H, J=12.32, 2.88 Hz), 7.23 (m, 1H), 7.31 (m, 4H), 7.37 (d, 1H, J=7.95 Hz), 8.49 (d, 1H, J=4.21 Hz).^{13}C NMR (400 MHz, $CDCl_3$) δ 19.5, 26.5, 29.2, 41.2, 42.6, 121.1, 125.9, 128.2, 129.3, 132.4, 136.8, 141.1, 146.9, 159.7. Elemental analysis calculated for $C_{16}H_{17}N$: C 86.05, H 7.67, N 6.27 found C 83.86, H 7.67, N 6.07.

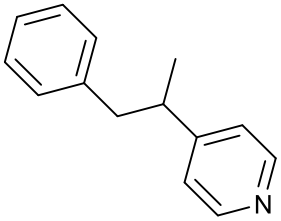

4-(1-phenylpropan-2-yl)pyridine: Synthesized using Method A. The product was obtained as an orange oil in 51% yield. ^{1}H NMR (400 MHz, $CDCl_3$) δ 1. 1.28 (d, 3H, J=6.84 Hz), 2.92 (d, 1H, J=13.5 Hz), 3.01 (m, 1H), 3.22 (d, 1H, J= 13.3 Hz), 6.83 (m, 1H), 7.08 (m, 2H), 7.15 (m, 3H), 7.25 (m, 1H), 8.50 (d, 1H, J=5.76 Hz), 8.52 (d, 1H, J=5.96 Hz).^{13}C NMR (400 MHz, $CDCl_3$) δ 20.5, 21.6, 41.3, 43.4, 44.2, 49.2, 122.6, 122.8, 123.2, 126.3, 127.7, 128.3, 129.1, 130.4, 137.4, 139.7, 149.5, 149.7, 155.6, 155.6. Elemental analysis calculated for $C_{14}H_{15}N$: C 85.24, H 7.66, N 7.10 found C 84.82, H 7.48, N 5.84.

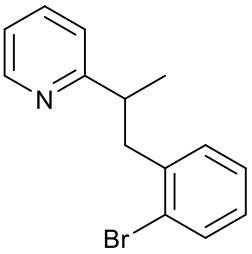

2-(1-(2-bromophenyl)propan-2-yl)pyridine: Synthesized using Method A. The product was obtained as a dark orange oil in 45% yield. ^{1}H NMR (400 MHz, $CDCl_3$) δ 1.34 (d, 3H, J=6.86 Hz), 3.04 (dd, 1H, J=7.6, 13.32 Hz), 3.19 (dd, 1H, J=7.16, 13.32 Hz), 3.32 (m, 1H, J=7.1 Hz), 7.01 (m, 3H), 7.08 (m, 2H), 7.51 (m, 2H), 8.60 (d, 1H, J=4.13 Hz).^{13}C NMR (400 MHz, $CDCl_3$) δ 19.9, 41.8, 43.2, 121.3, 122.3, 124.8, 126.9, 127.6, 131.4, 132.7, 136.2, 139.9, 149.2, 165.1. Elemental analysis calculated for $C_{14}H_{14}BrN$: C 60.89, H 5.11, N 5.07 found C 61.43, H 5.28, N 4.96.

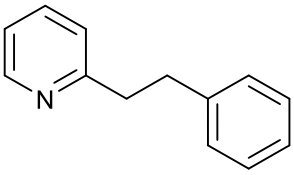

2-phenethylpyridine: Synthesized using Method A. The product was obtained as a yellow-orange oil-in 45% yield. ^{1}H NMR (400 MHz, $CDCl_3$) δ 3.10 (m, 4H), 7.09 (d, 2H, J=7.85 Hz), 7.13 (m, 1H), 7.22 (m, 3H), 7.29 (m, 2H), 7.57 (td, 1H, J=7.63, 1.61 Hz), 8.58 (d, 1H, J=4.27 Hz).^{13}C NMR (400 MHz, $CDCl_3$) δ 36.0, 40.2, 121.1, 123.0, 125.9, 128.3, 128.5, 136.3, 141.5, 149.3, 161.2. Data matched that published by Loh, Teck-Pent et al. *Angew. Chem. Int. Ed*. **2010**, 511-514.

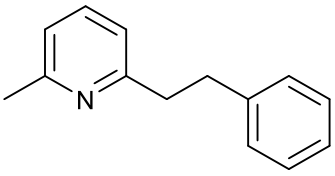

2-methyl-6-phenethylpyridine: Synthesized using Method A. The product was obtained as a yellow-orange oil in 21% yield. ^{1}H NMR (400 MHz, $CDCl_3$) δ 2.58 (s, 1H), 3.08 (m, 4H, J=2.56, 8.61, 16.6 Hz), 6.90 (d, 1H, J=7.64 Hz), 6.98 (d, 1H, J=7.63 Hz), 7.23 (m, 3H), 7.29 (m, 2H), 7.46 (t, 1H, J=7.65 Hz).^{13}C NMR (400 MHz, $CDCl_3$) δ 24.6, 36.2, 40.2,

119.7, 120.6, 125.8, 128.3, 128.5, 136.4, 141.7, 157.8, 160.6. Data matches that reported by Selikhov, A; Boronin, E.; Cherkasov, A.; Fukin, G.; Shavyrin, A.; Trifonov, A. *Adv. Synth. Catal.* **2020**, 5432-5443.

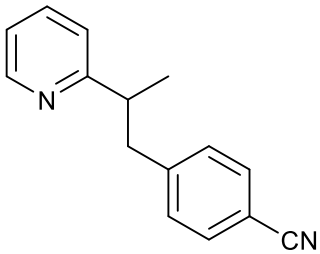

4-(2-(pyridin-2-yl)propyl)benzonitrile: Synthesized using Method B. The product was obtained as a light yellow oil in 17% yield. ^{1}H NMR (400 MHz, $CDCl_3$) δ 1.31 (d, 3H, J=6.44 Hz), 2.93 (dd, 1H, J=8.00, 16.1), 3.17 (m, 2H), 6.98 (d, 1H, J=7.80 Hz), 7.11 (t, 1H, J=6.6 Hz), 7.15 (d, 2H, J=8.12 Hz), 7.49 (d, 2H, J=8.16 Hz), 7.54 (td, 1H J=1.70, 7.88, 15.2 Hz), 8.57 (d, 1H, J=4.16 Hz). ^{13}C NMR (300 MHz, $CDCl_3$) δ 20.3, 43.2, 43.5, 109.7, 119.0, 121.5, 122.0, 129.8, 131.9, 136.4, 146.4, 149.3, 164.3.

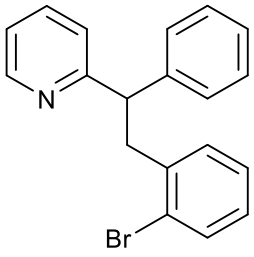

2-(2-(2-bromophenyl)-1-phenylethyl)pyridine: Synthesized using Method B. The product was obtained as a dark orange oil in 35% yield. ^{1}H NMR (400 MHz, $CDCl_3$) δ 3.49 (dd, 1H, J=7.21, 13.6 Hz), 3.79 (dd, 1H, J=8.07, 13.6 Hz), 4.52 (t, 1H, J=7.59 Hz), 6.86 (m, 1H), 6.99 (t, 2H, J=), 7.10 (m, 2H), 7.20 (m, 1H), 7.27 (t, 2H, J=7.46 Hz), 7.36 (m, 2H), 7.52 (m, 2H), 8.64 (d, 1H, J=4.38 Hz).^{13}C NMR (400 MHz, $CDCl_3$) δ 41.6, 52.9, 121.4, 123.6, 124.8, 126.5, 126.8, 127.6, 128.1, 128.3, 131.6, 132.6, 136.3, 139.5, 143.2, 149.2, 162.4. Elemental analysis calculated for $C_{19}H_{16}BrN$: C 67.47; H 5.01; N 4.14 found C 67.18; H 5.01; N 4.02.

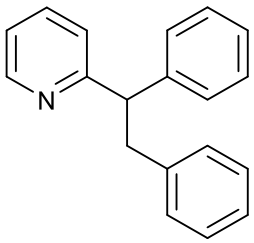

2-(1,2-diphenylethyl)pyridine: Synthesized using Method B. The product was obtained as a yellow-orange oil in 45% yield. ^{1}H NMR (400 MHz, $CDCl_3$) δ 3.40 (dd, 1H, J=7.58, 13.64 Hz), 3.70 (dd, 1H, J=7.98, 13.64 Hz), 4.40 (t, 1H, J=7.73 Hz), 7.10 (m, 3H), 7.14 (m, 1H), 7.20 (m, 3H), 7.29 (t, 2H, J=7.40 Hz), 7.36 (m, 2H), 7.53 (td, 1H, J=7.66, 15.30 Hz), 8.63 (d, 1H, J=4.25 Hz).^{13}C NMR (400 MHz, $CDCl_3$) δ 41.3, 55.4, 121.4, 123.2, 125.8, 126.5,

126.4, 128.0, 128.2, 128.4, 129.1, 126.3, 140.4, 143.3, 149.2, 163.0. Data match that reported by Sterckx, H.; Sambiagio, C.; Lemière, F.; Tehrani, K.; Maes, B. *Synlett.* **2017**, 1564-1569

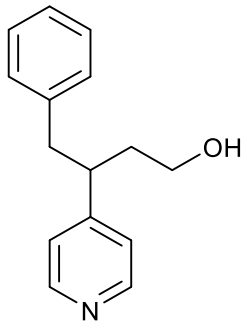

4-phenyl-3-(pyridin-4-yl)butan-1-ol: Synthesized using Method A. The product was obtained as an orange oil in 45% yield. ^{1}H NMR (400 MHz, $CDCl_3$) δ 1.89 (m, 1H), 2.02 (m, 1H), 2.88 (dd, 1H, J=8.20, 13.4 Hz), 2.95 (dd, 1H, J= 6.73, 13.5 Hz), 3.08 (m, 1H), 3.42 (m, 1H), 3.57 (m, 1H), 7.02 (d, 2H, J=6.92 Hz), 7.06 (d, 2H, J=4.67 Hz), 7.19 (m, 3H), 8.43 (d, 2H, J=4.68 Hz)^{13}C NMR (400 MHz, $CDCl_3$) δ 29.7, 37.6, 42.9, 43.7, 60.3, 123.3, 126.2, 128.2, 129.0, 139.2, 149.6, 153.5

5.4 Enamine NMR's

All NMR's are in CD_3CN after base addition and 30 minutes – 1 hour.

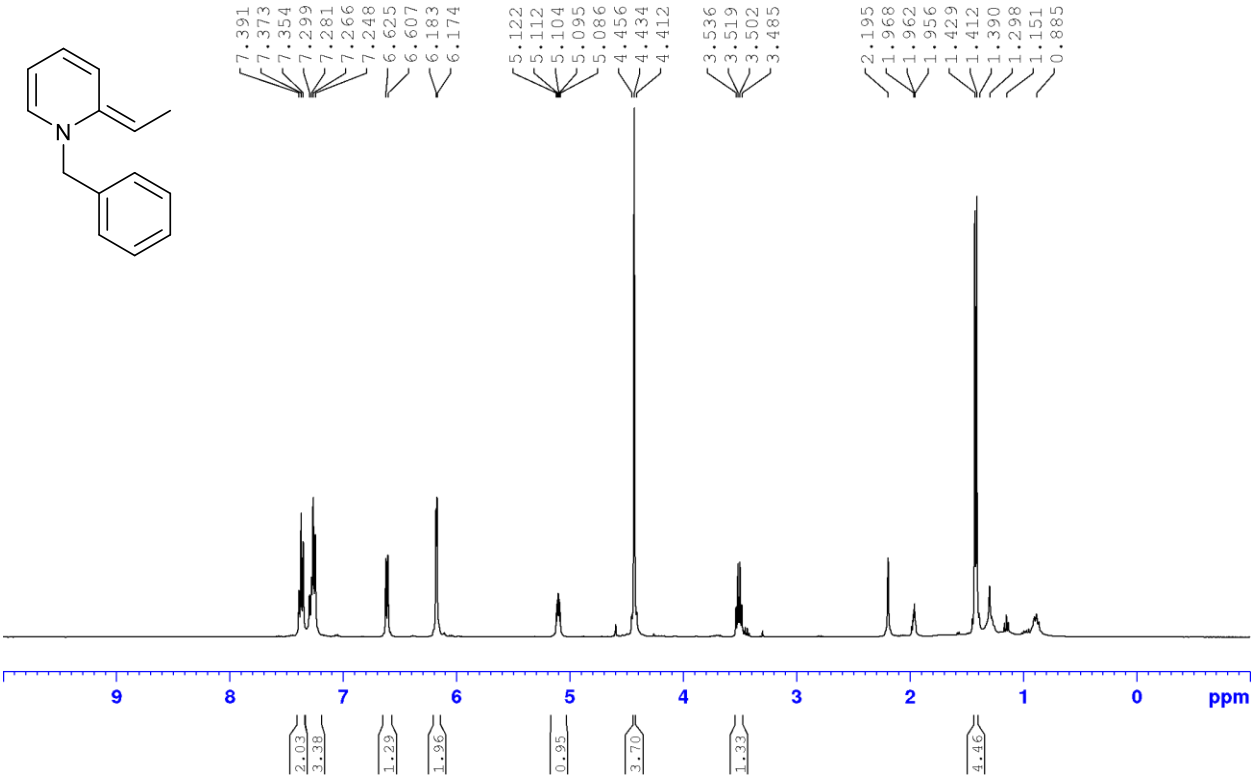

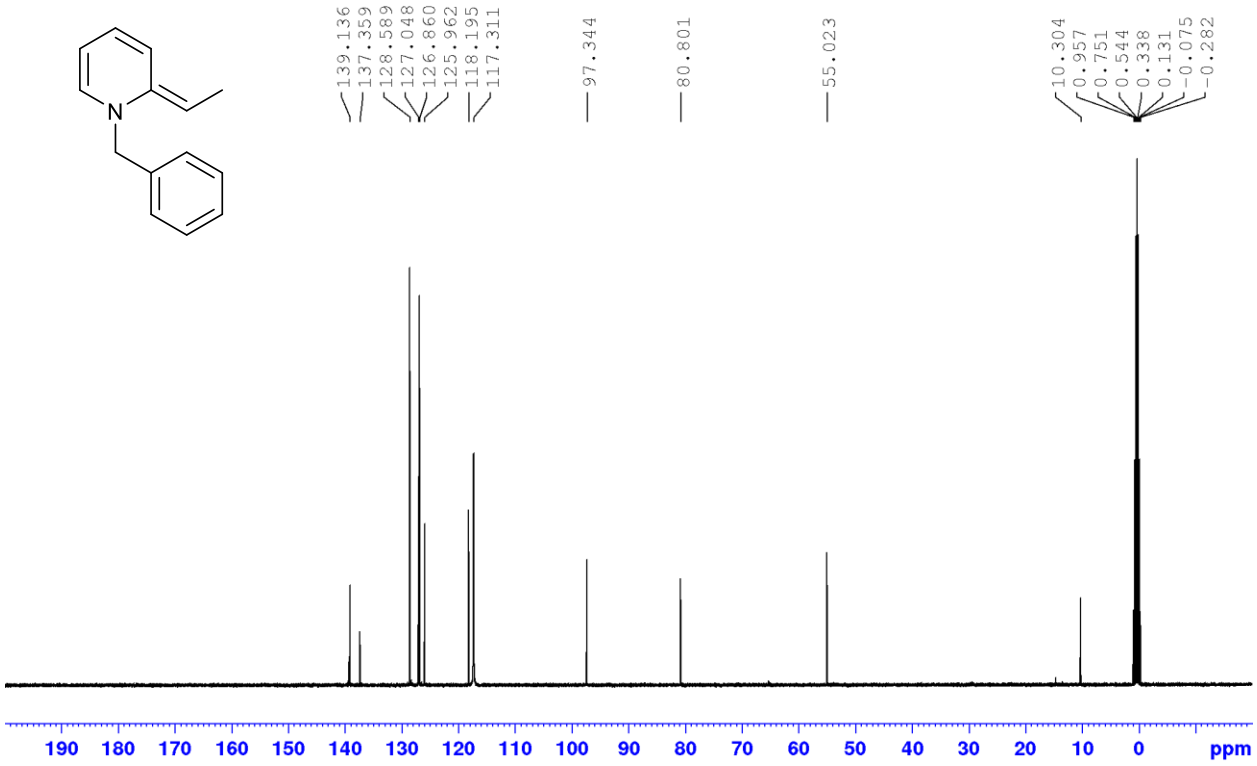
139.136
137.359
128.589
127.048
126.860
125.962
118.195
117.311
97.344
80.801
55.023
10.304
0.957
0.751
0.544
0.338
0.131
-0.075
-0.282
190 180 170 160 150 140 130 120 110 100 90 80 70 60 50 40 30 20 10 0 ppm

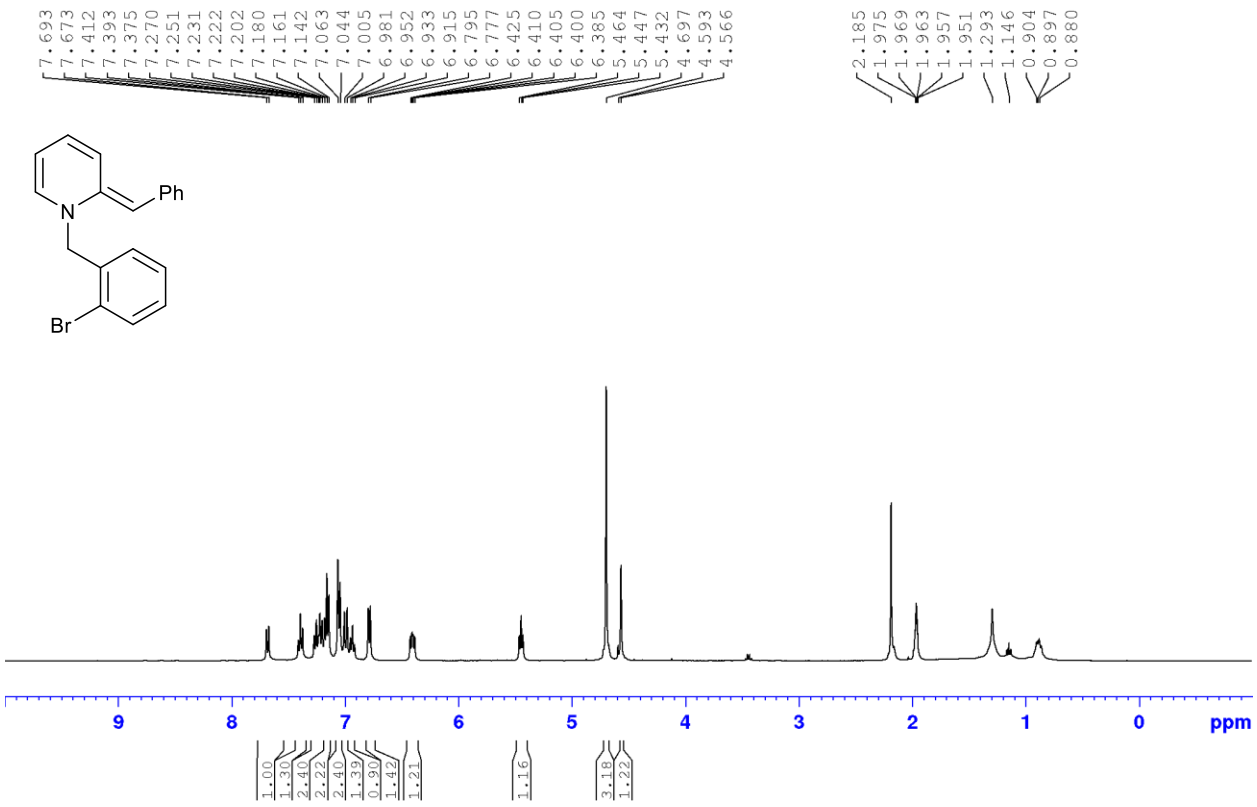
7.693
7.673
7.412
7.393
7.375
7.270
7.251
7.231
7.222
7.202
7.180
7.161
7.142
7.063
7.044
7.005
6.981
6.952
6.933
6.915
6.795
6.777
6.425
6.410
6.405
6.400
6.385
5.464
5.447
5.432
4.697
4.593
4.566
2.185
1.975
1.969
1.963
1.957
1.951
1.293
1.146
0.904
0.897
0.880
Ph
Br
9 8 7 6 5 4 3 2 1 0 ppm
1.00
1.30
2.40
2.22
2.40
1.39
0.90
1.42
1.21
1.16
3.18
1.22

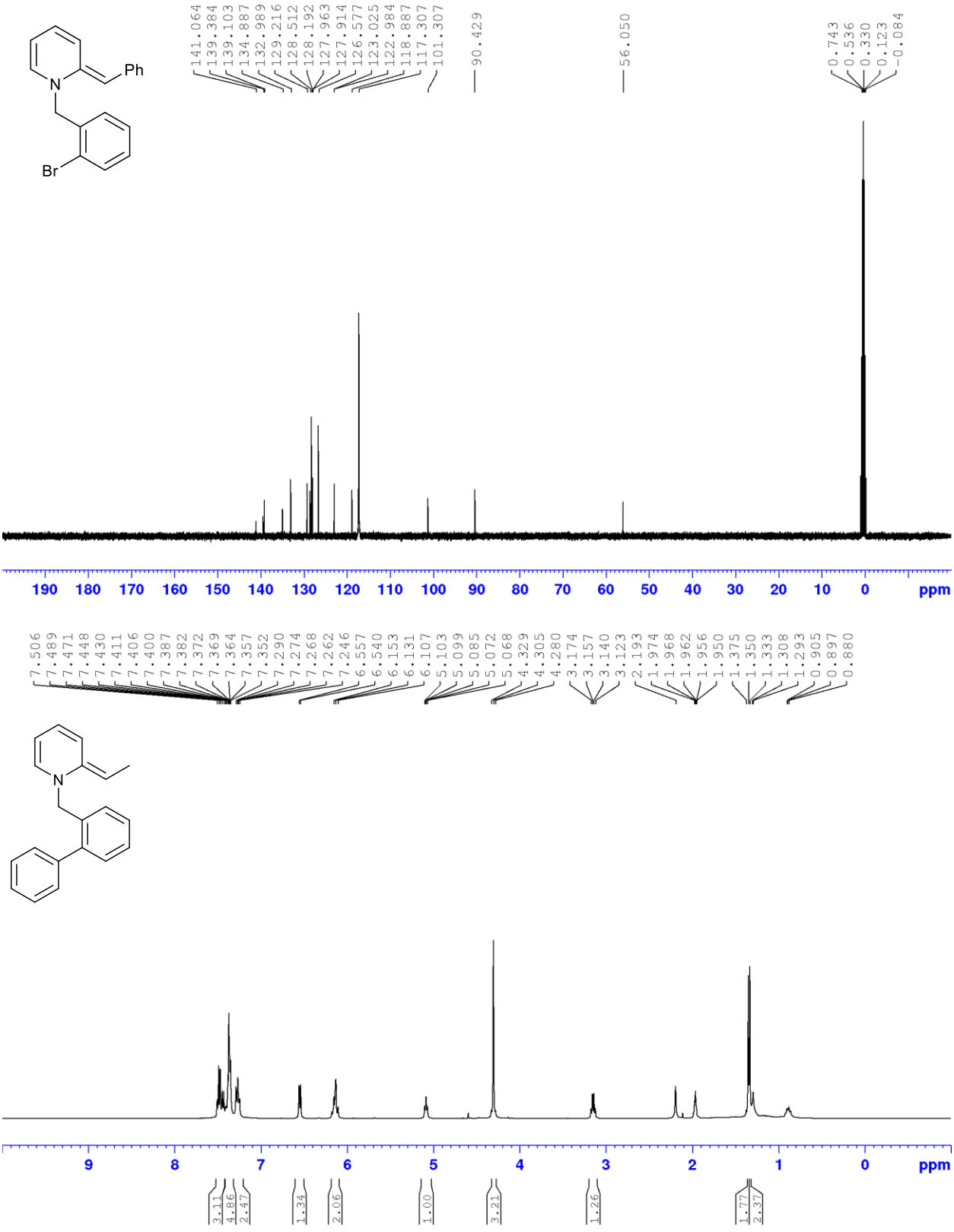
Ph
N
Br
141.064
139.384
139.103
134.887
132.989
129.216
128.512
128.192
127.963
127.914
126.577
123.025
122.984
118.887
117.307
101.307
90.429
56.050
0.743
0.536
0.330
0.123
-0.084
190 180 170 160 150 140 130 120 110 100 90 80 70 60 50 40 30 20 10 0 ppm
7.506
7.489
7.471
7.448
7.430
7.411
7.406
7.400
7.387
7.382
7.372
7.369
7.364
7.357
7.352
7.290
7.274
7.268
7.262
7.246
6.557
6.540
6.153
6.131
6.107
5.103
5.099
5.085
5.072
5.068
4.329
4.305
4.280
3.174
3.157
3.140
3.123
2.193
1.974
1.968
1.962
1.956
1.950
1.375
1.350
1.333
1.308
1.293
0.905
0.897
0.880
N
9 8 7 6 5 4 3 2 1 0 ppm
3.11
4.86
2.47
1.34
2.06
1.00
3.21
1.26
1.77
2.37

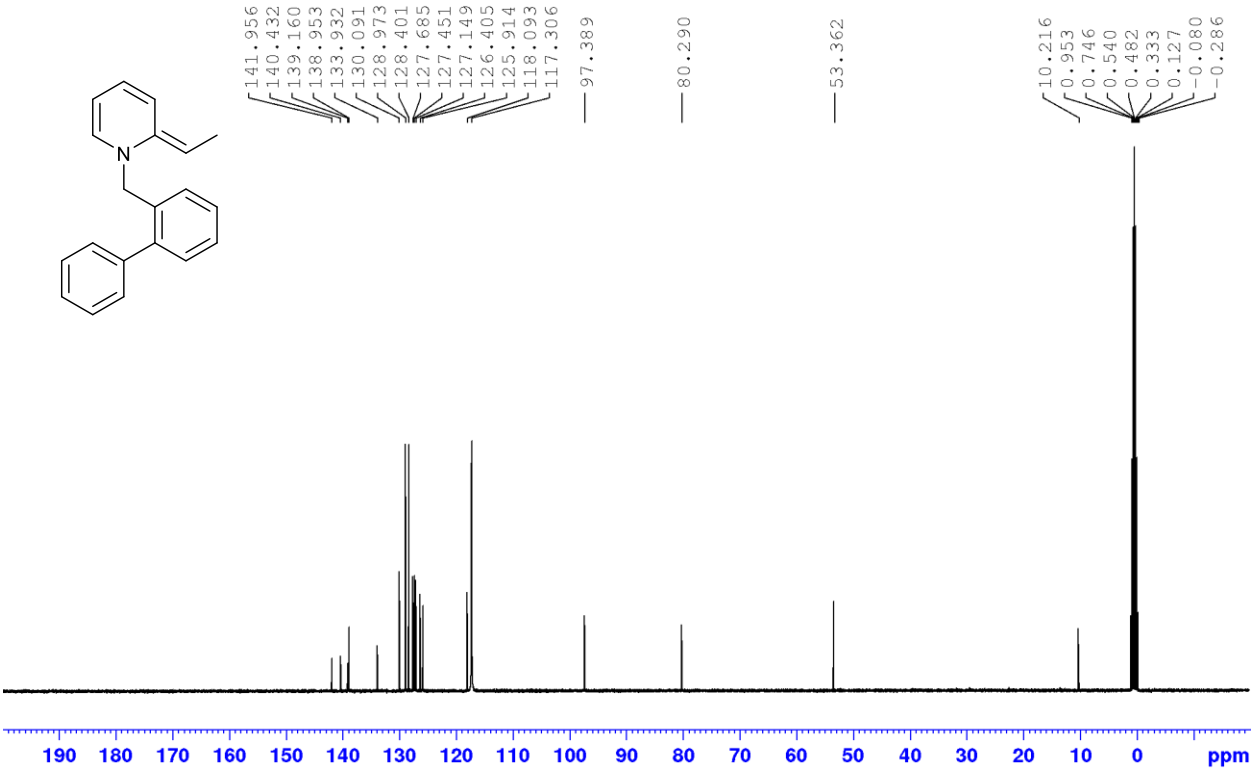
141.956
140.432
139.160
138.953
133.932
130.091
128.973
128.401
127.685
127.451
127.149
126.405
125.914
118.093
117.306
97.389
80.290
53.362
10.216
0.953
0.746
0.540
0.482
0.333
0.127
-0.080
-0.286
190 180 170 160 150 140 130 120 110 100 90 80 70 60 50 40 30 20 10 0 ppm

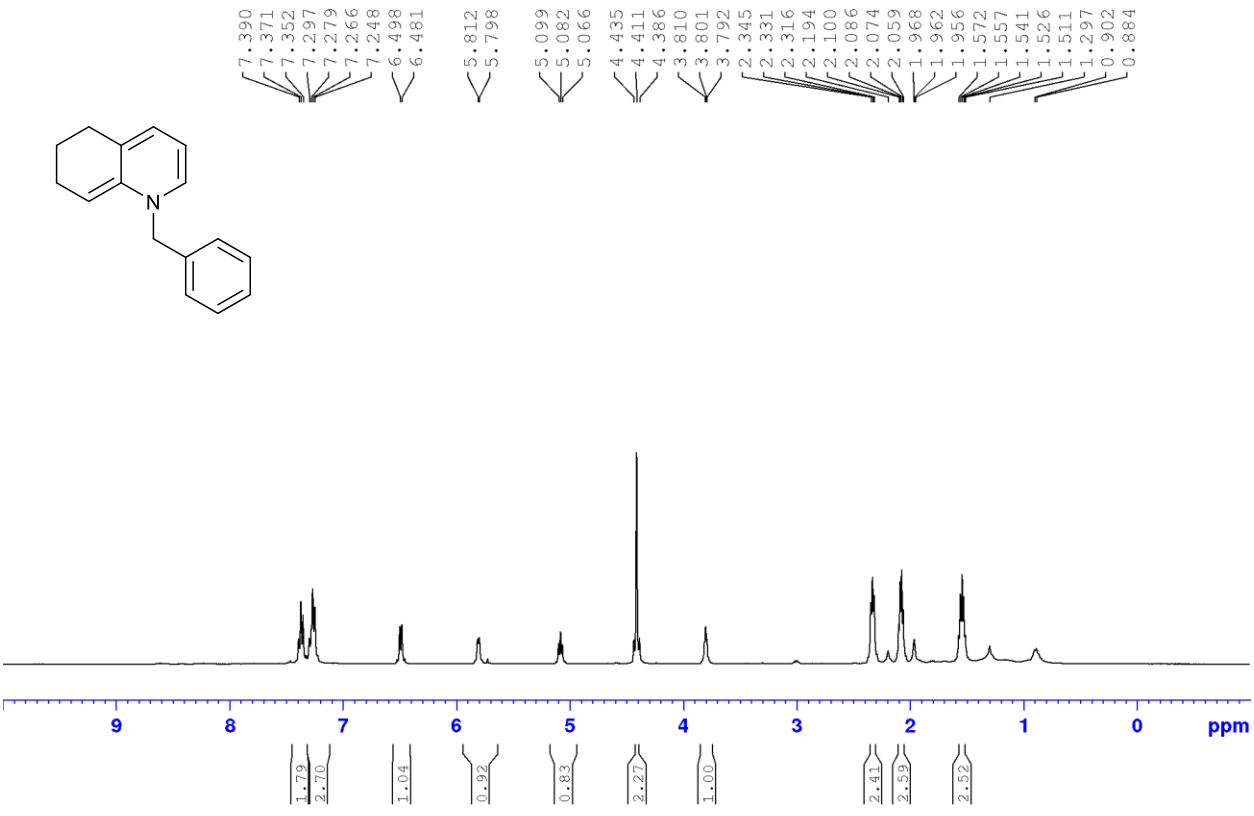
7.390
7.371
7.352
7.297
7.279
7.266
7.248
6.498
6.481
5.812
5.798
5.099
5.082
5.066
4.435
4.411
4.386
3.810
3.801
3.792
2.345
2.331
2.316
2.194
2.100
2.086
2.074
2.059
1.968
1.962
1.956
1.572
1.557
1.541
1.526
1.511
1.297
0.902
0.884
9 8 7 6 5 4 3 2 1 0 ppm
1.79
2.70
1.04
0.92
0.83
2.27
1.00
2.41
2.59
2.52

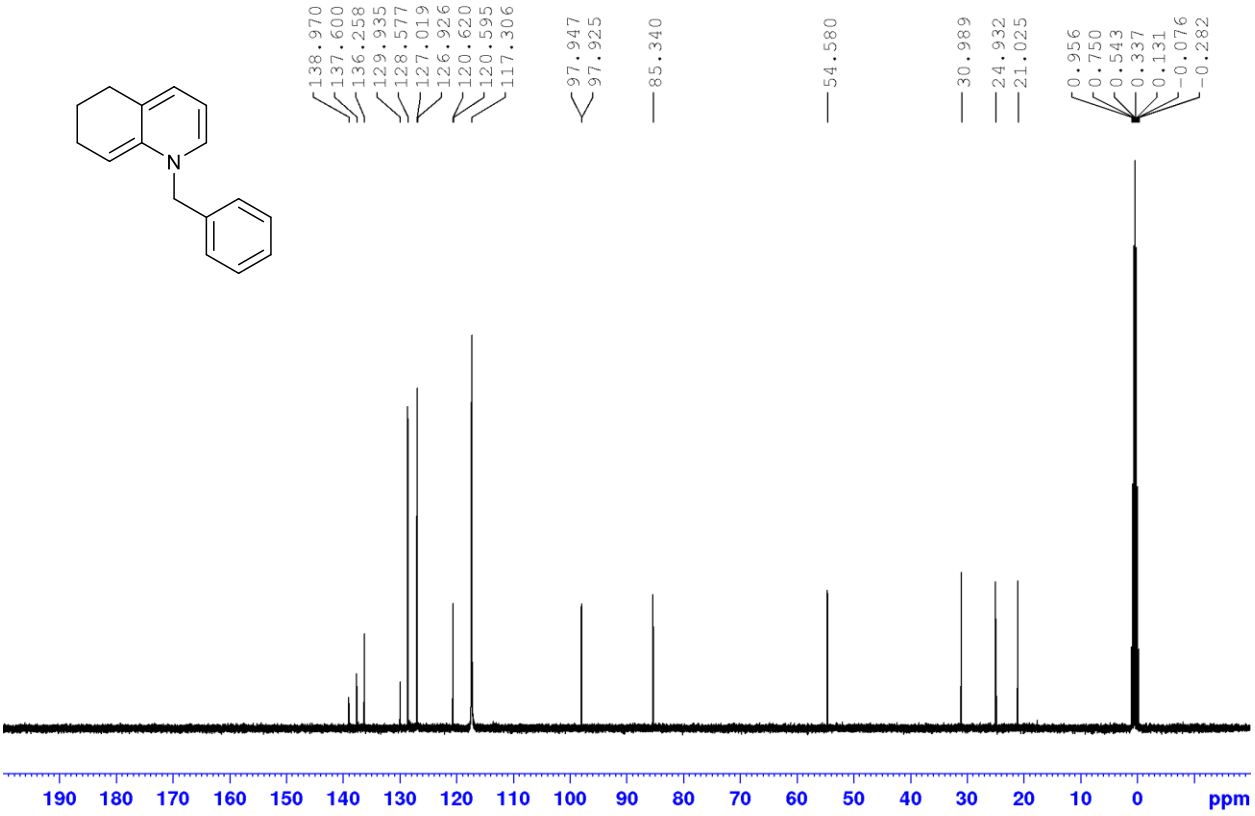
138.970
137.600
136.258
129.935
128.577
127.019
126.926
120.620
120.595
117.306
97.947
97.925
85.340
54.580
30.989
24.932
21.025
0.956
0.750
0.543
0.337
0.131
-0.076
-0.282
N
190 180 170 160 150 140 130 120 110 100 90 80 70 60 50 40 30 20 10 0 ppm

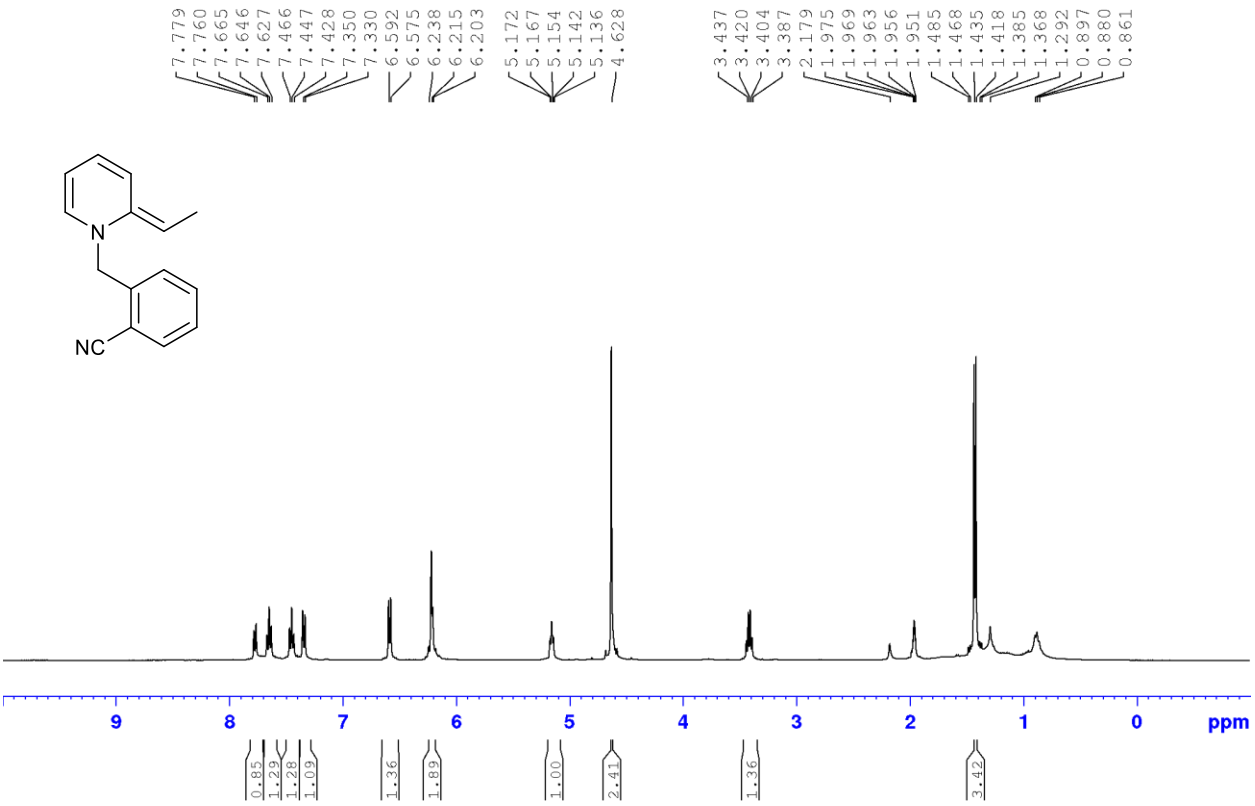
7.779
7.760
7.665
7.646
7.627
7.466
7.447
7.428
7.350
7.330
6.592
6.575
6.238
6.215
6.203
5.172
5.167
5.154
5.142
5.136
4.628
3.437
3.420
3.404
3.387
2.179
1.975
1.969
1.963
1.956
1.951
1.485
1.468
1.435
1.418
1.385
1.368
1.292
0.897
0.880
0.861
N
NC
9 8 7 6 5 4 3 2 1 0 ppm
0.85
1.29
1.28
1.09
1.36
1.89
1.00
2.41
1.36
3.42

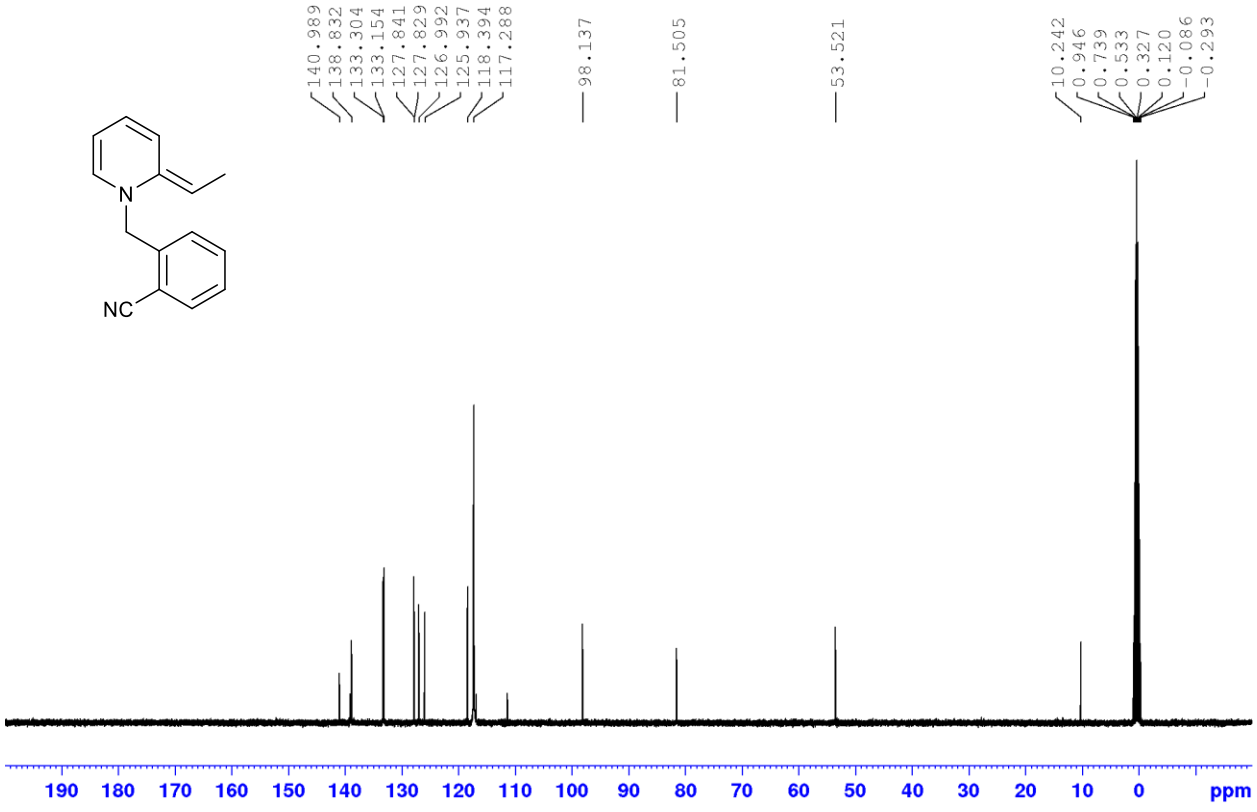
140.989
138.832
133.304
133.154
127.841
127.829
126.992
125.937
118.394
117.288
98.137
81.505
53.521
10.242
0.946
0.739
0.533
0.327
0.120
-0.086
-0.293
N
NC
190 180 170 160 150 140 130 120 110 100 90 80 70 60 50 40 30 20 10 0 ppm

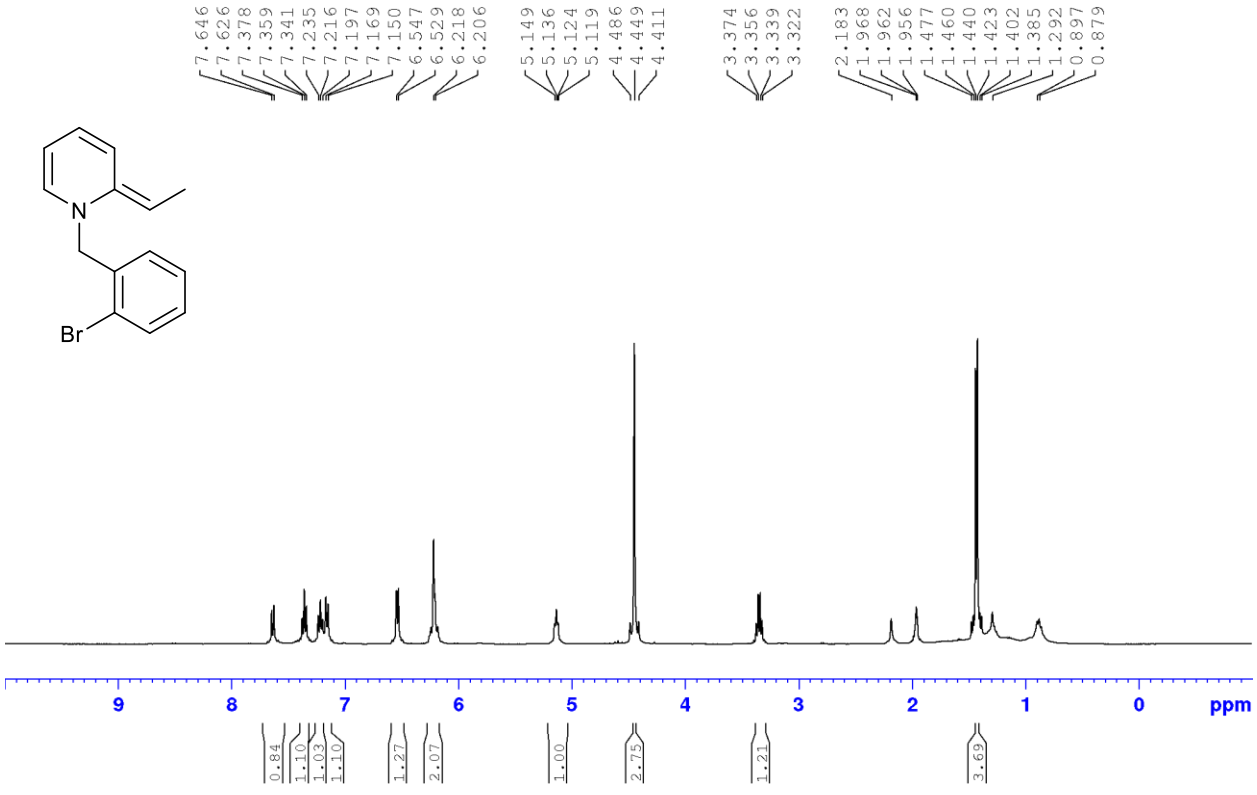
7.646
7.626
7.378
7.359
7.341
7.235
7.216
7.197
7.169
7.150
6.547
6.529
6.218
6.206
5.149
5.136
5.124
5.119
4.486
4.449
4.411
3.374
3.356
3.339
3.322
2.183
1.968
1.962
1.956
1.477
1.460
1.440
1.423
1.402
1.385
1.292
0.897
0.879
N
Br
9 8 7 6 5 4 3 2 1 0 ppm
0.84
1.10
1.03
1.10
1.27
2.07
1.00
2.75
1.21
3.69

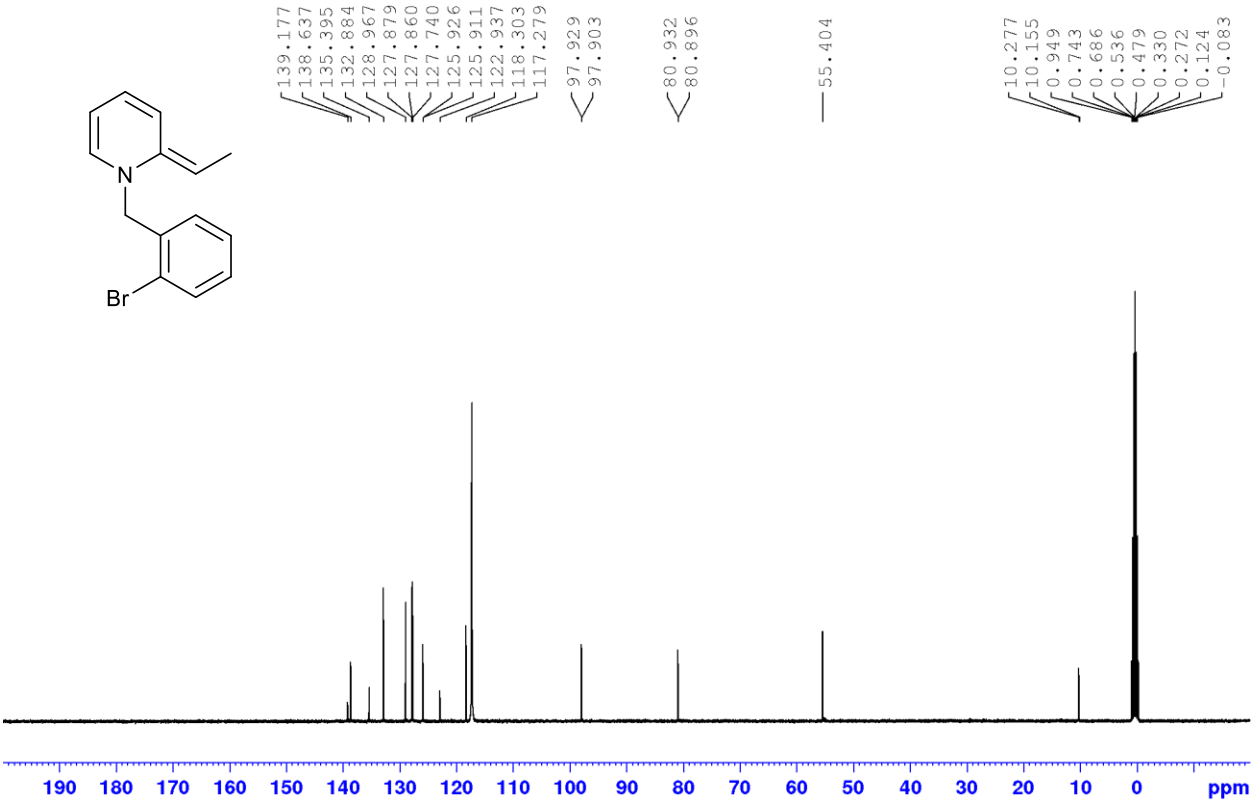
139.177
138.637
135.395
132.884
128.967
127.879
127.860
127.740
125.926
125.911
122.937
118.303
117.279
97.929
97.903
80.932
80.896
55.404
10.277
10.155
0.949
0.743
0.686
0.536
0.479
0.330
0.272
0.124
-0.083
N
Br
190 180 170 160 150 140 130 120 110 100 90 80 70 60 50 40 30 20 10 0 ppm

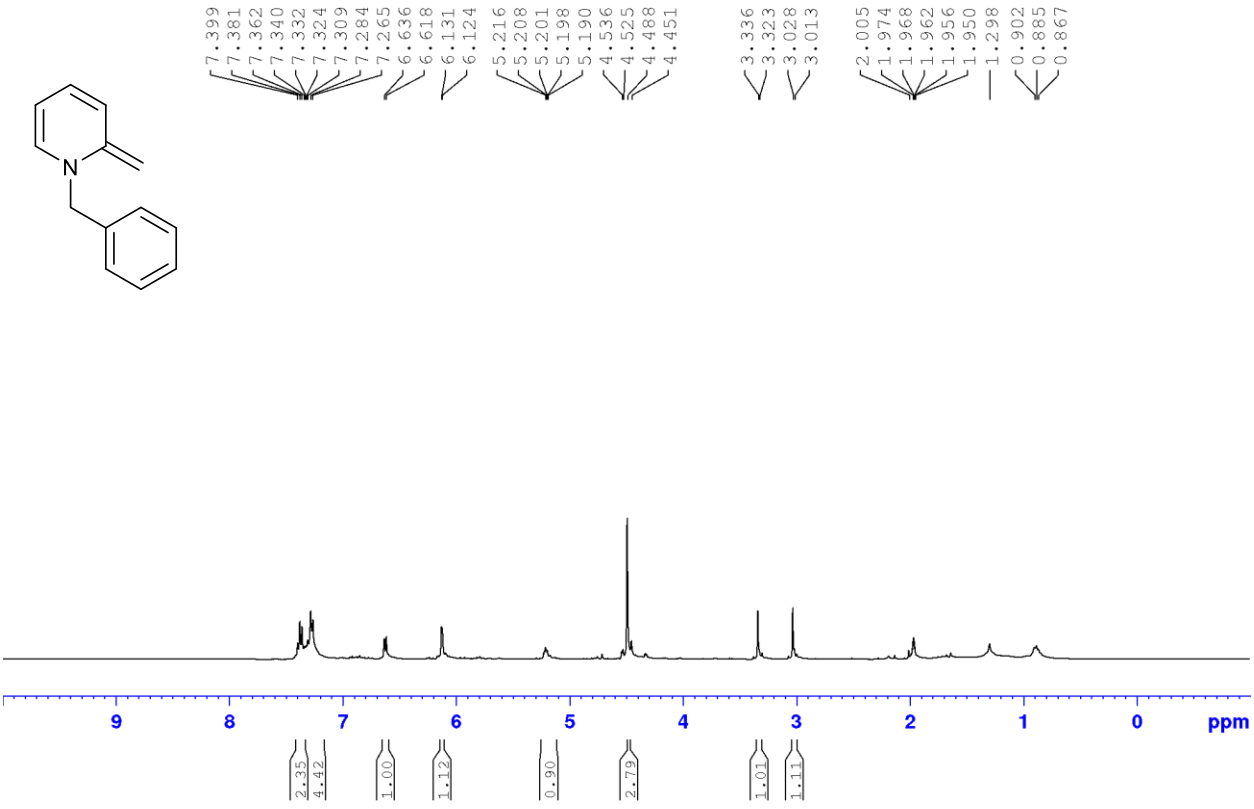
7.399
7.381
7.362
7.340
7.332
7.324
7.309
7.284
7.265
6.636
6.618
6.131
6.124
5.216
5.208
5.201
5.198
5.190
4.536
4.525
4.488
4.451
3.336
3.323
3.028
3.013
2.005
1.974
1.968
1.962
1.956
1.950
1.298
0.902
0.885
0.867
N
9 8 7 6 5 4 3 2 1 0 ppm
2.35
4.42
1.00
1.12
0.90
2.79
1.01
1.11

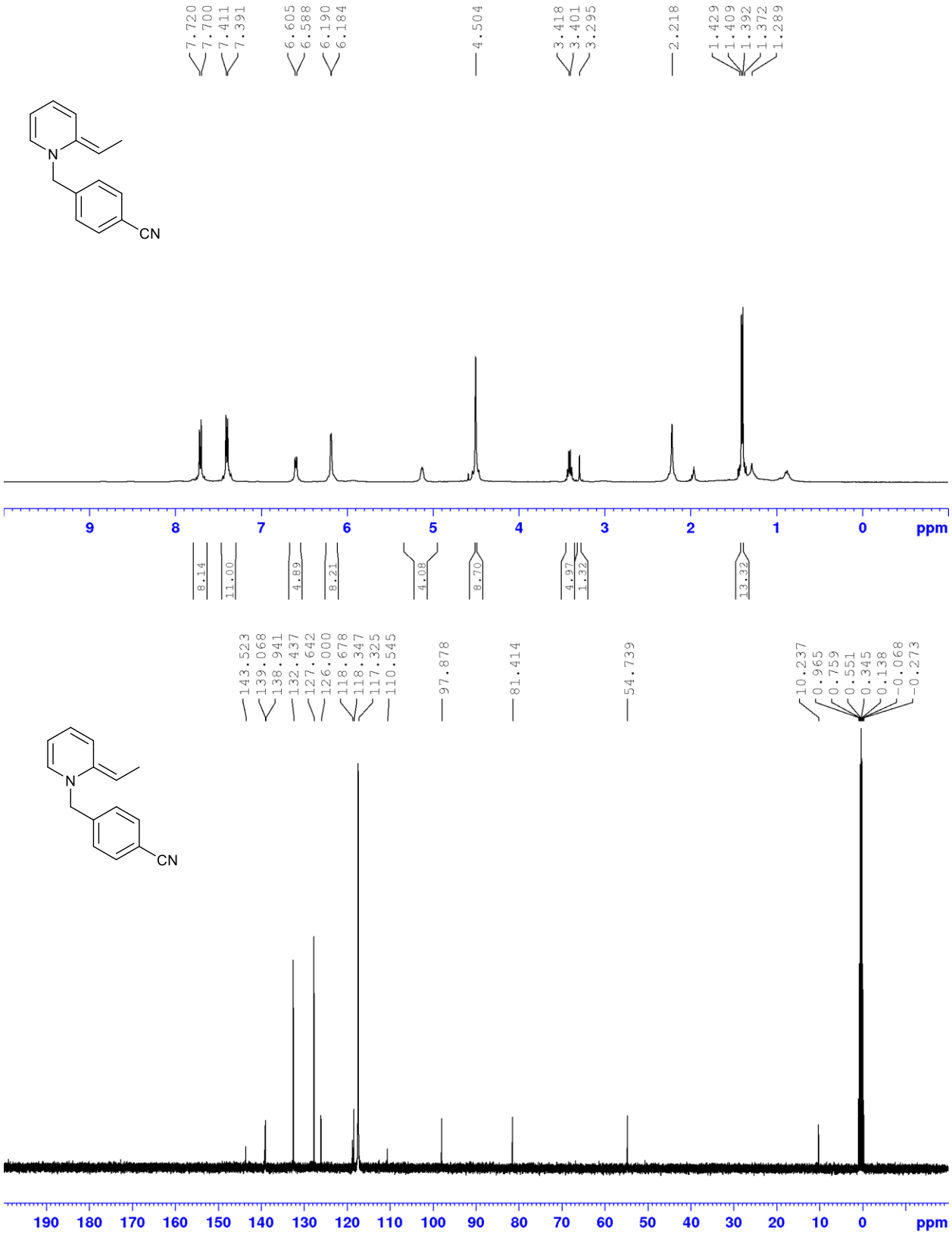
7.720
7.700
7.411
7.391
6.605
6.588
6.190
6.184
4.504
3.418
3.401
3.295
2.218
1.429
1.409
1.392
1.372
1.289
N
CN
9
8
7
6
5
4
3
2
1
0
ppm
8.14
11.00
4.89
8.21
4.08
8.70
4.97
1.32
13.32
143.523
139.068
138.941
132.437
127.642
126.000
118.678
118.347
117.325
110.545
97.878
81.414
54.739
10.237
0.965
0.759
0.551
0.345
0.138
-0.068
-0.273
N
CN
190
180
170
160
150
140
130
120
110
100
90
80
70
60
50
40
30
20
10
0
ppm

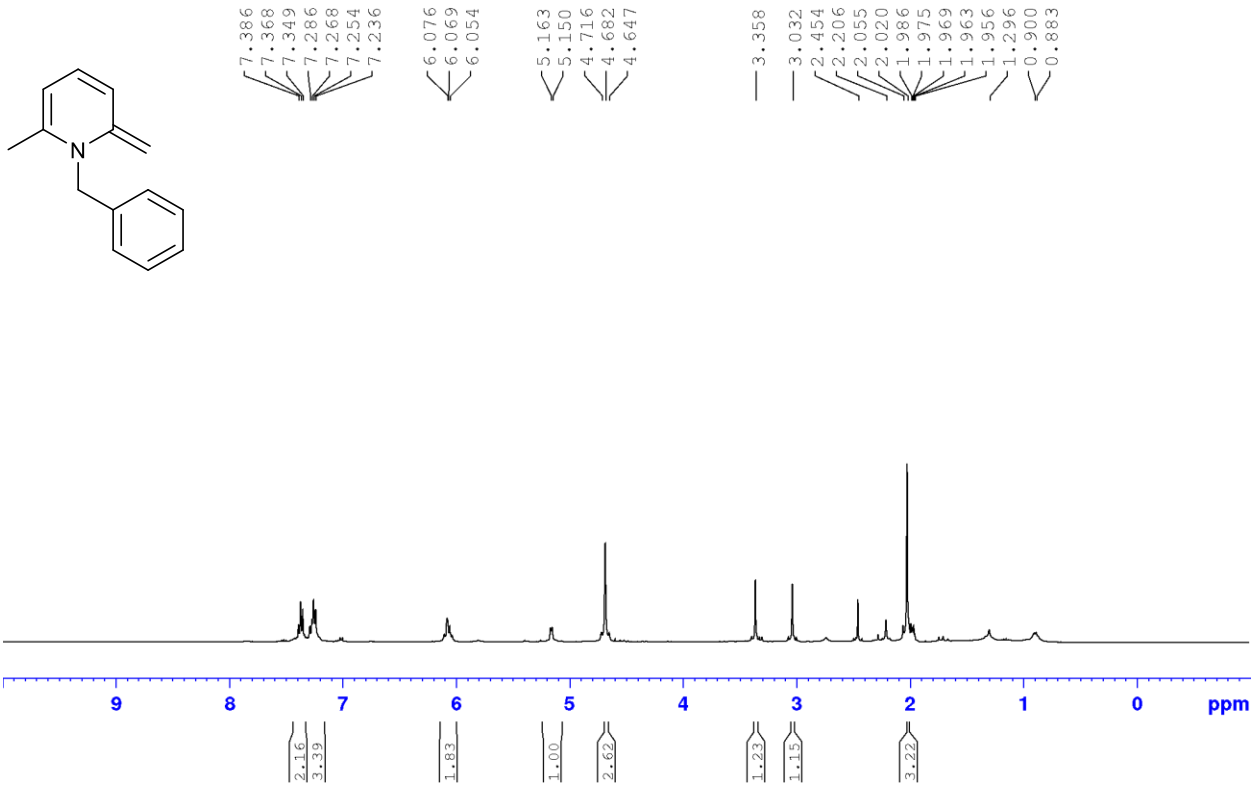
7.386
7.368
7.349
7.286
7.268
7.254
7.236
6.076
6.069
6.054
5.163
5.150
4.716
4.682
4.647
3.358
3.032
2.454
2.206
2.055
2.020
1.986
1.975
1.969
1.963
1.956
1.296
0.900
0.883
9
8
7
6
5
4
3
2
1
0
ppm
2.16
3.39
1.83
1.00
2.62
1.23
1.15
3.22

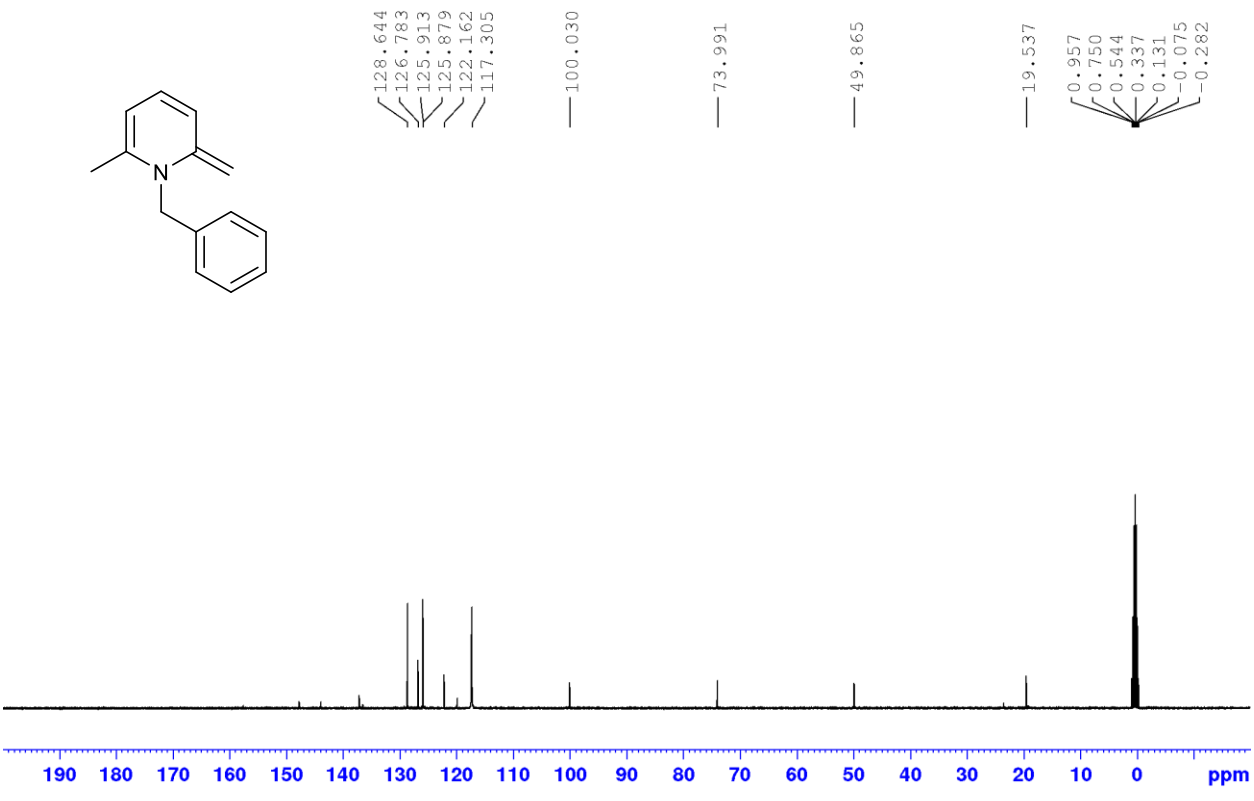
128.644
126.783
125.913
125.879
122.162
117.305
100.030
73.991
49.865
19.537
0.957
0.750
0.544
0.337
0.131
-0.075
-0.282
190
180
170
160
150
140
130
120
110
100
90
80
70
60
50
40
30
20
10
0
ppm

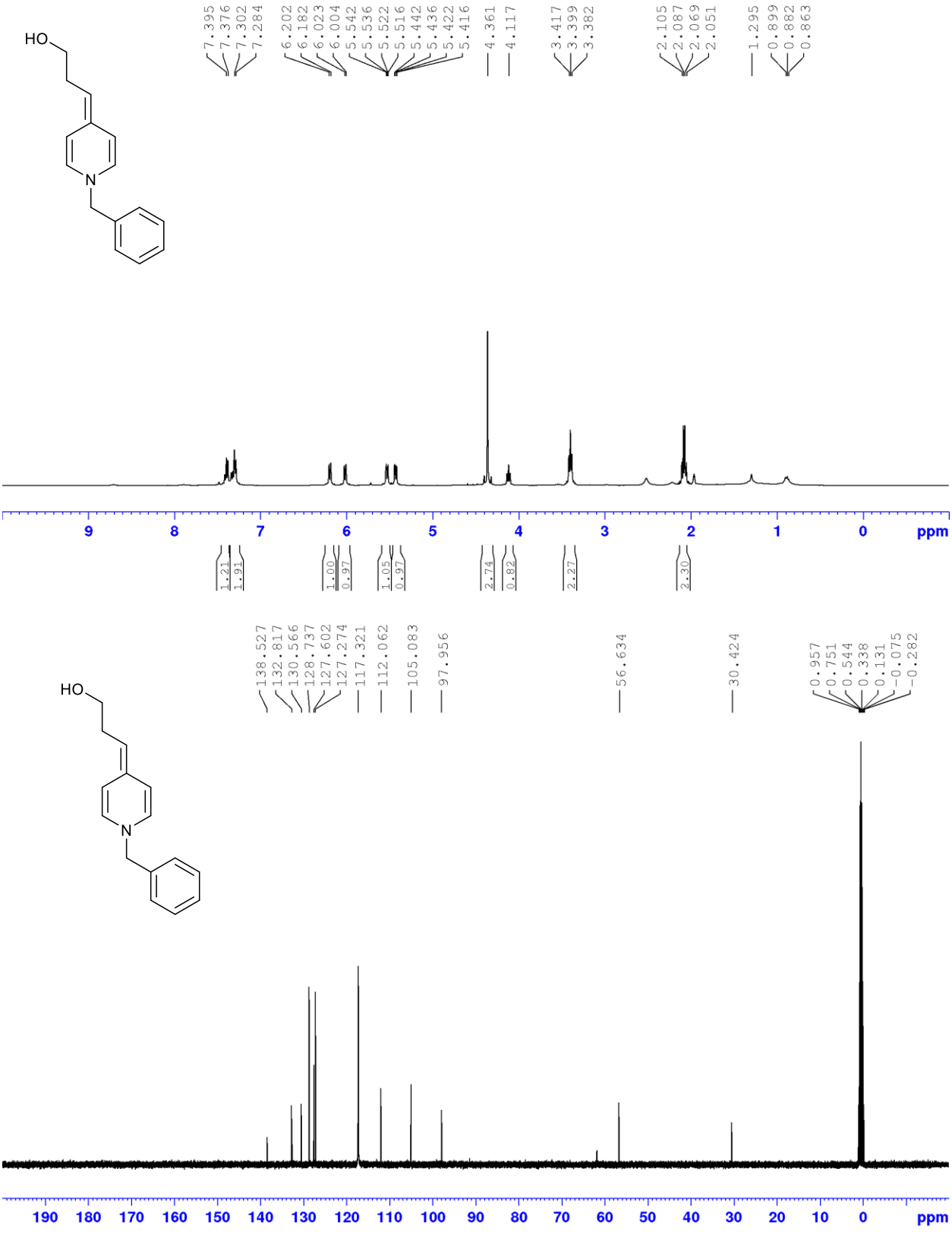
HO
N
7.395
7.376
7.302
7.284
6.202
6.182
6.023
6.004
5.542
5.536
5.522
5.516
5.442
5.436
5.422
5.416
4.361
4.117
3.417
3.399
3.382
2.105
2.087
2.069
2.051
1.295
0.899
0.882
0.863
9
8
7
6
5
4
3
2
1
0
ppm
1.21
1.91
1.00
0.97
1.05
0.97
2.74
0.82
2.27
2.30
138.527
132.817
130.566
128.737
127.602
127.274
117.321
112.062
105.083
97.956
56.634
30.424
0.957
0.751
0.544
0.338
0.131
-0.075
-0.282
190
180
170
160
150
140
130
120
110
100
90
80
70
60
50
40
30
20
10
0
ppm